

Does the lower limb kinematic CGM2.i model form a suitable alternative to the PiG model in a clinical setting?

Louise Missault

Student number: 01409686

Supervisors: Prof. Malcolm Forward, Prof. Frank Plasschaert

Master's dissertation submitted in order to obtain the academic degree of
Master of Science in Biomedical Engineering

Academic year 2018-2019

Does the lower limb kinematic CGM2.i model form a suitable alternative to the PiG model in a clinical setting?

Louise Missault

Student number: 01409686

Supervisors: Prof. Malcolm Forward, Prof. Frank Plasschaert

Master's dissertation submitted in order to obtain the academic degree of
Master of Science in Biomedical Engineering

Academic year 2018-2019

Acknowledgments

Firstly, I would like to express my gratitude to my supervisor Prof. Dr. Eng. M. Forward for the insightful feedback, his knowledge about gait analysis and for responding to all my questions. My sincere thanks also goes to Ellen De Dobbelaere, who was always there with a smile to help me with the data collection.

A very sincere thank you to T. Rodriguez Moliner, who is head of the team responsible for the installation of the gait analysis lab in Havana but who was above all a major support during my stay in Cuba. I also thank my fellow engineering students of the university 'Instituto Superior Politecnico Jose Antonio Echeverria' in Havana for the lovely five months together and Maarten Roose for the stimulating discussions and the Cuban friendship. I am also grateful to Dra. C. Heidi Trujillo Fernandez, Eng. Rosaime Glez. de los Reyes and Prof. Dr. Eng. P. Segers for the administrative help.

Finally, I must express my very profound gratitude to my family, housemates, friends, fellow students, ... Basically to everyone who supported and encouraged me during the five past years at the university. Thank you!

Permission for usage

The author gives permission to make this master dissertation available for consultation and to copy parts of this master dissertation for personal use. In all cases of other use, the copyright terms have to be respected, in particular with regard to the obligation to state explicitly the source when quoting results from this master dissertation.

Louise Missault, *May 31st 2019*

Does the lower limb kinematic CGM2.i model form a suitable alternative to the PiG model in a clinical setting?

by

Louise Missault

Supervisors: Prof. Dr. Eng. Malcolm Forward

Master's dissertation submitted in order to obtain the academic degree of
Master of Science in Biomedical Engineering

Faculty of Engineering and Architecture
Ghent University

Academic year 2018-2019

Abstract

Currently, a research group from the University of Salford, Manchester is working on the promising CGM2.i project. The aim of the project is to develop a new model, the CGM2 model, which preserves the strengths of the widely used Plug-In-Gait model (PiG) but improves its weaknesses with the intention to replace the PiG model in clinical services. The objective of this thesis is to address the question: 'Does the CGM2.i model form a suitable alternative for the PiG model in clinical service?' The CGM2.i models that are investigated as alternative for the PiG model in this study are the CGM1.0Kad, CGM1.0Med, CGM1.1Kad, CGM1.1Med, CGM2.1, CGM2.2 and CGM2.3 model.

The first part of the thesis consists of a detailed theoretical review of the PiG and CGM2 models, focusing on the kinematics. The second part of the work provides the design descriptions and result discussions of an experimental data analysis which addresses the research question by focusing on 3 pillars: a pairwise comparison of the models, the repeatability and how well the real physical gait is represented.

Keywords

CGM2, accuracy, repeatability, kinematics, Plug-In-Gait, comparison

Does the lower limb kinematic CGM2.i model form a suitable alternative for the PiG model in a clinical setting?

Louise Missault

Supervisors: Prof. ir. M. Forward

Abstract— Currently, a research group from the University of Salford is working on the promising CGM2.i project. The aim of the project is to develop a new model, the CGM2 model, which preserves the strengths of the currently used Plug-In-Gait model (PiG) but improves its weaknesses [1]. The CGM2 model, the conventional gait model 2, is designed with the intention to replace the PiG model in clinical services. A detailed theoretical review of the PiG and CGM2 models, focusing on the kinematics, forms the background for design of an investigation of the appropriateness of CGM2 for clinical practice. This question is addressed through data analysis which focuses on 3 pillars: a pairwise comparison of the models, assessment of repeatability and how well the real physical gait is represented.

Keywords— CGM2, accuracy, repeatability, kinematics, Plug-In-Gait, comparison

I. INTRODUCTION

The Plug-In-Gait model, developed in 1990, is still used in different forms worldwide for clinical gait assessment. The strengths of the PiG model are not only its simplicity and comprehensibility but also that it's relatively well validated [2]. Moreover, the repeatability that can be obtained with the PiG model has to some extent been documented. Unfortunately, beside these strengths, the conventional PiG model contains also some well-known weaknesses [2].

- Since the introduction of the PiG model there has been a concern about the position of the hip joint center (HJC) [3].
- In the current PiG model, the femoral coronal plane can be defined by placement of the knee alignment device (KAD). The use of the KAD is associated with an inconsistent determination of the medio-lateral knee axis in the transverse plane and thus also with an intersession variability of the femoral coronal plane [2].
- The PiG model is more an algorithm that generates kinematic and kinetic output. It is not considered by some as a biomechanical model as the segment lengths are not constant [2].
- The skin markers move as a rigid cluster relative to the underlying bone structure and they also move relatively to each other. This movement is caused by skin movement, muscle contractions and inertial effects on fat. Due to this soft tissue artefact (STA) the PiG model does not represent the real physical gait [4].
- The foot is modelled as one segment, which is an oversimplification of the real foot. Alternative foot models are developed and validated but are still not implemented in clinical practice [2].
- One might expect that the upper body also has an influence on a subjects gait. However, no studies offer convincing prove whether or not the upper body must be taken into account in the PiG model[2].

Consideration of these weaknesses leads to the question of whether there is an alternative to the PiG model which is more suitable for clinical application.

The CGM2 seems an appropriate alternative, as the aim of the CGM2.i project is to develop a model that 'preserves the strengths of the PiG model and addresses its weaknesses' [1]. The CGM2.i project incorporates different submodels. Each submodel consists of the previous submodel with one specific adaptation added, improving a specific limitation of the PiG model.

This master dissertation compares the following 8 kinematic models: the PiG, the CGM10Kad, CGM10Med, CGM11Kad, CGM11Med, CGM21, CGM22 and the CGM23 model. The first part of the report provides a complete and detailed overview of the theory behind the PiG model and the CGM2.i project. Since currently the theoretical background of the CGM2 model has not been published in a compact form. In the second part, data analysis of a repeatability study using 2 normal subjects is presented with the aim of identifying if any of the 8 models is the most appropriate for clinical application.

II. THE THEORY BEHIND THE CGM2 MODEL

In order to evaluate the clinical suitability of the CGM2 model, a thorough knowledge of the theoretical background of the CGM2 model is required. In particular how the submodels of the CGM2.i project (up to CGM23) differ from the PiG model.

A. CGM10Kad & CGM10Med

The CGM10Kad model is designed with the aim of developing a clone of the PiG model. The CGM10Kad model serves as the base of the subsequent submodels and allows the users to familiarize with the pyCGM2 package [2]. Although, caution is needed because the PiG and CGM10Kad models are not exact clones.

In the PiG model the KAD is applied in the static trial but no medial ankle markers are applied. The tibia is divided into a torsioned and untorsioned segment in both the static and dynamic trials. The untorsioned segment is aligned with the femur and is used for the calculation of the knee angles. The torsioned segment, used for ankle angle calculation, is obtained by rotating the untorsioned segment around the longitudinal axis of the tibia by the tibial torsion value (Figure 1). The PiG model uses the tibia torsion value is obtained from the anthropometric measurements as the amount to rotate the torsioned version of the tibia segment.

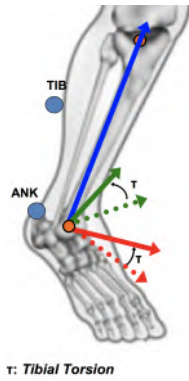


Fig. 1. The tortioned and untortioned tibia [5]

In the CGM10Kad model, the KAD and medial ankle markers are applied during the static trial. During the static trial the tibial torsion value is calculated based on the orientation of the line between the ankle markers relative to the femoral coronal plane [6]. In the static trial the necessary detail for (re)construction of the segments is derived and in the dynamic trials, the tibia is modelled as both a tortioned and untortioned segment.

The discrepancy between the way of defining the tibia, leads to a knee rotation offset in the static trial, equal to the tibial torsion value. In the dynamic trials of both models, the untortioned tibia is used for knee angle calculation. However, because the way of measuring the tibial torsion values differs in the PiG and CGM10Kad model, a difference occurs between the knee angles of the models. In the CGM10Med model, the KAD is replaced by a medial and lateral knee marker for the knee alignment in the static trial but the principle at least remains the same.

B. CGM11Kad & CGM11Med

In the CGM11 models, two adaptation in terms of kinematics are introduced in order to clarify the clinical interpretation while preserving the base of the model.

The first adaptation is related to the Cardan rotation sequence of the pelvic angles. The original 'Tilt-Obliquity-Rotation' sequence is replaced by 'Rotation-Obliquity-Tilt' in the CGM11 models [6]. The latter sequence corresponds to the clinical interpretation that the pelvic tilt is the rotation of the pelvis relative to the lab around the medio-lateral axis of the pelvis rather than around an axis fixed in the lab and related to the direction of progression.

Secondly, the tibia is modelled as one tortioned segment in the dynamic trials of the CGM11Kad and CG11Med models. This should lead to a knee rotation offset equal to the tibial torsion value between the CGM10 and CGM11 models in the dynamic trials [6].

C. CGM21

A number of studies suggest that the equation used in the Plug-In-Gait model results in a physically incorrect hip joint center position. Both, functional calibration methods and other regression equations are proposed as alternatives. In CGM21 the original regression equation for the HJC is replaced by those

from Hara et al. [7] (calculated in the same pelvic coordinate system as used in PiG):

$$HJC_x = 11 - 0.063 * LL \quad (1)$$

$$HJC_y = 8 + 0.086 * LL \quad (2)$$

$$HJC_z = -9 - 0.078 * LL \quad (3)$$

LL stands for leg length and is expressed in mm. A positive X-, Y- and Z-coordinate represent respectively a HJC anterior, lateral and superior to the pelvic origin.

D. CGM22

In the conventional PiG model, the dynamic processing is done using a 'direct method'. This implies that the orientation of the segments is determined by calculating for each time frame separately, the segment origin and axes using the positions of the measured markers. In the CGM22 model, the direct method is replaced by the so called 'Inverse Kinematics' (IK) method [8]. During the static trial, a lower body segment model is created which consists of a chain of rigid body segments connected by 'ball-in-socket' joint constraints. In the dynamic trials, the best match between this lower body segment model and the measured markers is searched. This is done by minimizing the cost function, which is the weighted root mean square distance between modelled markers and the measured markers. This ensures that the segment length remains constant and that the CGM22 model can thus be considered more as a true biomechanical model.

E. CGM23

In the CGM23 model the lateral thigh and tibia wand markers are each replaced by a non rigid cluster of 3 skin mounted markers. The skin markers are generally applied to anatomical landmarks which are felt to be least prone to soft tissue artefact. The lateral thigh wand marker is thus replaced by (1) a proximal anterior thigh marker, THAP, (2) a distal anterior thigh marker, THAD and (3) a lateral thigh skin mounted marker, THI [9]. The lateral tibia wand marker is replaced by (1) a proximal anterior tibia marker, TIAP, (2) a middle anterior thigh marker, TIAD and (3) a lateral tibia skin mounted (without wand) marker, TIB. The lateral wand markers and their replacing clusters of skin markers are shown in figure 2. Exploiting the inverse kinematics with a larger number of markers, in theory makes the dynamic processing less susceptible to particular markers prone to STA.

III. DATA ANALYSIS: MATERIALS AND METHODS

Data was collected from two healthy subjects (subject 1: female, 65kg, 176 cm, 22 years and subject 2: male, 77kg, 185cm, 22 years) without gait disorder during 3 sessions with one week between the sessions. The data capturing and processing was executed using VICON Nexus 2.8.1 and data processing was carried out using the 'PlugInGait LowerBody Ai Functional VST' work flow and the pyCGM2 package, version 3.0.8.

Each session consisted of a static trial with the knee alignment device applied, a static trial with a lateral and medial knee marker applied and 10 dynamic trials. The corresponding

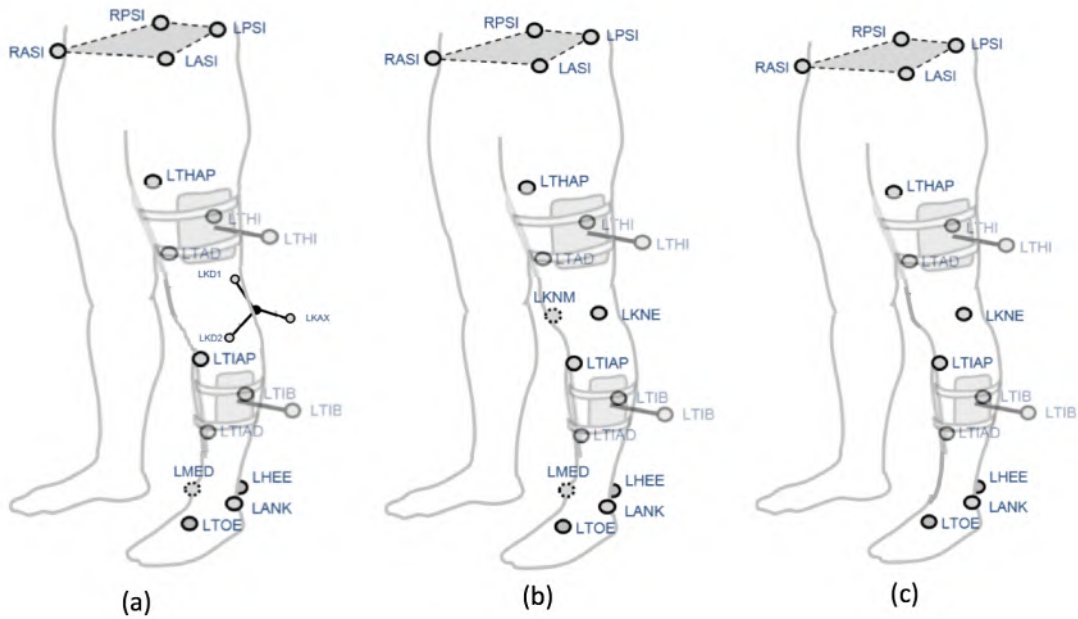


Fig. 2. The marker placement in the static trial with KAD (a), in the static trial with the lateral and medial knee marker (b) and in the dynamic trials (c) [9]

marker placements can be found in figure 2 a, b and c respectively. The 10 dynamic trials are all modelled using the 8 different models. For each model, the necessary markers are selected and the other markers are left unlabeled. With this methodology, the difference in kinematic output is for a single trial related only to the differences between the models and not due to biological variability.

In assessing if the CGM2.i model is an appropriate alternative for the PiG model for clinical application, the collected data was analyzed from 3 different points of view: the pairwise comparison of the models, the repeatability and how well the models represent the real gait.

IV. DATA ANALYSIS: A PAIRWISE COMPARISON OF THE SEGMENT AXES AND THE KINEMATIC OUTPUT

In order to be suitable for clinical practice, the kinematic model should be clearly defined since good comprehension of the model is the basis for a correct interpretation of the model output. The differences between the models are examined in the context of the model output. An overview of the pairwise com-

parison of the segments and the relative angles is shown in figure 3. The pyCGM2 package of the CGM10Med model was found to result in obvious errors in the knee axis alignment and was eliminated from further analysis because of this software bug.

A. CGM10Kad & PiG

The tibial torsion value in the CGM10Kad model comes from transverse orientation of the ankle markers with respect to the femoral coronal plane and in the PiG model from the anthropometric measurements. Hence, the definition of the tibial coronal plane and therefore as well the position of the ankle joint center, differ between the two models, leading to a difference in the ankle rotation angle. Furthermore, a medio-lateral (ML) shift in the foot origin and an anterior-posterior (AP) shift in the HJC were observed. The latter causes hip flexion/extension and knee flexion/extension offset between the models. Both, the shift in the hip joint center and the one in the foot origin shouldn't be present according to the published description of CGM10Kad.

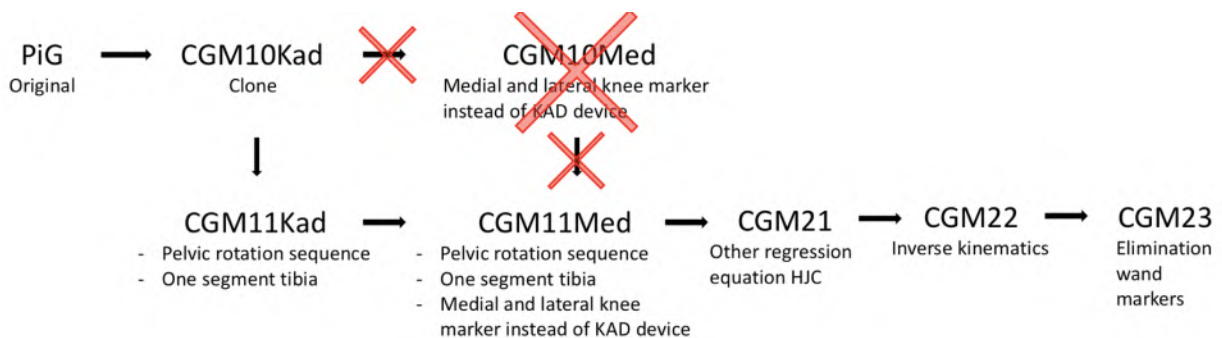


Fig. 3. A scheme representing the pairwise comparison with the elimination of the CGM10Kad model

B. CGM11Kad & CGM10Kad

In the dynamic trials of the CGM11Kad model, the untortioned and tortioned tibia segment are replaced by only one tortioned tibia. This leads to a knee rotation offset between the models that equals the tibia torsion value. In addition a superior-inferior (SI) shift in the foot origin was observed, causing an ankle dorsi/plantar flexion offset. As this shift is not mentioned in the description of CGM11Kad, it may be considered as an error. As this report focuses only the relative angles between body segments, the effect of the adaptation of the alternative Cardan sequence for the pelvic angles (the orientation of the pelvis with respect to the lab) is not discussed.

C. CGM11Med & CGM11Kad

The CGM11Med and CGM11Kad model differ in terms of knee alignment method. Because of the top-down approach (from the pelvis to the foot), a different knee alignment does not only affect the femur and the knee joint definition, but also the tibia and ankle. In order to establish whether the observed kinematic differences are a consequence of the difference in knee alignment, further investigation is required. An AP shift in the hip joint center (about 30mm), which causes a hip flexion/extension and knee flexion/extension offset, and an AP shift in the foot origin are observed. The change in hip joint center in particular was unexpected and will compound any changes in knee axis location/orientation.

D. CGM21 & CGM11Med

The CGM21 model positions the hip joint center more lateral and superior compared to the CGM11Med. The magnitude of the total shift is subject dependent (subject 1: 20mm, subject 2: 30mm). This shift in the HJC is a consequence of the use of alternative regression equations for the HJC location and causes a hip abduction/adduction (subject1: about $0,5^\circ$, subject 2: about 3°) and knee varus/valgus offset (subject1: about -1° , subject 2: about $-3,5^\circ$). The difference between the CGM21 and CGM11Med model is totally in line with expectations from theory, with no contradictions observed.

E. CGM22 & CGM21 and CGM23 & CGM22

The static processing is the same in the CGM21 and CGM22 model. The segment model, generated in the static trial, is fitted to measured markers during the dynamic processing in CGM22. This fitting is done by the 'OpenSim IK Solver', which generates the joint angles corresponding to the minimal distance between the measured and modeled markers without outputting the corresponding segments and joint centers. Hence, the segments and joint centers shown in Nexus are not the ones of CGM22, which makes it harder to interpret the kinematic output. Further, it can be concluded that the difference in kinematic output of CGM21 and CGM22 is probably related to soft tissue artefact and knee axis misalignment but that further investigation is required. The exact same reasoning, drawbacks and conclusions apply for the differences between the CGM22 and CGM23 model.

V. DATA ANALYSIS: THE REPEATABILITY

In order to be suitable for clinical practice, a model needs to be repeatable. A high intersession repeatability enables for example better distinction between a subject's pre-and postoperative gait.

The biological variability, an inconsistent walking speed and soft tissue artefact are considered as the main sources of the intrasession variability [10]. For the intersession variability, these sources also play a role but their effect is generally swamped by other larger errors. An inconsistent marker placement is considered as the main source of the intersession variability.

Both the intersession and intrasession repeatability are investigated using 3 parameters: the average standard deviation (ASD) of 9 kinematic parameters, the intraclass correlation coefficient (ICC) of selected summary parameters and the minimal detectable change (MDC), again of selected summary parameters.

A. The Averaged Standard Deviation (ASD)

A.1 Definition

The averaged standard deviation [$^\circ$] is an absolute parameter which represents variability while taking into account the whole gait cycle. How the ASD values are calculated, is schematized in figures 4 and 5 for respectively the intersession and intrasession repeatability.

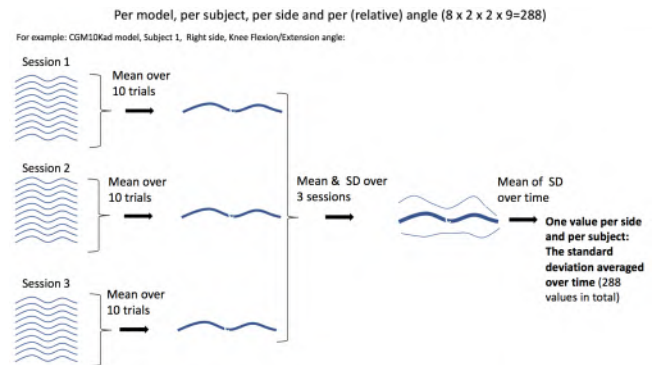


Fig. 4. Scheme of the calculation of the intersession averaged standard deviation

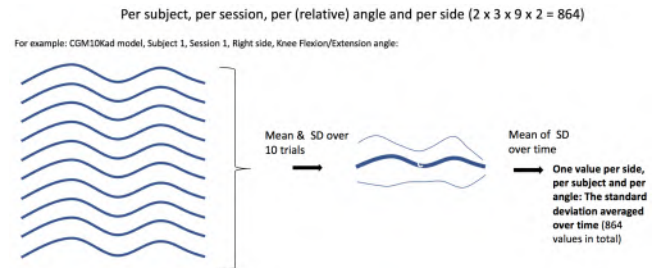


Fig. 5. Scheme of the calculation of the intrasession averaged standard deviation

A.2 Results and Discussion

Table 1 shows a ranking of the repeatability of all the models based on the intersession and intrasession ASD values. Although the repeatability is very angle dependent, this work evaluates the overall repeatability of the models without distinguishing between the different angles. This is justified because the model most suitable for clinical practice, is the model which performs best generally over all angles. The CGM10Med model is not considered in the ranking as the pyCGM2 package of the model contains a software bug, which leads to questionable output.

Table 1. Overall ranking of the repeatability of the models based on averaged standard deviation

	ASD Inter	ASD Intra
Best	CGM23	PiG
	CGM21	CGM23
	CGM11Med	CGM21
	CGM22	CGM11Med / CGM11Kad
	CGM11Kad	CGM10Kad
	PiG	CGM22
worst	CGM10Kad	

CGM23, the inverse kinematics method with a large number of markers (as an alternative to wand markers), shows the highest intersession repeatability. The low intrasession repeatability of the CGM22 model is probably related to the combination of wand markers with rigid segment modelling creating its sensitivity to STA. The CGM23 model expected to be less prone to STA shows indeed a better intrasession repeatability.

B. Intraclass Correlation Coefficient (ICC)

The ICC values lay between 0 and 1 and represents the variability due to error relative to the heterogeneity of the population of a particular summary parameter (Peak and Range of Motion in this study). This work provides a thorough analysis of the ICC as a lot of haziness exists about correct way to calculate and interpret it.

The computational formulas differ for the inter- and intrasession ICC, according to the system of McGraw and Fleiss [11](inter: $k=3$, $n=2$ and intra: $k=10$, $n=2$).

$$ICC_{Inter} = \frac{MS_B - MS_E}{MS_B + (MS_T - MS_E)/n} \quad (4)$$

$$ICC_{Intra} = \frac{MS_B - MS_E}{MS_B + (k-1)MS_E + k(MS_T - MS_E)/n} \quad (5)$$

MS_B , MS_T and MS_E result from the 2-way ANOVA and represent respectively the between subject variability, the variability due to systematic measurement error and the variability due to random measurement error.

An analysis of the ICC results of the experimental data in this work indicates that the ICC is actually not suitable to represent the repeatability in this study since:

1. Many ICC values lay outside interval [0,1] and are thus not interpretable.
2. The value of the ICC is more determined by the between subjects variability than by the variability due to error, which leads to misinterpretation.

C. The standard error measurement (SEM) and the minimal detectable change (MDC)

C.1 Definition

The SEM is the precision with which kinematic output can be measured in an individual test and is quantified as $SEM = \sqrt{MS_E}$, with MS_E the mean square of the variability due to random error [12]. It should be noted that by definition only the random measurement errors are considered and not the systematic ones. The MDC is the smallest difference between two tests that can be considered as a real physical change in kinematics and not due to (random) measurement errors [12]. The minimal detectable change is calculated as $MDC = SEM * \sqrt{2} * 1,96$.

C.2 Results and Discussion

All the models, except from the CGM10Med model, are ranked from lowest to highest MDC, so from best to worst repeatability (Table 2).

Table 2. Overall ranking of the repeatability of the models based on the minimal detectable change

	MDC Inter	MDC Intra
Best	CGM23/CGM21	CGM23
	CGM11Med	CGM21/PiG
	PiG	-
	CGM22	-
	CGM11Kad	-
Worst	CGM10Kad	-

Considering all the angles, both the intersession and intrasession repeatability are the highest in the CGM23 model, based on the MDC values. This is probably due to the fact that the CGM23 model is designed to be less sensitive to soft tissue artefact. The PiG and CGM21 model score the second best in terms of intrasession repeatability, but for the ranking of MDC values of other models, no consistent conclusions can be drawn over the 3 sessions.

VI. DATA ANALYSIS: HOW WELL IS THE REAL PHYSICAL GAIT REPRESENTED

The most accurate model, is the one which contains least errors (such as software bugs) and which is least prone to errors (such as STA and marker misplacement). All the models studied make the assumption that the knee functions somewhat as a hinge joint during normal gait and that as a consequence the Knee Varus/Valgus is close to a constant value in reality. Under this assumption, a range of motion of the Knee Varus/Valgus angle different from zero and in particular a correlation between the Knee Flexion/Extension and Varus/Valgus angles indicate a non realistic kinematic output knee axis misalignment.

A. The crosstalk between the Knee Flexion/Extension and Knee Varus/Valgus angles

In the case of a knee axis misalignment in the transverse plane, a physical knee flexion/extension movement is in the model partially considered as a knee flexion/extension and partially as knee varus/valgus. The model with the lowest crosstalk value is hence likely to be least prone to transverse plane knee alignment error.

The PiG, CGM10Kad and CGM11Kad rely on KAD placement for correct knee axis alignment and the results reflect indeed that the three models result in similar knee axis misalignment. Considering the models using the medial and lateral knee marker for the knee alignment, analysis of the crosstalk between the knee flexion/extension and varus/valgus demonstrates that CGM21 and CGM11Med result in a similar knee alignment which is more realistic than the knee alignment in CGM22 and CGM23. No conclusions can be drawn about whether the KAD or the two knee markers result in the best knee axis alignment.

B. The range of motion (ROM) of the Knee Varus/Valgus angle

When there are no errors present, the range of motion of the Varus/Valgus angle will be minimal. A misalignment of the knee axis and soft tissue artefact are two types of errors that increase the Varus/Valgus ROM. The model with the lowest varus/valgus range of motion, is then the model which is least sensitive to soft tissue artefact and less susceptible to knee alignment errors.

Table 3. Ranking of the models from smallest to largest Varus/Valgus range of motion (All session and subjects considered)

Smallest Varus/Valgus ROM	CGM23
	PiG
	CGM10Kad/CGM11Kad
	CGM11Med/CGM21
Largest Varus/Valgus ROM	CGM22

Table 3 presents the ranked order of the model output in terms of varus/valgus ROM. The CGM23 model has over all the sessions and subjects the smallest Varus/Valgus range of motion. This is probably because CGM23 is designed to minimize soft tissue artefact. CGM22 has the largest Varus/Valgus range of motion probably because it's very prone to soft tissue artefact. Hence, the ranking in table 3 is in line with the expectations.

VII. CONCLUSIONS

The research question of this study is: Do the lower limb kinematic CGM2.i models form a suitable alternative to the PiG model in a clinical setting? The CGM2.i models that are investigated in this study are the CGM10Kad, CGM10Med, CGM11Kad, CGM11Med, CGM21, CGM22 and CGM23 model. The 3 pillars on which the data analysis focuses, in order to answer the question, are: a pairwise comparison of the

underlying segment definitions and the kinematic output, the repeatability and how well the physical gait is represented.

Evaluating the values of both the averaged standard deviation and minimal detectable change, leads to the unambiguous conclusion that the CGM23 model has overall the highest intersession repeatability. The intrasession repeatability of the CGM23 and PiG model is comparable.

Considering the knee axis misalignment issues together with likely benefit of soft tissue artefact reduction, leads to the conclusion that the kinematic output of the CGM23 model is least prone these types of errors. The analysis of the crosstalk between the knee flexion/extension and varus/valgus demonstrates that CGM21 and CGM11Med result in a more realistic knee alignment than CGM22 and CGM23.

Based on the repeatability and the accuracy, the CGM23 model seems a suitable alternative to the PiG model. When looking to the segment definition question on the other hand, the CGM23 model is a black box with unknown (or at least unseen) joint centers and segment axes. Besides the 3 pillars on which the data analysis focused, there is a fourth important criteria to consider: the ease of use. Certainly version 3.0.8 of the pyCGM2 packages is very sensitive to user errors and therefore the PiG is felt to be more user friendly.

Leading to the conclusion that the CGM23 will be more appropriate for clinical practice than the PiG model once the following points are addressed:

1. Although the unexpected shifts in HJC's and foot origins in the CGM2.i models are found to have a predictable impact on the kinematics in a range of patient pathologies, an explanation of the shifts is desired as the previous CGM2.i models form the basis for CGM23.
2. The joint centers and segment axes of the CGM23 model need to be available in Nexus. This allows to confirm that the segment length is constant and that the CGM23 model is compatible with other biomechanical models.
3. For all the CGM2.i models, the pyCGM2 package must become more user friendly.

REFERENCES

- [1] F. Leboeuf, CGM2.i Project: Design Criteria, 2018.
- [2] F. Leboeuf, The CGM2.i project, 2018.
- [3] A. Leardini, A. Cappozzo, F. Catani, S. Toksvig-Larsen, A. Petitto, V. Sforza, G. Casanelli, and S. Giannini, Validation of a functional method for the estimation of hip joint centre location, tech. rep., 1999.
- [4] A. Peters, B. Galna, M. Sangeux, M. Morris, and R. Baker, Quantification of soft tissue artifact in lower limb human motion analysis: A systematic review, 1 2010.
- [5] G. Paolini, Plug in Gait WebEx Training Session 3 Interpreting PiG results: PiG biomechanical modelling, tech. rep.
- [6] F. Leboeuf, R. Baker, A. Barre, J. Reay, R. Jones, and M. Sangeux, The conventional gait model, an open-source implementation that reproduces the past but prepares for the future, *Gait and Posture*, vol. 69, pp. 126129, 3 2019.
- [7] R. Hara, J. McGinley, C. Briggs, R. Baker, and M. Sangeux, Predicting the location of the hip joint centres, impact of age group and sex, *Scientific Reports*, vol. 6, 11 2016.
- [8] F. Leboeuf, CGM2.2 Overview, 2018.
- [9] F. Leboeuf, CGM2.3 Removal of Thigh Wands, 2018.
- [10] J. L. McGinley, R. Baker, R. Wolfe, and M. E. Morris, The reliability of three-dimensional kinematic gait measurements: A systematic review, 4 2009.
- [11] T. K. Koo and M. Y. Li, A Guideline of Selecting and Reporting Intraclass Correlation Coefficients for Reliability Research, *Journal of Chiropractic Medicine*, 2016.
- [12] J. P. Weir, QUANTIFYING TEST-RETEST RELIABILITY USING THE INTRAClass CORRELATION COEFFICIENT AND THE SEM, *Tech. Rep.* 1, 2005.

Contents

Nomenclature	XV
I Context of the master thesis	1
I.1 Introduction	1
I.2 Motivation	2
I.3 Course of the book	2
II Literature study	3
II.1 What is gait analysis?	3
II.1.1 Lab installation to collect input data	3
II.1.2 Output data that describes gait	5
II.2 The Plug-In-Gait model: the kinematics	6
II.2.1 Marker placement	7
II.2.2 The segment definitions	9
II.2.3 The joint definitions	17
II.2.4 The angle definitions	18
II.2.5 Overview of the axis notations	19
II.2.6 Limitations	19
II.3 CGM2: An alternative model	21
II.3.1 CGM1.0	22
II.3.2 CGM1.1	24
II.3.3 CGM2.1	26
II.3.4 CGM2.2	27
II.3.5 CGM2.3	29
II.3.6 CGM2.4, CGM2.5 and CGM2.6	32
II.4 Research question	32
III Data analysis: Materials and Methodology	34
III.1 Participants	34
III.2 Instrumentation	34
III.3 Data Collection and Processing	34
III.4 Data Analysis: Pairwise comparison of the models	36
III.5 Data Analysis: Repeatability	38

III.5.1 Sources of variability	38
III.5.2 Averaged standard deviation (ASD)	39
III.5.3 Intraclass correlation coefficient (ICC)	41
III.5.4 The Standard Error Measurement (SEM) and the Minimal De- tectable Change (MDC)	44
III.6 Data Analysis: How realistically do the models represent the physical gait? 45	
III.6.1 The crosstalk between the knee flexion/extension angle and the knee varus/valgus angle	45
III.6.2 The range of motion (ROM) of the knee varus/valgus angle	46
III.6.3 The distance between the hip joint centers	46
IV Results and Discussion	47
IV.1 Pairwise comparison of the models	47
IV.1.1 CGM10Kad & Plug-In-Gait	47
IV.1.2 CGM11Kad & CGM10Kad	54
IV.1.3 CGM11Kad & CGM11Med	58
IV.1.4 Software bug in CGM10Med	66
IV.1.5 CGM21 & CGM11Med	67
IV.1.6 CGM22 & CGM21	72
IV.1.7 CGM23 & CGM22	77
IV.2 Repeatability	79
IV.2.1 The averaged standard deviation (ASD)	79
IV.2.2 Intraclass Correlation Coefficient (ICC)	84
IV.2.3 The Standard Error Measurement (SEM) and the Minimal De- tectable Change (MDC)	88
IV.2.4 Conclusions	90
IV.3 How realistically is the physical gait represented?	92
IV.3.1 The crosstalk between the knee flexion/extension and the varus/- valgus angle	92
IV.3.2 The range of motion of the knee varus/valgus	94
IV.3.3 Conclusions	95
V Additional remarks	96
V.1 The ease of use of the pyCGM2 package	96
V.2 Future work	96
VI Conclusions	98
Bibliography	102
Appendices	106

A	Averaged Standard Deviation	107
B	Intraclass Correlation Coefficient	117
C	Standard Error Measurement	121
D	Minimal Detectable Change	125

Nomenclature

Abbreviations

α	The static plantarflexion offset
β	The static rotation offset
τ	Kendall's tau
τ	Tibial torsion
θ	Thigh rotation offset parameter
θ	Tibia rotation offset parameter
MS_B	Mean square of between subject variability
MS_E	Mean square of variability due to random error
MS_T	Mean square of variability due to systematic error
AJC	Ankle Joint Center
AO	Ankle Offset
AP	Anterior-Posterior
ASD	Averaged Standard Deviation
CGM10Kad	Conventional gait model version 1.0 with knee alignment device applied in the static trial
CGM10Med	Conventional gait model version 1.0 with medial and lateral knee marker in the static trial
CGM10Med	Conventional gait model version 1.0 with medial and lateral knee markers applied in the static trial
CGM11Kad	Conventional gait model version 1.1 with knee alignment device applied in the static trial

CGM11Med	Conventional gait model version 1.1 with medial and lateral knee markers applied in the static trial
CGM2	Conventional gait model version 2
CGM21	Conventional gait model version 2.1
CGM22	Conventional gait model version 2.2
CGM23	Conventional gait model version 2.3
CGM24	Conventional gait model version 2.4
CGM25	Conventional gait model version 2.5
CGM26	Conventional gait model version 2.6
HJC	Hip Joint Center
ICC	Intraclass Correlation Coefficient
IK	Inverse Kinematics
IR	Infrared
KAD	Knee Alignment Device
KJC	Knee Joint Center
KO	Knee Offset
LL	Leg Length
MDC	Minimal Detectable Change
ML	Medio-lateral
PiG	Plug-In-Gait
ROM	Range of Motion
SEM	Standard Error Measurement
SI	Superior-Inferior
STA	Soft Tissue Artefact
Markers	
KAX	Lateral marker on the knee alignment device

KD1	Upper marker on the knee alignment device
KD2	Lower marker on the knee alignment device
LANK	Lateral marker on left ankle
LASI	Left Anterior Superior Illiac marker
LHEE	Marker on left heel
LKNE	Lateral marker on left knee
LKNM	Medial marker on left knee
LMED	Medial marker on left ankle
LPSI	Left Posterior Superior Illiac marker
LTHAD	Left Distal Anterior Thigh marker
LTHAP	Left Proximal Anterior Thigh marker
LTHI	Marker on left thigh
LTIAD	Left Distal Anterior Tibia marker
LTAP	Left Proximal Anterior Tibia marker
LTIB	Marker on left tibia
LTOE	Marker on left toe
RANK	Lateral marker on right ankle
RASI	Right Anterior Superior Illiac marker
RHEE	Marker on right heel
RKNE	Lateral marker on right knee
RKNM	Medial marker on right knee
RMED	Medial marker on right ankle
RPSI	Right Posterior Superior Illiac marker
RTHAD	Right Distal Anterior Thigh marker
RTHAP	Right Proximal Anterior Thigh marker
RTHI	Marker on right thigh

RTIAD	Right Distal Anterior Tibia marker
RTIAP	Right Proximal Anterior Tibia marker
RTIB	Marker on right tibia
RTOE	Marker on right toe
SACR	Sacral marker

Chapter I

Context of the master thesis

I.1 Introduction

Parkinson's disease, stroke, cerebral palsy, tendonitis, arthritis, multiple sclerosis, ... All causes of abnormal gait, affecting a patient's daily activities and social life. Resolving the walking disorder can take away a large discomfort for the patient. Muscular botox injection, surgery and orthoses are few of the most common treatments for abnormal gait. In order to determine the appropriate type of treatment and the exact place of application, the walking disorder needs to be investigated in more detail. Abnormalities in someone's way of walking are obvious and can be noticed by anyone. But as basis for a successful treatment, gait analysis, a quantitative way of describing the patient's gait, is indispensable. Gait analysis is the systematic measurement, description and assessment of the quantities that characterize human locomotion [1]. In the clinical application gait analysis doesn't fulfill a diagnostic role, it only serves as an evaluation tool. On the one hand, it's used to evaluate quantitatively how advanced an already diagnosed disease is. Comparing the abnormal walking pattern with a normal walking pattern doesn't only give an idea of the severeness of the disorder but also indicates what exactly is abnormal (hip angles, knee moments, stride length,...). On the other hand, the gait analysis gives insight in the effect of a treatment. The walking patterns with or without orthoses, before or after a surgery,... can be compared quantitatively.

It's critical that the results of the gait analysis describe as perfectly as possible the gait of the subject. Although this seems evident, this is one of the largest stumbling blocks current gait analysis is facing. In the gait analysis, the trajectories of reflective markers, placed on the subject, are captioned during walking by a system of infrared cameras. Starting from those marker trajectories, the joint rotation angles are determined on the basis of a kinematic model such as the Plug-In-Gait model. This model has some shortcomings leading to joint angles as output of the analysis that differ from the real joint angles. In theory, an alternative model, the CGM2 model, addresses some of

these shortcomings. This master dissertation attempts to investigate, if in practice the the CGM2 model generates kinematics that are a better approximation of the real joint angles than the widely used Plug-In-Gait (PiG) model.

I.2 Motivation

During my Erasmus in Cuba at university 'Instituto Superior Politecnico Jose Antonio Echeverria' in Havana, I got the opportunity to work together with the team responsible for the installation of the first gait analysis lab in Havana. This project is in cooperation with the University of Ghent. The installation of the lab is still ongoing and the gait analysts are currently being trained. At this moment in the process, it's interesting to question the use of the conventional Plug-In-Gait model. The model is in different forms widely used for clinical application but has some well-known limitations that can be improved. A research group from the Salford University in Manchester is currently developing a new model, the CGM2 model, designed to replace the PiG in a clinical setting. An objective investigation whether the CGM2 is a valuable alternative to the PiG model for clinical practice in Ghent and Havana, could lead to interesting insights.

I.3 Course of the book

This report starts-off with a detailed theoretical review of the PiG and CGM2 models, focusing on the kinematics (Chapter II). This literature study forms the background for design of a data analysis which investigates the appropriateness of the PiG and CGM2 models for clinical application. The experimental data analysis, using 2 normal subjects, focuses on 3 pillars: a pairwise comparison of the models, assessment of repeatability and how well the real physical gait is represented. The design of the experimental data analysis is described in chapter III and the results are discussed in chapter IV. This report ends with some additional remarks and final conclusions.

Chapter II

Literature study

II.1 What is gait analysis?

The basic principle of gait analysis is schematized in figure II.1.1 [2]. The Plug-In-Gait model is widely used in clinical application to convert the collected input data into the desired output data that describes the gait. What the input and output data exactly consists of is explained respectively in section II.1.1 and section II.1.2. The structure and details of the Plug-In-Gait model is described in section II.2.

Besides the actual recording of the subject's walking, several anthropometric measurements also need to be taken during the assessment. Body length, body mass, leg length, knee width, tibial torsion, ... are a few examples of necessary measurements.

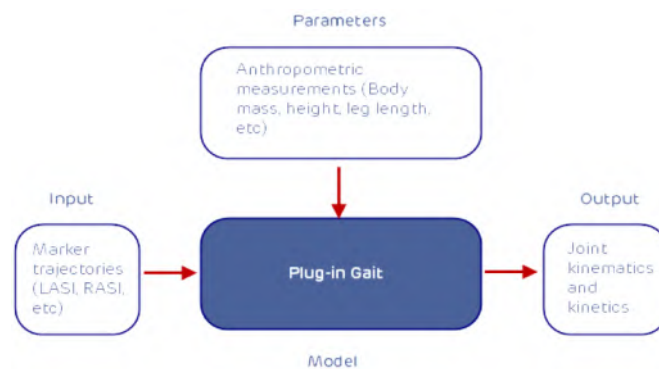


Figure II.1.1: Basic principle of gait analysis

II.1.1 Lab installation to collect input data

Reflective markers and system of infrared cameras

The first type of data that is collected during the gait analysis are the trajectories of the reflective markers placed on the subject's skin. A system of infrared cameras measures the position of the reflective markers over time during walking. The cameras emit infrared

light that is reflected by the reflective markers. Using multiple cameras, the positions of the markers in the 3 dimensional calibrated space of the lab can be determined. In the gait analysis lab in the University Hospital in Ghent, UZ Gent, 24 infrared cameras are arranged in a circular array around the walls of the laboratory focusing on the central volume of the lab. Figure II.1.2 shows a picture of the lab in UZ Gent and few of the 24 IR cameras are indicated in red.

The exact location of the reflective skin markers on the body depends on which model is used. The marker placement for the Plug-In-Gait model is explained in section II.2.1.

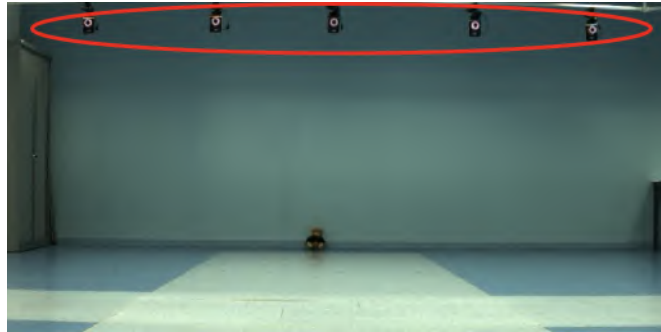


Figure II.1.2: Infrared cameras in the gait analysis lab in UZ Gent

Force plates

Along the subject's walking path, there are force plates built into the floor. These force plates measure the ground reaction forces during walking. Attention must be paid that the subject is not aware of these force plates, otherwise this would affect the walking pattern. The force platform measures the ground reaction vector in 3 perpendicular directions during foot contact. In figures II.1.3 and II.1.4 one can see the 5 force plates in the lab in UZ Gent indicated in blue.



Figure II.1.3: Force plates in the gait analysis lab in UZ Gent

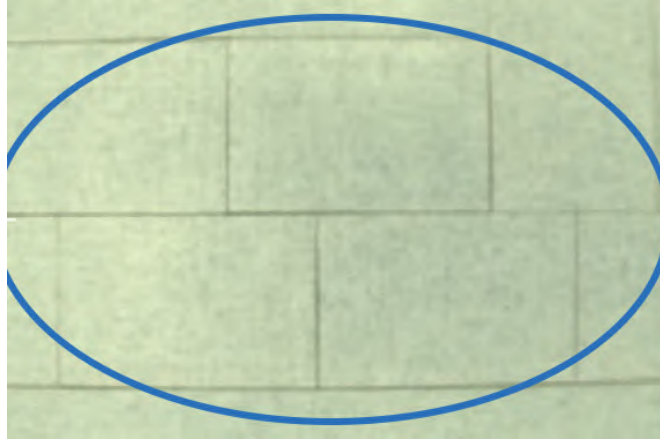


Figure II.1.4: Detail of 5 the force plates

Video

Although quantitative kinematic and kinetic data offer a good insight in the gait abnormalities, the general visual aspect is also sometimes desired. In the gait analysis lab in UZ Gent, 4 video cameras are used to record the sagittal, frontal and transverse planes of the subject including a close up view of the subjects feet and ankles.

II.1.2 Output data that describes gait

Kinematics

Within the kinematics 5 groups of rotation angles can be distinguished:

1. Hip angles: the rotation angles between the pelvic and the femur.
2. Knee angles: the rotation angles between the femur and the tibia.
3. Ankle angles: the rotation angles between the tibia and the foot.
4. Pelvic angles: the angles between the pelvic and the coordinate system of the lab.
5. Foot Progression angles: the angles between the foot and the coordinate system of the lab.

The first three groups, the relative angles, describe the position of one body segment relative to another. This is expressed by rotation angles around 3 perpendicular axes. These groups are called 'the relative angles'. In the case of the absolute angles, the last two groups, the orientation of body segments in the lab coordinate system is determined. The angles are expressed by an Euler rotation and as a function of time. This allows us to quantify the joint angles (how segments move relative to each other) during walking. The kinematic data is calculated starting from the reflective marker trajectories. Each

model has a specific way of converting the marker trajectories into kinematic output. How this is done in the PiG model is explained in section II.2.

Kinetics

The kinetic data consists of both joint moments and joint powers. Joint moments give among others information about the tension in the ligaments and muscles crossing the joint. Joint powers on the other hand give information about the nature of the muscle contraction. Power absorption is related to eccentric muscle contraction and power generation indicates that the muscle contracts concentrically [3].

The kinetic data is derived from the ground reaction forces measured by the force plates in conjunction with the kinematics of the segments. The way of going from the ground reaction forces to the joint moments and powers depends on the model. The calculation requires the mass, the moment of inertia and the center of gravity of each limb segment. This exact information is not available for the subject but can be derived from the anthropometric measurements done during the assessment. How exact the PiG model defines the joint moments and powers won't be explained in this report as the focus of this master thesis is on the kinematic part.

Temporal-spatial parameters

The temporal gait parameters are among others the velocity (m/s), the cadence (steps per minute), the time of the stance phase (s), the time of the swing phase (s), ... The spatial parameters are the foot progression angle ($^{\circ}$), the step width (m), the stride length (m), ... The most important spatial parameters are represented in figure II.1.5.

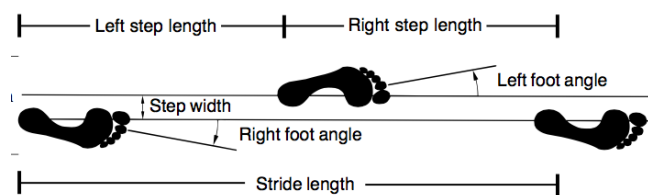


Figure II.1.5: Representation of the main spatial parameters

II.2 The Plug-In-Gait model: the kinematics

To convert the marker trajectories into kinematic data and the ground reaction forces into joint moments and powers, an appropriate model is needed. In clinical practice the Plug-In-Gait model is widely used. First, the marker placement used in the PiG model is discussed. Next, it is explained how the kinematic data is obtained in the PiG model [4]

II.2.1 Marker placement

The marker placement is dependent on which version of the Plug-In-Gait lower body model is used. In Vicon Nexus 2.8.1 the following PiG variations are implemented [5]:

- The PiG Lower Body Ai. The 'Ai' stands for the use of 2 posterior superior illiac spine markers (LPSI and RPSI) instead of the the sacral marker (SACR) which is used in the original PiG model.
- The PiG Lower Body Ai Functional. This variation is similar to the PiG Full Body Ai version but contains 4 extra markers. These 4 markers are the THIA and TIBA markers on both the left and the right side. These are extra markers placed on respectively the thigh and the tibia in order make the SaRa/ScoRe/OCST processing possible.

In this study the Plug-In-Gait Lower Body Ai model is used. Therefore, the marker placement and the corresponding processing in order to obtain the joint angles, of only this version are discussed.

The markers are placed on the skin, through palpation, on locations which correspond to anatomical landmarks of the underlying bone structure. The markers and their corresponding bone segment are:

- Pelvis: LASI, RASI, LPSI and RPSI.
- Femur: LTHI and RTHI.
- Tibia: LTIB, RTIB, LANK and RANK. The ankle markers are placed on the lateral malleoli.
- Foot: LHEE, RHEE, LTOE and RTOE.

The markers listed above are applied during the static and the dynamic trials. The markers at the height of the knee differ in the static and dynamic trials and are therefore not mentioned above. On the epicondyles of the femur, a 'Knee Alignment Device' (KAD) is applied during the static trial. This device contains 3 makers (KAX, KD1 and KD2) and is used to find the alignment of the knee joint, more specifically for part of the definition of the femoral coronal plane. During the dynamic trials the KAD is removed and replaced by one lateral knee marker (LKNE and RKNE). The markers placed during the dynamic trials are shown in figures II.2.1, II.2.2 and II.2.3 . The KAD device is indicated in figure II.2.4.

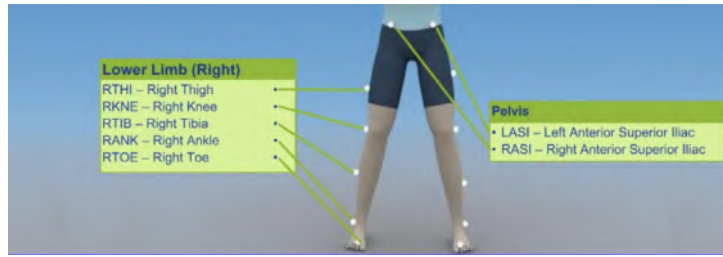


Figure II.2.1: Anterior view of the PiG marker placement in the dynamic trials



Figure II.2.2: Posterior view of the PiG marker placement in the dynamic trials

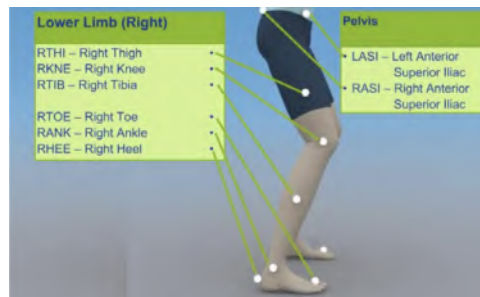


Figure II.2.3: Side view of the PiG marker placement in the dynamic trials

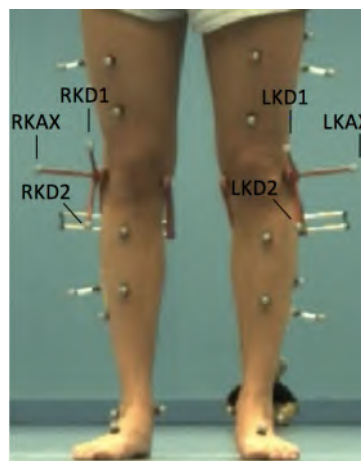


Figure II.2.4: The Knee Alignment Device with its 3 markers indicated (KAX, KD1, KD2)

II.2.2 The segment definitions

The starting point of the PiG model is the 'rigid body hypothesis'. This hypothesis states that the lower body consists of the several 'rigid body segments'. Based on the physical markers and the anthropometric measurements, virtual markers are determined. Both the physical reflective markers and the virtual markers define the rigid segments. Each time frame, the segments are defined again. The definition of the segments is done by determining a segment origin and a segment axes system starting from the physical and virtual markers [4].

The PiG model divides the lower body into 7 segments: The pelvis, the left femur, the right femur, the left tibia, the right tibia, the left foot and the right foot. There are also 3 joints defined between the segments: the hip, the knee and the ankle joint [4]. For the definition of the segments, a top-down approach is used: from the pelvis to the foot.

The pelvis

Definition of the pelvis segment

Four markers are placed on the pelvis segment in the PiG model: RASI, LASI, RPSI and LPSI. The sacral marker was used in the original PiG model but is in the current model replaced by the LPSI and RPSI markers. The sacral marker is shown for completeness but is thus not used in the current PiG model (figure II.2.5 a). The origin of the pelvis segment lays on the midpoint between the anterior pelvis markers (b). The axis Y_{Pelvis} is oriented from the pelvis origin to LASI marker (c). In the next step, a virtual point which is the midpoint between the LPSI and RPSI markers, is created. A plane going through (1) this virtual point, (2) the LASI and (3) the RASI marker, is constructed (d). Z_{Pelvis} is defined as a vector perpendicular to this plane in the superior direction (e). X_{Pelvis} is the crossproduct of Y_{Pelvis} and Z_{Pelvis} .

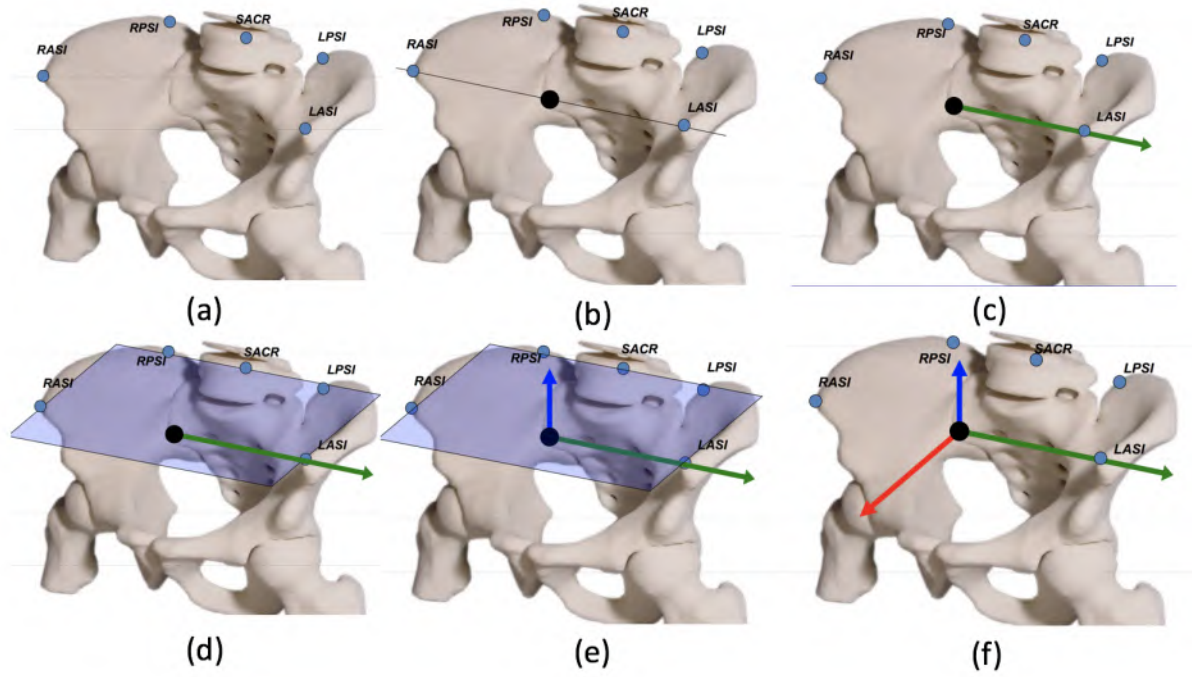


Figure II.2.5: Definition of pelvis origin and axes system [4]

The pelvis origin as defined in this section is only valid for the first part of the processing. Once the hip joint centers are determined, the pelvis origin is defined as the midpoint between the left and the right hip joint center.

Definition of the Hip Joint Center (HJC)

The hip joint centers are calculated based on equations defining its position in the pelvic coordinate system (with the midpoint between the RASI and LASI marker as origin). Based on the leg length and inter ASIS distance measurements, the hip joint center is determined through following equations [4]:

$$HJC_x = C * \cos(\theta) * \sin(\beta) - (AsisTrocDist + r) * \cos(\beta) \quad (II.1)$$

$$HJC_y = -(C * \sin(\theta) - a) \quad (II.2)$$

$$HJC_z = -C * \cos(\theta) * \cos(\beta) - (AsisTrocDist + r) * \sin(\beta) \quad (II.3)$$

with

$$C = MeanLegLength * 0.115 - 48.56$$

$$a = (InterASISdistance)/2$$

$$AsisTrocDist = 0.1288 * LegLength - 48.56$$

$$r = \text{MarkerRadius}$$

$$\theta = 0.5\text{rad}$$

$$\beta = 0.314\text{rad}$$

All the parameters are expressed in millimeter and the Asis Trochanter Distance can also be entered as an anthropometric measurement. A positive X-, Y- and Z-coordinate corresponds respectively to a hip joint center anterior, lateral and superior to the pelvic origin. In the case of non pathological subjects the HJC is positioned posterior, lateral and inferior with respect to the pelvic origin.

The pelvis origin is now positioned on the midpoint between the left and right hip joint center (figure II.2.6). The orientation of the 3 perpendicular axes, Y_{Pelvis} , Z_{Pelvis} and X_{Pelvis} , does not change.

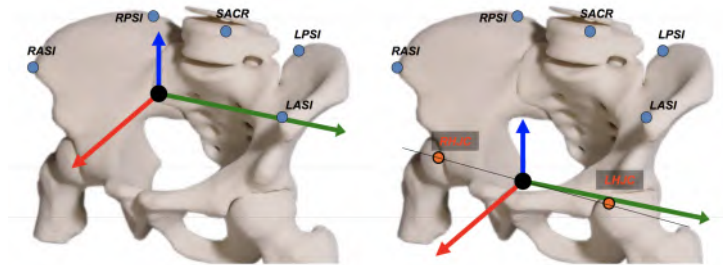


Figure II.2.6: Definition of femur origin and axes system [4]

The Femur

On the femur segment 2 markers are applied: the lateral knee marker (KNE) and the lateral thigh marker (THI) (figure II.2.8 a). The HJC is modeled as a virtual marker on the femur segment. The origin of the femur is by definition the equal to the knee joint center. Therefore it is necessary to first explain how the knee joint center is defined.

Definition of the Knee Joint Center (KJC)

The Knee Width is an anthropometric measurement from which the Knee Offset can be calculated as: $KO = (\text{MarkerDiameter} + \text{KneeWidth})/2$. The knee joint center is defined as the point that fulfills the following three requirements. (1) The point lays in the femoral coronal plane, defined as $\langle \text{HJC}, \text{THI}, \text{KNE} \rangle$. (2) The distance between the knee joint center and the lateral knee marker is equal to KO. (3) The angle between the KNE-KJC line and the HJC-KJC line is 90° . As there is only one position satisfying all 3 conditions, the KJC is defined unambiguously (see figure II.2.8 (b) and (c)).

In this way, the knee joint was originally determined in the PiG model. Unfortunately, this method has one large disadvantage: the definition of the femoral coronal plane

and therefore as well the definition of the knee joint center, is highly dependent on the anterior-posterior position of the THI marker. As there is no anatomical landmark on which the lateral thigh marker can be positioned, an anterior-posterior positioning error this marker occurs frequently. A solution for this problem is the use of the KAD.

Figure II.2.7 (a) represents how the knee joint center is defined in the static trials using the knee alignment device. First, a virtual point, KNE, is created that is positioned equidistantly from the KAX, KD1 and KD2 markers. Then, the knee joint center is defined as the point (1) laying in the $\langle KAX, KNE, HJC \rangle$ plane, (2) laying at a distance KO from the virtual point KNE and (3) with the lines KJC-HJC and HJC-KNE perpendicular to each other. The projection of the thigh marker on the plane perpendicular to the axis KJC-HJC is called THI_{proj} . The thigh rotation offset parameter, θ , is the angle THI_{proj} -KJC-KNE, measured in the plane perpendicular to KJC-HJC, and is stored to use in the processing of the dynamic trials. θ reflects how much the THI markers deviates from the femoral coronal plane. The thigh rotations offset parameters enables finding the femoral coronal plane in the dynamic trials, without the KAD device but with the lateral thigh marker. In the dynamic trials the KJC is the point that satisfies the following 3 conditions: (1) The lines KJC-HJC and KJC-KNE are perpendicular, (2) the KJC lays at a distance KO from the KNE marker and (3) the angle between the lines THI-KJC and KNE-KJC, projected in the plane perpendicular to KJC-HJC, is equal to θ (see figure II.2.7 (b)). The method as explained in figure II.2.7 is how the knee joint center is defined in the currently used PiG model.

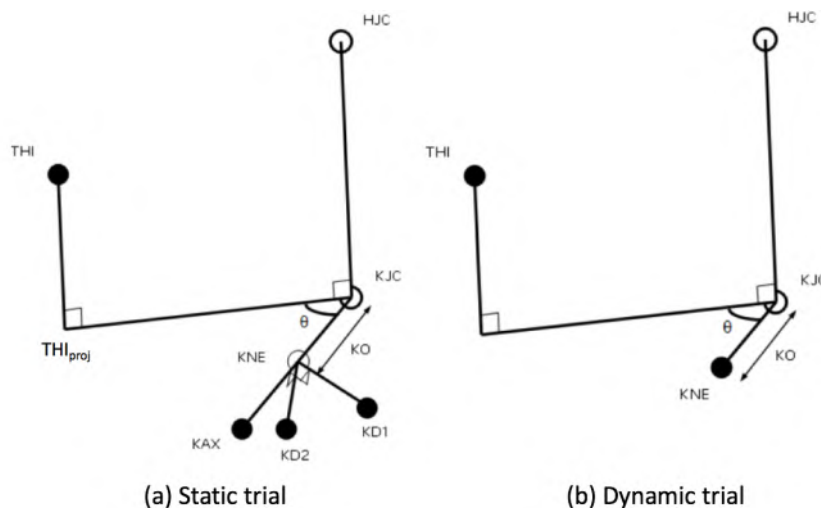


Figure II.2.7: Definition of the Knee Joint Center using the KAD [5]

Definition of the femur segment

The origin of the femur segment is by definition equal to the knee joint center. The

axis Z_{Femur} is oriented from the KJC to the HJC and lays as a consequence in the femoral coronal plane, $\langle HJC, KJC, KNE \rangle$ (figure II.2.8 d). X_{Femur} is defined as the vector in the anterior direction perpendicular to the femoral coronal plane (f). Y_{Femur} is the crossproduct of Z_{Femur} and X_{Femur} and lays as a consequence also in the $\langle HJC, KJC, KNE \rangle$ plane (g).

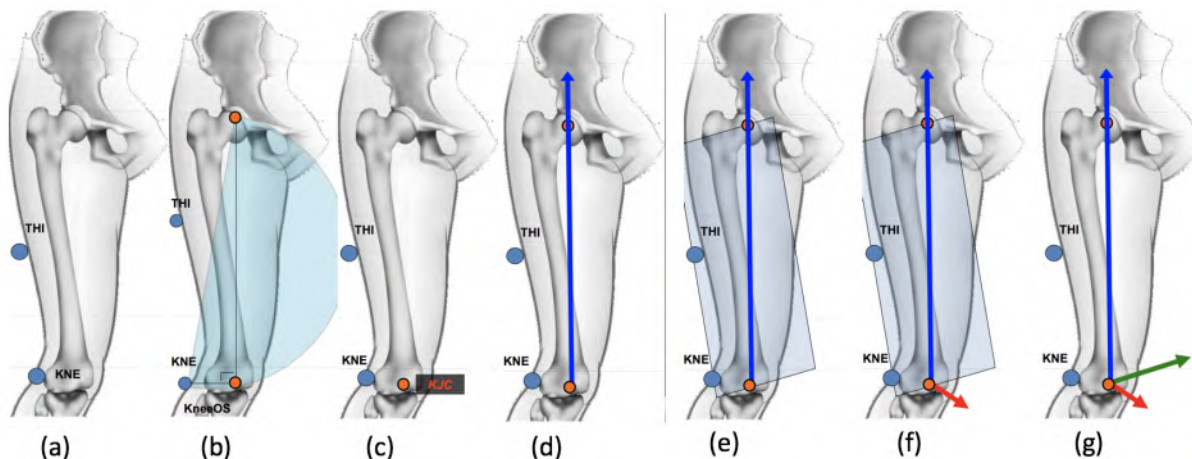


Figure II.2.8: Definition of femur origin and axes system [4]

The Tibia

Definition of the Ankle Joint Center (AJC)

In order to determine the position of the ankle joint center, 2 anthropometric measurements are necessary: The Ankle Width to calculate the ankle offset ($AO = (MarkerDiameter + AnkleWidth)/2$) and the Tibial Torsion (τ). The tibial torsion [$^{\circ}$] is known from the subject measurements and is equal to the angle between the femoral coronal plane and the tibial coronal plane. The ankle joint center in the static trials is found as the point that fulfills the following conditions (see figure II.2.9 a):

1. The distance between the AJC and the ANK marker is equal to the ankle offset.
2. The line AJC-ANK is perpendicular to the AJC-KJC line.
3. The angle between ANK-AJC and KAX_{Proj} -AJC equals the tibial torsion value. KAX_{Proj} is the projection of the KAX marker on the knee alignment device in the plane through the AJC and perpendicular to the KJC-AJC axis.

In order to make the positioning of the ankle joint center also possible in the dynamic trials, the shank rotation offset value, θ , needs to be calculated in the static trial. θ is the angle TIB_{Proj} -AJC-ANK measured in the plane perpendicular to KJC-AJC axis (figure II.2.9 b). The shank rotation offset fulfills a similar role in the tibial segment as the thigh

rotation offset does in the femoral segment. It makes it possible to find the tibial coronal plane in the dynamic trials based on the TIB marker without the KAD.

In the dynamic trials the AJC is defined as the point (1) that lies at a distance AO from the ANK marker, (2) with $AJC-KJC$ and $AJC-ANK$ perpendicular to each other and (3) with the angle $TIB_{Proj}-AJC-ANK$ equal to θ (figure II.2.9 c).

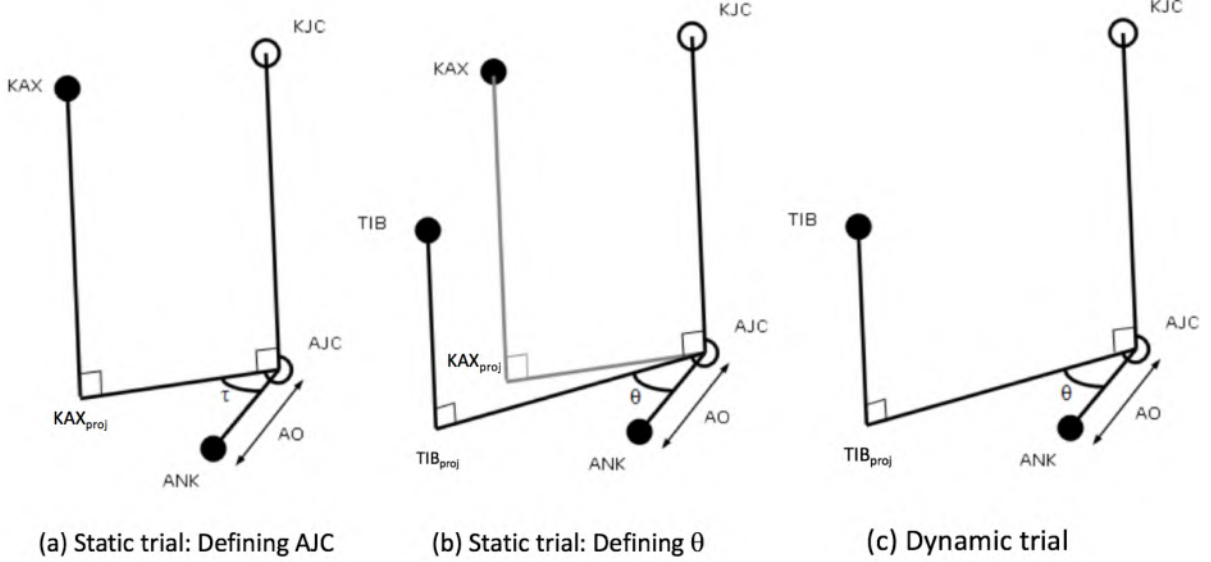


Figure II.2.9: Definition of Ankle Joint Center [5]

Definition of the tibia segment

The Plug-In-Gait model (without the use of a medial ankle marker) generates 2 tibia segments: A proximal untortioned and a distal tortioned tibia segment. The distal tortioned segment is aligned with the trans-malleolar axis of the ankle and is used to calculate the ankle angles. The proximal untortioned tibia segment is aligned with the knee joint and is used for the knee angles calculation. The untortioned segment is by definition equal to the tortioned segment rotated over the negative tibial torsion value around the KJC-AJC axis. As one can see in figure II.2.9 (a), the coronal plane of the tortioned segment is $\langle ANK, AJC, KJC \rangle$. As the untortioned segment is the tortioned segment rotated over $-\tau$ around the KJC-AJC axis, figure II.2.9 (a) makes clear that the coronal plane of the untortioned segment is the $\langle KAX, AJC, KJC \rangle$ plane.

The origin of the tortioned tibia segment is the ankle joint center (figure II.2.10 a). $Z_{Tibia,tor}$ is the vector from the AJC to the KJC (b). $X_{Tibia,tor}$ is pointed in the anterior direction and perpendicular to the tibial coronal plane $\langle ANK, AJC, KJC \rangle$ (d) and $Y_{Tibia,tor} = \text{crossproduct}(Z_{Tibia,tor}, X_{Tibia,tor})$ (e).

The origin of the untortioned segment is also the ankle joint center. When the tortioned tibia segment is known, the untortioned tibia segment can be obtained by a rotation around KJC-AJC. This rotation axis is $Z_{Tibia,tor}$ and as a consequence, the Z-axis for both tibia segments is the same ($Z_{Tibia,tor} = Z_{Tibia,untor}$). $X_{Tibia,untor}$ and $Y_{Tibia,untor}$ can be found by rotating respectively $X_{Tibia,tor}$ and $Y_{Tibia,tor}$ over the negative of the tibial torsion value (figure II.2.10 e). In non-pathological patients, the tibial torsion value is mostly negative, which corresponds an external rotation ankle mediolateral axis relative to the mediolateral axis of the knee. A rotation over the opposite of the tibial torsion value (a positive value) corresponds thus to an internal rotation of the tortioned tibia in order to get it aligned with the knee joint (also shown in figure II.2.10 f).

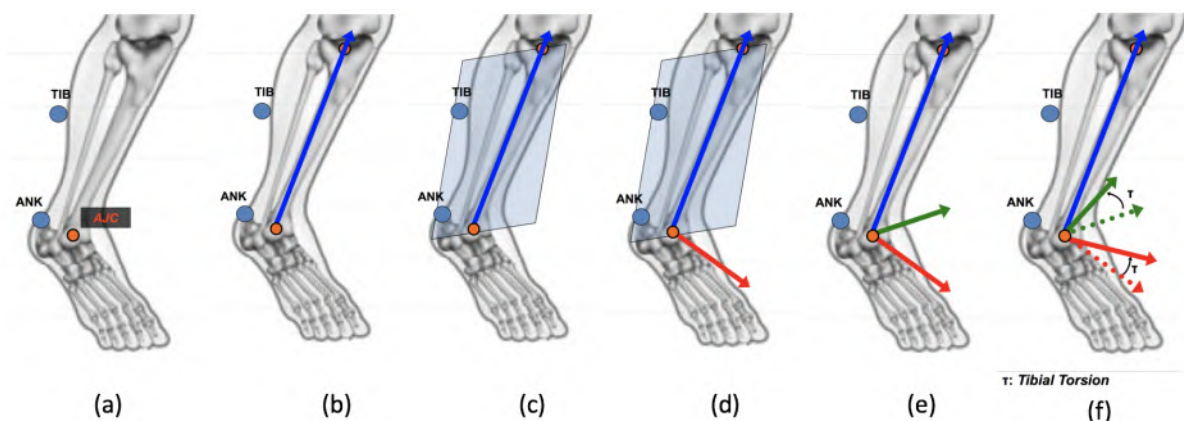


Figure II.2.10: Definition of tibia origin and axes system [4]

In the Plug-In-Gait model without medial ankle markers, the tibia is divided in 2 segments in both the static and dynamic trials. In this case, the tibial torsion is entered as a anthropometric measurement. In the case of a PiG model with medial ankle markers, the tibial torsion is not entered as subject measurement but measured during the static trial based on the ANK-MED axis. Therefore, when medial ankle markers are used, the tibia is modelled as one tortioned segment in the static trials and as an untortioned and tortioned segment in the dynamic trials. This will be explained in more detail in section II.3.1.

The Foot

On the foot segment two markers are applied: The heel marker and the toe marker (see figure II.2.11 a). The origin of the foot segment is the TOE marker and the axis Z_{Foot} is oriented from the toe marker to the ankle joint center (figure II.2.11 b). In the next step, a virtual plane is created through 3 points: $\langle TOE, AJC, KJC \rangle$ (c). The axis Y_{Foot} is defined as perpendicular to this virtual plane and pointed to the left side (d). Finally, X_{Foot} is the crossproduct of Y_{Foot} and Z_{Foot} .

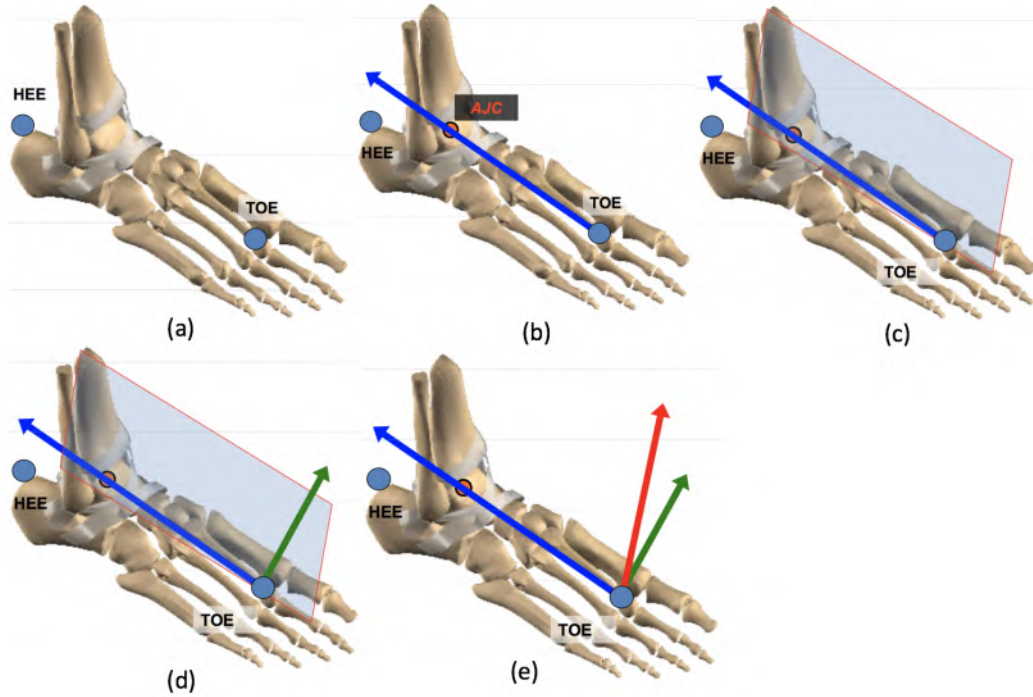


Figure II.2.11: The uncorrected definition of foot origin and axes system [4]

Unfortunately, this way of defining the axes system of the foot generates a longitudinal foot axis foot, Z_{Foot} , which is not parallel to the ground. This problem is resolved by creating a corrected reference foot system when the 'assume foot flat' option' is selected. A new virtual ankle joint center (RF) is created with the same X and Y coordinate as the original AJC but positioned at the height of the toe marker (Z coordinate) (figure II.2.12 a). For the dynamic processing it's necessary to know how the vector TOE-RF is oriented relative to the vector TOE-AJC in the static trial. The relative position of the 2 vectors is described in the static trial through 2 parameters: the static plantarflexion offset and the static rotation offset. The plantarflexion offset is the rotation of the RF-TOE relative to the AJC-TOE with respect to the medio-lateral axis of the distal tibia segment (α). The rotation offset (β) is the rotation of the RF-TOE relative to the AJC-TOE in the plane perpendicular to the longitudinal axis of the distal tibial segment (figure II.2.12 b). Thanks to the parameters α and β , the RF can also be found in the dynamic trials which allows to generate as well a corrected foot segment system in the dynamic trials [4]. The heel marker does not participate in the definition of the foot segment and is only used to calculate the rotation of the foot around its longitudinal axis [6].

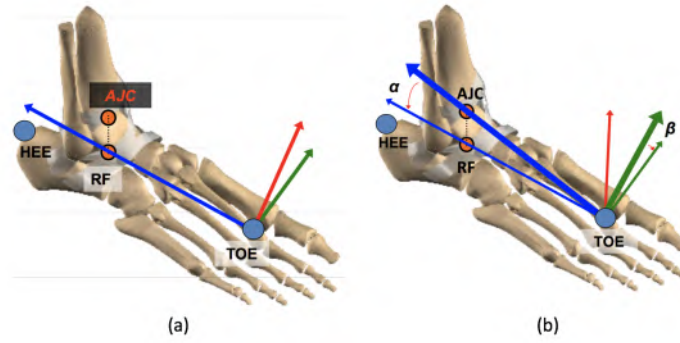


Figure II.2.12: The corrected definition of foot origin and axes system [4]

II.2.3 The joint definitions

For each joint (hip, knee and ankle), a joint center and 3 joint rotation axes are defined. The rotations axes are numbered in this report using the following convention. The first axis is allocated to the proximal segment. The second axis is associated with the distal segment and axis three is the crossproduct of the first two axes. This corresponds to the rotation sequences of the relative angles as described in the PiG Reference Guide of Vicon [5].

The Hip

The hip is the joint between the pelvis and the femur and the hip joint center is defined as explained in section II.2.2. The axes are:

- Hip1=Hip Flexion/Extension axis= Y_{Pelvis} .
- Hip2=Hip Rotation axis= Z_{Femur} .
- Hip3=Hip Abduction/Adduction axis= $Crossproduct(Hip1,Hip2)$.

The Knee

The knee is the joint between the femur and the tibia. The knee joint center (KJC) is defined as explained in section II.2.2. The knee rotation axes are:

- Knee1=Knee Flexion/Extension axis= Y_{Femur} .
- Knee2=Knee Rotation axis= Z_{Tibia} .
- Knee3=Knee Varus/Valgus axis= $Crossproduct(Knee1,Knee2)$.

The Ankle

The ankle joint is located between the tibia and foot segment. The ankle joint center (AJC) is defined as explained in section II.2.2. The ankle rotation axes are:

- Ankle1=Ankle Dorsi/Plantar Flexion axis= Y_{Tibia} .
- Ankle2=Ankle Inversion/Eversion axis= Z_{Foot} .
- Ankle3=Ankle Rotations axis= $\text{Crossproduct}(\text{Ankle1}, \text{Ankle2})$.

II.2.4 The angle definitions

The relative angles

For the calculation of the relative angles, three axes play a role: a joint rotation axis, a proximal segment axis and a distal segment axis. The 2 segment axes are projected to the plane perpendicular to the joint rotation axis. The relative angle is defined as the angle between the projections of the 2 segment axes. Table II.2.1 shows in the first 3 columns, the three axes that participate for all 9 relative angles [5]. The last column represents in which direction the angle is considered as positive. The notation of the axes is conform with how they are described in section II.2.2 and II.2.3.

Table II.2.1: Relative Angles Definition

	Rotation axis	Proximal Segment axis	Distal Segment axis	Positive
Hip Flexion/Extension	Hip1	X_Pelvis	Projection of X_Femur	Flexion
Hip Adduction/Abduction	Hip3	Projection of Z_Pelvis	Projection of Z_Femur	Adduction
Hip Rotation	Hip2	Projection of X_Pelvis	X_Femur	Internal
Knee Flexion/Extension	Knee1	X_Femur	Projection of X_Tibia	Flexion
Knee Varus/Valgus	Knee3	Projection of Z_Femur	Projection of Z_Tibia	Varus
Knee Rotation	Knee2	Projection of X_Femur	X_Tibia	Internal
Ankle Dorsi/PlantarFlexion	Ankle1	X_Tibia	Projection of Z_Foot	DorsiFlexion
Ankle Inversion/Eversion	Ankle2	Projection of Z_Tibia	X_Foot	Inversion
Ankle Rotation	Ankle3	Projection X_Tibia	Z_Foot	Internal

A small remark needs to be made about the knee and ankle angles. For the knee angles $X_{tibia,untor}$ is used and for the ankle angles $X_{tibia,tor}$ is used.

Absolute Angles

The absolute angles are between a body segment and the laboratory reference system. Both the pelvic angles and the foot angles fall under this category. As the focus in this study lays on the relative angles, the definition of the absolute angles won't be explained here. For a detailed explanation, one can consult the Vicon Plug-In-Gait Reference Guide [7].

II.2.5 Overview of the axis notations

Because the notations allocated in this section are used in the whole report, an overview of the notations of both the segment axes and joint rotations axes is shown in figure II.2.13.

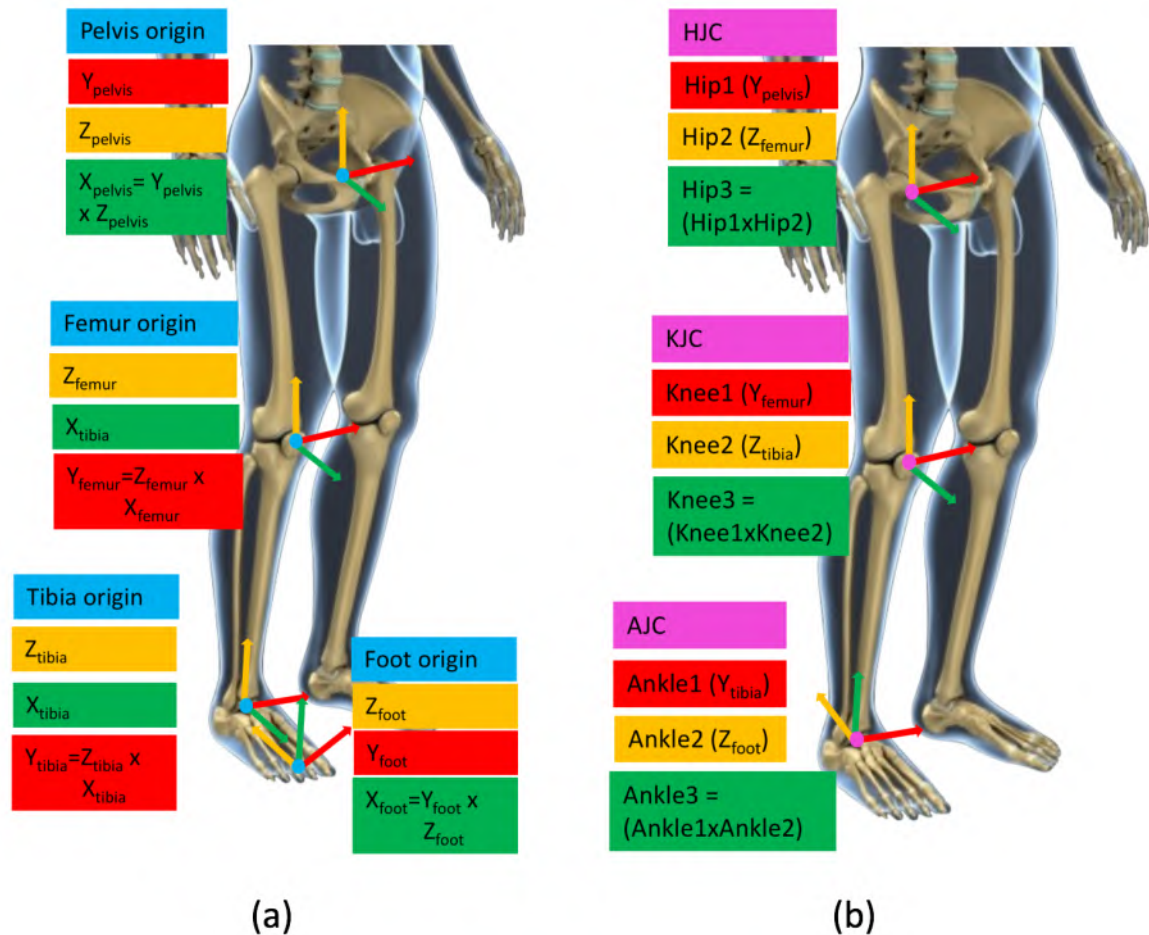


Figure II.2.13: Overview of the notations and orientations of the segment axes (a) and the joint rotation axes (b)

Figure II.2.13 (a) shows the segments origins and axes (origin in blue, Y-axis in red, Z-axis in yellow and X-axis in green). Figure II.2.13 (b) shows the joint axes systems with the joint centers in pink. The first 2 axes of every joint, are equal to a segment axis shown in (a) in the same color.

II.2.6 Limitations

The biggest strengths of the PiG model are that it is widely used and considered, validated and repeatable. However, being only repeatable is not enough to be suitable for clinical practice. It's also important that the model represents well the real movement of the

underlying bones during the gait and in this respect a number of limitations have been expressed [8].

The position of the hip joint center

Since the beginning of the PiG model there has been a concern about the true anatomical position of the hip joint center [9]. Studies have suggested both functional calibration methods and alternative predictive equations that generate a more physically correct HJC position than the currently used equations [10]. However, these alternatives are still not implemented in clinical practice [8].

The definition of the femoral coronal plane

In the original PiG model, the definition of the femoral coronal plane was highly dependent on the placement of the THI marker (as explained in section II.2.2). As this thigh marker is not placed on an anatomical landmark, the position of the thigh marker and thus as well the definition of the femoral coronal plane varies a lot between different sessions. Using the KAD leads to a more consistent but still too variable determination of the femoral coronal plane [8] .

The error that causes most of the variability is the orientation of the knee axis in the transverse plane due to non optimal KAD and lateral knee marker placement and skin movement during the process. A non consistent determination of the femoral coronal plane between multiple sessions results thus in a high intersession variability of the hip rotation angle. In the currently used PiG the intersession repeatability of the hip rotation angle is still felt by clinical users to be too high. Suggested alternatives for the definition of the knee axis and thus the femoral coronal plane are the use of medial knee markers or functional knee calibration.

No real biomechanical model

In some ways the PiG model is no longer considered as a real biomechanical model. It is then thought of an algorithm that develops kinematic and kinetic data. The segment lengths are not constant because the segments are not defined as rigid objects. This aspect makes the PiG model incompatible with other biomechanical models that calculate for example the muscle length, muscle force,...

Soft tissue artefact

Stereophotogrammetry with skin markers is based on the idea that the skin markers are a perfect representation of the skeletal structure. Unfortunately the markers move as a rigid cluster relative to the bone structure and they also move relatively to each other. This movement of the skin relative to the bone structure is caused by skin movement,

muscle contractions, inertial effects on fat, The error arising from this undesired phenomena is called the soft tissue artefact (STA). The exact nature of the soft tissue artefact (direction of relative movement, effect on the kinematic output,..) is highly dependent on the subject and the task that is executed [11].

Subjects having a gait disorder are particularly prone to weight gain. Additional abdominal fat is then present on the pelvis and creates difficulty in palpation and correct location of the markers. It also leads to more soft tissue artefact of the pelvis markers. The currently used PiG model does not address this problem.

The foot segment model

The foot is modelled as one segment, which is an oversimplification of the real foot. Alternatives such as the Oxford foot model have been developed but are not routinely utilised in clinical practice [12].

II.3 CGM2: An alternative model

The overall idea of the CGM2.i project is to "develop a model that preserves the strengths of the original model while addressing its weaknesses" [13]. A detailed overview of the CGM2.i project can be found on it's website [14].

The aim of the CGM2.i project is to develop a standardized biomechanical model for application in clinical services. The CGM2.i model is not designed for research centers where specific cases are investigated. The model needs to be both biomechanically rigorous and simple to make it practical to use in clinical setting [15].

The Python code for the CGM2 is implemented as a Nexus plug-in modele, supported by Vicon and developed by a team of the University of Salford in cooperation with the Royal Children's Hospital in Melbourne. It is available at GitHub [14]. The CGM2.i model consists of different submodels, each focusing on one specific limitation of the original model. Each model consists of the previous submodel with one specific adaption added. This allows investigation of the impact of each individual adaption on the kinematic and kinetic output.

In what follows in this section all the submodels, from CGM1.0 up to CGM2.6, are described. There will be only focused on the lower body models of the CGM2 project, not on the full body models. What is different from the previous submodel, the marker placement, joint axes and centers definitions, ... are explained per submodel. The last 3 submodels are mentioned but won't be discussed in detail as this master dissertation only focuses on the models up to CGM2.3.

II.3.1 CGM1.0

The CGM1.0 model is a clone in Python of the PiG model. On the one hand this is created to give the users the opportunity to get used to the Python operations. On the other hand, this also forms the base for the subsequent models wherein specific adaptations will be implemented in order to improve the original model. The user can check whether the CGM1.0 gives the same output as the PiG model.

As different variations on the Plug-In-Gait model exist, it's necessary to have a more critical look on the CGM1.0 model to evaluate which variation is 'cloned'. In this study, 2 variations of the PiG model are of interest: 'The PiG with KAD' and 'The PiG with KAD and medial ankle markers' [16].

The Plug-In-Gait with KAD and medial ankle markers

The KAD is a device applied to the medial and lateral epicondyles of the femur that determines the femur coronal plane. During the static trial, besides the KAD on the knee, also markers are placed on both the medial and lateral malleolus. This allows determination of the tibia coronal plane in the same way the KAD determines the femoral coronal plane. Knowing those two coronal segment planes allows calculation of the tibial torsion (the angle between the knee flexion-extension axis and the ankle dorsi-plantar axis) in the static trial. After the static trial the KAD and the medial malleolar marker can be removed.

During the dynamic processing the tibia segment is divided into 2 segments: a proximal untortioned segment and a distal tortioned segment [16]. The distal and tortioned segment is aligned with the trans-malleolar axis and is used to calculate ankle angles. The proximal and untortioned segment is aligned with the femur and used for the knee angle calculations. The untortioned tibia is obtained by rotating tortioned tibia around its vertical Z axis by the negative of the tibial torsion [17] (Fig. II.3.1).

This division of the tibial segment in the dynamic trials results in knee rotation angles fluctuating around zero. However, in the static trial, the tibia consists of only one tortioned segment and the knee rotation equals thus the value of the tibial torsion.

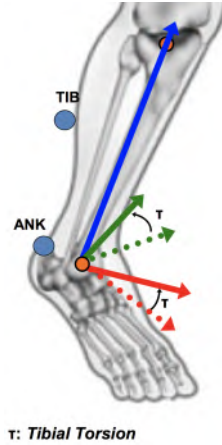


Figure II.3.1: Difference between tortioned and untortioned tibia [4]

The Plug-In-Gait with KAD and without medial ankle markers

In this variation of the PiG model, no medial ankle markers are applied. This means that the tibial torsion value can't be calculated in the static trials and needs to be entered as a subject measurement. The way of determining the AJC, the tortioned tibia and the untortioned tibia in this case, is already explained in section II.2.2. This results in some important differences compared to the PiG model with medial ankle markers.

- In the static trial, the PiG without medial markers models the tibia as 2 segments and but when medial markers are applied, the tibia consists of only one tortioned segment in the static trial. This leads to a knee rotation angle around zero in the 'PiG without medial markers', where this is around the tibial torsion value in the case with the medial ankle markers.
- In the dynamic trials, the tortioned and untortioned tibia are rotated by an angle τ relative to each other. However in theory, the tibial torsion value is the same in both the PiG with or without medial marker, this is not true in practice. Because the tibial torsion is a subject measurement in one method and a calculated value based on the position of the ankle markers on the other method, there is a difference between them. This error in the tibial torsion values, leads to differences in the tibia coronal planes and the determination of the AJC in the dynamic trials.

The CGM1.0 model is a clone of the 'Plug-In-Gait model with KAD and with medial markers' [16]. Dependent on what variation of the PiG model is used to compare with, it is possible that the results contain slight differences. When the 'PiG-KAD-without medial ankle markers' is used, the dynamic output will be the same but the static knee rotations angles and the tibial segment coordinate system will differ. Moreover, the definition of the tibial coronal plane and thus the position of the ankle joint center will differ as well.

The CGM1.0 model can be executed using the KAD or using a medial knee marker fulfilling the same role as the KAD.

II.3.2 CGM1.1

The CGM1.1 model addresses 3 weaknesses of the Plug-In-Gait model. The 3 adaptations are made in order to clarify the clinical interpretation of the kinematic and kinetic output, while preserving the base of the original model. The adaptations implemented in the CGM1.1 model relate to: (1) the Cardan sequence for the pelvis kinematics, (2) the tibia coordinate system and the corresponding tibial torsion and (3) the decomposition of the joint moments [16]. The decomposition the joint moments in the PiG model is done in the distal segment coordinate system. Studies [18] and [19] state that projection of the joint moments in the joint coordinate system results in different and better clinically interpretable kinetic output. As this report focuses on the kinematics, the third adaptation in the CGM1.1 model won't be discussed in detail. The first two adaptations are discussed below.

The Cardan sequence for the pelvic kinematics

The pelvic rotation sequence determines the rotation axes: The first rotation corresponds to an axis of the laboratory coordinate system, the third rotation is around an axis of the pelvic coordinate system and the second rotation is about the axis perpendicular to the first and the third rotations axis. In the conventional Plug-In-Gait model the rotation sequence of the pelvic angles is: Tilt-Obliquity-Rotation [20]. This implies that the pelvic tilt in the PiG model is the rotation of the pelvis around the transversal axis of the laboratory. However, the clinical interpretation of the pelvic tilt is the rotation around the transversal or medio-lateral axis of the pelvis itself. In order to have a pelvic tilt corresponding to the clinical definition, the pelvic tilt needs to be in third position in the rotation sequence. Therefore, the original sequence is replaced by Rotation-Obliquity-Tilt in the CGM1.1 model [16]. It needs to be noted that as a consequence the pelvic rotation in the CGM1.1 is around the vertical axis of the laboratory and not around the vertical axis of the pelvis as in the PiG model.

It's clear that the Rotation-Obliquity-Tilt sequence is in agreement with the clinical definition of the pelvic tilt but the effect of the change in rotation sequence on the kinematic output needs to be investigated. Studies showed that the effect on a normative database is minimal but that the change in rotation sequence induces a larger change in pathological subjects with a large pelvic obliquity and rotation [21] [16].

Tibial torsion and the definition of the tibial segment

As explained in section II.3.1, in the CGM1.0 model the tibial torsion is calculated in the static trial with the aid of the medial ankle marker and the KAD or medial knee marker. Based on this static tibial torsion, the tibia segment is divided in a untorted and a tortioned segment during the dynamic processing. This results in knee rotation angles oscillating around zero instead of around the tibial torsion value. This can be a cause of clinical misinterpretation as the tibial torsion is subtracted from the real knee rotation over the whole gait cycle in the dynamic kinematic output. This clinical misinterpretation needs to be avoided because large tibial torsion is a common phenomena in pathological patients. Therefore, in the CGM1.1 model, the tibial segment is modelled as one tortioned segment, resulting in a knee rotation output that equals the real knee rotation of the subject (tibial torsion included) in both the static and dynamic trials. [16].

The use of only one tibia segment also has a small influence on the ankle inversion/eversion and ankle rotation angles [16]. As explained in section II.2.2 the Plug-In-Gait model creates a corrected static foot reference system when the 'assume foot flat' option is selected. This foot reference system is created in the static trial but can be created again in the following dynamic trials thanks to the 2 stored parameters: plantarflexion offset α and rotation offset β . The plantarflexion offset is the rotation of the RF-TOE relative to the AJC-TOE with respect to the medio-lateral axis of the distal tibia segment (α). The rotation offset (β) is the rotation of the RF-TOE relative to the AJC-TOE in the plane perpendicular to the longitudinal axis of the distal tibial segment (see figure II.3.2).

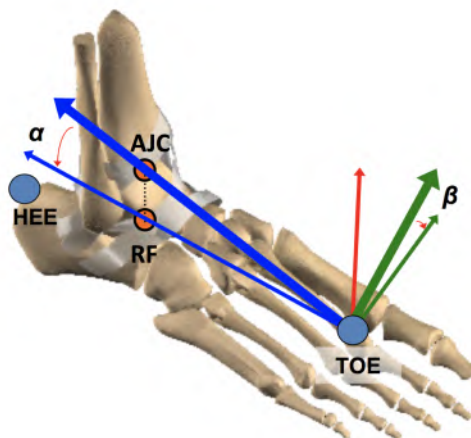


Figure II.3.2: Static plantarflexion offset α and static rotation offset β [4]

In the 'The Plug-In-Gait with KAD and medial ankle markers' a processing error is present: The static plantarflexion offset and the static rotation offset are calculated with respect to the axis system of the proximal tibial segment instead of the distal tibial segment [16]. The proximal tibia is obtained by rotating the distal tibia around its

longitudinal axis by the negative value of tibial torsion. As a result, the longitudinal axis of the proximal and distal segment are the same leading to no error in the static rotation offset. However, the the medio-lateral axis of the proximal and distal segment differ. The resulting error in the static plantarflexion offset leads to a small error in the ankle inversion/eversion angles and the ankle rotation angles. As the CGM1.0 is a clone of the 'The Plug-In-Gait with KAD and medial ankle markers', this error is also present in the CGM1.0. In the CGM1.1 model on the other hand, the tibia is modelled as only one segment thus the error in the ankle inversion/eversion and rotation kinematics is no longer present.

II.3.3 CGM2.1

Multiple studies state that the Plug-In-Gait model generates the hip joint center in a wrong position and propose alternatives to find the physical correct hip joint center [22] [9] [23]. Other regression equations and functional calibration are frequently suggested alternatives. Functional calibration has been shown to be a better way of estimating the HJC than the currently used regression equations. However, Sangeux et al. demonstrated that alternative regression equations can perform almost as well as the functional calibration methods [10].

Many patients experience difficulties executing the required functional exercise due to the effects of their pathology. A regression equation that estimates the hip joint center as accurate as the functional calibration methods is thus highly desirable. Moreover, the CGM2.i project develops a model for the application in clinical services. A regression equation is more suited for this design criteria than a functional calibration.

Hara et al. performed a study on alternative regression equations [24][25]. Multiple regression equations using different predictors (inter ASIS distance, leg length, pelvic depth,..) and taking into account sex and age, are compared on 157 subjects in the study. The resulting regression equation estimates the HJC with a similar accuracy as the functional calibration methods and regression equation investigated in the study of Sangeux et al. [10][25]. The only predictor used in the final equation of Hara et al. is the leg length. This is advantageous compared to the other regression equations as the leg length is easy to measure in clinical practice and less sensitive to the marker placement. The Hara et al. regression equations are a better estimation of the hip joint center than the regression equations in the PiG model, but there is a lot of discussion about the effect on the kinematic and kinetic output. Furthermore, the selection criteria of the study of Hara et al. is that subjects with affected musculoskeletal structure (due to trauma, growing disorder,..) must be excluded. The resulting regression equations are thus only valid for subjects whose leg length is in balance with the overall anatomy of the subject.

In the CGM2.1 model the original regression equations for the hip joint center are replaced by the Hara et al. regression equations. As the regression equations are only valid for subjects with unexceptional leg length, this forms a drawback of the CGM2.1 model. The Hara et al. regression equations implemented in the CGM2.1 model are [24]:

$$HJC_x = 11 - 0.063 * LL \quad (II.4)$$

$$HJC_y = 8 + 0.086 * LL \quad (II.5)$$

$$HJC_z = -9 - 0.078 * LL \quad (II.6)$$

LL stands for leg length and is expressed in mm. The hip joint centers are calculated in the pelvic coordinate system which is defined identically to the Plug-In-Gait model. A positive X-, Y- and Z-coordinate represent respectively a HJC anterior, lateral and superior to the pelvic origin. This sign convention is the same as for the regression equations in the Plug-In-Gait model as described in section II.2.3.

II.3.4 CGM2.2

The Plug-In-Gait model is based on the rigid body hypothesis, defining the rigid body segments individually for each time frame. The method used to calculate the position of the rigid segments is called the 'Direct Method'. At least 3 markers are placed on each segment, from which 2 vectors can be formed. These 2 vectors and its cross-product form the segment reference frame. The direct method calculates these 3 vectors for each time frame in order to find the segment position. [26] [27]

The calculated vectors and the corresponding determination of the position the body segment are prone to the skin movement. Moreover, there is no joint constraint between the different segments, which can lead to mismatch (overlay, gap, translation,...) at the joints.

In the CGM2.2 model a method dealing with the soft tissue artefact is implemented to define the body segment positions: The 'Inverse Kinematics' or the 'Kinematic Fitting'. The inverse kinematics is implemented by exploiting the 'Open Sim Inverse Kinematics Solver' [28] [29]. During the static trial, a segment model is created based on the physical and virtual markers. This segment model is a chain in which each body segment represents a rigid link connected through ball-in-socket joint constraints. The model anatomy, joint positions and axes orientations in the static trial are the same in the CGM21 and CGM22 model.

During dynamic processing, the best fit between the segment model and the measured markers is searched for each time frame. This is done by minimizing the weighted root mean square distance between modelled markers and the measured markers [30]. As for the lower body, all markers are of same importance, the same weight is given to all the markers in the CGM2.2 model.

A visualization of the basic idea of inverse kinematics is shown in figures II.3.3 and II.3.4. The pink markers represent the modelled markers fixed to the segment model generated in the static trial. The blue markers are the measured markers during the dynamic trial (Fig.II.3.3). For different positions of the segment model, the weighted cost function based on the distance between the modelled and the measured markers is calculated. The position of the segment model with the minimal cost function, is the best fit for that individual time frame (position B in figure II.3.4).

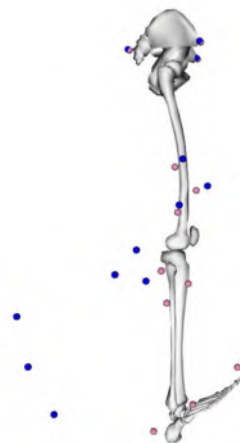


Figure II.3.3: Illustration of Inverse Kinematics: Modelled and measured markers [31]

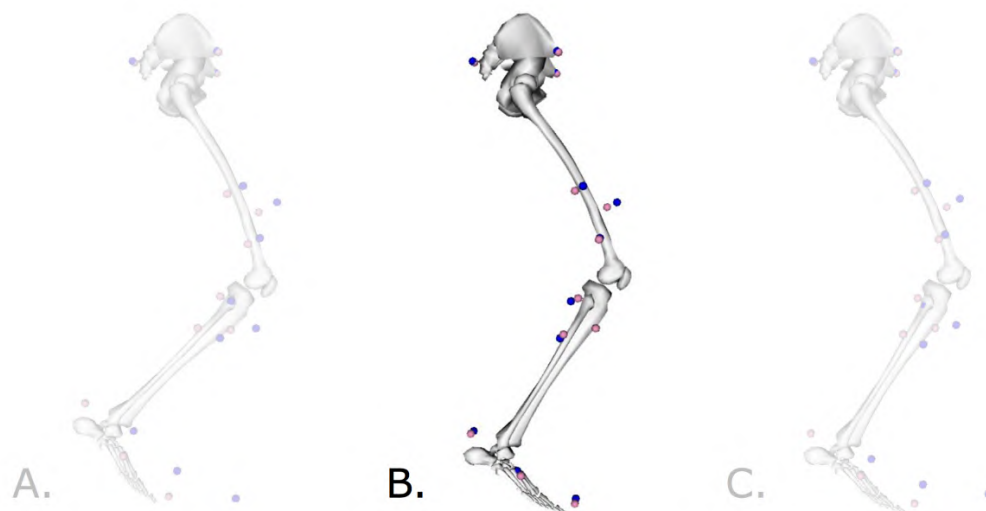


Figure II.3.4: Illustration of Inverse Kinematics: Searching best fit [31]

The different body segments are connected through ball-in-socket joint constraints and

the minimizing of the cost function is done for the whole model at the same time and not for each segment sequentially. This resolves the problem of the segment mismatches at the joints [26]. Through inverse kinematics, each segment preserves its constant length during the dynamic trials. This makes CGM2.2, in contrary with the PiG model, compatible with other biomechanical models for calculation of muscle length, muscle force estimation,... [30]. One study [27] states that replacing the direct method by the inverse kinematics only has a small influence on the kinematic and kinetic output. This needs to be confirmed by more studies using more varied and larger subject groups. If the impact on the kinematic and kinetic output is indeed small, there inverse kinematics can be implemented in clinical routine.

The major drawback of the OpenSim Inverse Kinematics solver is that it doesn't generate directly the joint angles corresponding to the minimal cost function. The intermediate steps such as generating axes, joint centers and segment origins in the dynamic trials, are not part of the OpenSim IK solver output. The CGM2.2 segments and joint centers are thus not known using the the OpenSim IK solver.

II.3.5 CGM2.3

At the beginning, it was necessary to use wand markers at the thigh and shank segment because with small number of low resolution cameras, a rotation of the thigh or shank segment could cover a normal skin marker for the cameras. As nowadays in clinical practice much more cameras with a better resolution are used, it's not necessary anymore to use wand markers. Furthermore, the wand markers have inertia and appear to wobble in the anterior-posterior direction at the initial contact. It is thus desired to eliminate the use of wand markers [32].

In the CGM2.3 model, the lateral thigh and shank wand markers are replaced by a non rigid cluster of 3 skin mounted markers. The position of the markers is chosen in order to reduce the soft tissue artefact. However, it is not as straightforward as it seems to identify the positions more resistant to soft tissue artefact. As already mentioned in section II.2.6, the precise nature of the soft tissue artefact is highly dependent on the subject and the performed task. A few general conclusions about the STA are of interest in this study and are listed below [11].

- The knee region, including the lateral and medial knee markers, are highly prone to soft tissue artefact.[33]
- The medial and lateral malleolus markers are not very sensitive to STA. [33]
- Markers on the anterior tibia (on the shin) experience only a very little effect of soft tissue artefact. [33]

- Many qualitative studies conclude that the tibia is less prone to soft tissue artefacts than the pelvis and the femur. [11]

The Femur

At the femur, the lateral thigh wand marker is replaced by the following 3 skin mounted markers [32]:

1. THAP: A proximal anterior thigh marker, about on third of the knee-hip distance at the anterior side of the thigh.
2. THAD: A distal anterior thigh marker, about two third of the knee-hip distance at the anterior side of the thigh.
3. THI: A lateral thigh marker in the middle between the hip and knee at the lateral side of the thigh.

In general, the femur is more prone to soft tissue artefacts than the tibia. No exact location on the femur is demonstrated to be less prone to STA, which complicates the choice of marker positions. On the website of the CGM2.i project, a study of Cockcroft et al. is used to justify the femur marker positions in the CGM2.3 model. Cockcroft et al. compared the soft tissue artefact of a distal lateral thigh marker and a proximal lateral thigh marker [34]. The movement of the markers relative to the underlying bone segment is the comparable for the distal and proximal marker. Yet, a proximal lateral thigh marker is less prone to soft tissue artefact as the skin-bone movement of the proximal marker affects less the knee axis alignment and position.

Firstly, the study was executed using lateral thigh markers and not using anterior thigh markers. Secondly, the height of the lateral thigh marker in the CGM2.2 model and the CGM2.3 model is the same (in the middle between the knee and the hip). Therefore, the study of Cockcroft et al. does not explain the choice of the THAP, THAD and THI marker in the CGM2.3 model.

The other markers on the femur segment, which are present in both the CGM2.2 and the CGM2.3 model, are (1) the lateral knee marker, used as a tracking marker for the inverse kinematics process in the dynamic trials, and (2) the medial knee marker, which is only used for calibration.

The Tibia

The lateral tibial wand marker is replaced by the following 3 skin mounted markers [32]:

1. TIAP: A proximal anterior tibia marker, positioned just below the tuberosity.
2. TIAD: A middle anterior tibia marker, in the middle between the knee and the ankle at the anterior aspect.
3. TIB: A lateral tibia marker in the half-way between the knee and the ankle.

In contrast with the femur, on the tibia there are some positions which have shown to exhibit only small amounts of soft tissue artefact. Peters et al. showed that the TIAP, TIAD, ANK and MED markers are rigid relative to each other during gait [33]. This indicates a low effect of soft tissue artefact on the markers and hence explains the choice of the anterior tibial markers TIAD and TIAP. The skin mounted lateral thigh marker is preserved to keep the process backwards compatible with the PiG model. Furthermore, the lateral ankle marker and the medial ankle marker are both present in the CGM2.2 and CGM2.3 model. The lateral ankle marker, ANK, is used as tracking marker in the inverse kinematics process and the medial ankle marker, MED, is only used for calibration during the static trial.

The CGM2.3 model is designed to be less prone to soft tissue artefacts than the CGM2.2 model. Firstly, the wand markers are eliminated. Secondly, one marker is replaced by 3 markers on positions less prone to soft tissue artefact (at least for the tibia). In that way, the process of the inverse kinematics, is less dependent on for example the lateral knee marker which is demonstrated to be very sensitive to soft tissue artefact.

The marker sets of the CGM1.0, CGM1.1, CGM2.1 and the CGM2.2 are the same apart from one point: in the CGM1.0 and CGM1.1 model one can choose to use the KAD for calibration or the lateral and medial knee marker for calibration. In the dynamic trials the marker sets are exactly the same for the four models (figure II.3.5 a). The marker set of the CGM2.3 is different and shown in figure II.3.5 b.

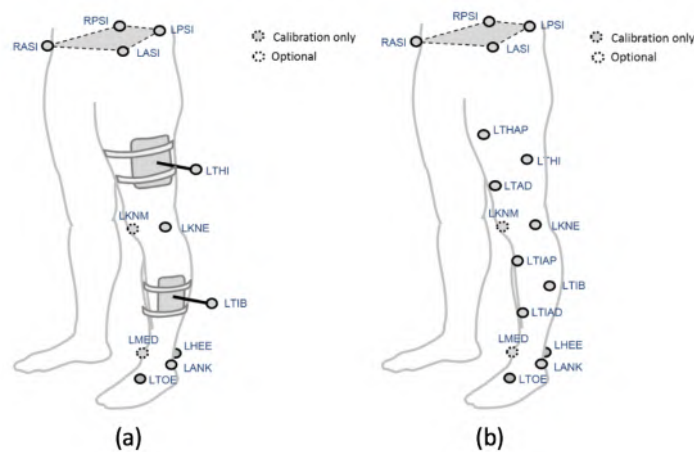


Figure II.3.5: The marker set of the CGM1.0/CGM1.1/CGM2.1/CGM2.2 model (a) and of the CGM2.3 model (b) [32]

II.3.6 CGM2.4, CGM2.5 and CGM2.6

As the CGM2.4, CGM2.5 and CGM2.6 won't be investigated in this study and the development of these model is still ongoing, no detailed theoretical background is given in this report about those three models. To give an idea what the following steps are in the development of the CGM2 model, they are listed shortly below:

- In the CGM2.4 model, the foot is modelled as two segments: a hindfoot segment, which is similar to the CGM1 foot model and a forefoot segment which is a modification of the Oxford Foot Model [6].
- In the CGM2.5 model the upper body is modelled as well.
- The CGM2.6 model implements a functional calibration of the knee axis [35].

II.4 Research question

The aim of this study is to answer the question: 'Does the CGM2.i model form a suitable alternative for the PiG model in clinical service?' The question is answered especially focusing on the application of the CGM2.i model in the gait analysis lab of the University Hospital in Ghent. The CGM2.i models that are investigated as alternative for the PiG model with KAD and without medial ankle marker in this study are the CGM1.0Kad, CGM1.0Med, CGM1.1Kad, CGM1.1Med, CGM2.1, CGM2.2 and CGM2.3 model. The question is addressed using unimpaired subjects as a precursor to evaluate the model's performance on patients.

The specific questions addressed in this study are:

- Are the underlying segment definitions and kinematic output of the processed experimental data in line with what is expected from the theory behind each model?
- Does the comparison of the intersession repeatability of the eight models reveal a model showing the best intersession repeatability?
- Does the comparison of the intrasession repeatability of the eight models reveal a model showing the best intrasession repeatability?
- What are the magnitudes of the minimal detectable changes and standard error measurements of the eight models?
- Which of the eight models is least susceptible to knee axis misalignment?
- Which of the eight models is least prone to soft tissue artefact?

The aim of this study is to provide an objective investigation of the CGM2.i project based on data collected at the University Hospital in Ghent. In reviewing the literature in this area, one can see that the majority is written by the same group of scientists (R.Baker, M.Sangeux, F.Lebeouf, etc.). These same scientists are developing the CGM2.i model. An independent study investigating the clinical value of the CGM2.i project is thus desired.

Chapter III

Data analysis: Materials and Methodology

III.1 Participants

Two healthy subjects (subject 1: female, 65kg, 176 cm, 22 years and subject 2: male, 77kg, 185cm, 22 years) without gait disorder participated voluntarily to the study. The data of both subjects, walking at self selected speed, is collected during 3 sessions with about one week between consecutive sessions. In all sessions and for both subjects, the same trained gait analyst carried out the marker placement and the anthropometric measurements.

III.2 Instrumentation

The trajectories of the retro-reflective markers are captured by a system of 24 calibrated infrared cameras with a frequency of 100Hz. The data capturing and processing is executed by the VICON Nexus 2.8.1 system. The PiG model is processed through the 'PlugInGait LowerBody Ai Functional VST' work flow. For the processing of the CGM2.i model the package pyCGM2, version 3.0.8 (available at GitHub (15/01/2019) [14]) is used. The gait analysis is performed in the gait analysis lab of the Cerebral Palsy Reference Centre, University Hospital Ghent.

III.3 Data Collection and Processing

The data of 2 subjects is collected in 3 sessions. Each session consists of a static trial with the knee alignment device and medial ankle marker applied, a static trial with the lateral and medial knee marker and medial ankle marker applied and 10 dynamic trials. The marker placement of the static trial with KAD (a), the static trial with two knee markers

(b) and the 10 dynamic trials (c) is shown in figure III.3.1. The same anthropometric measurements are used for the three sessions.

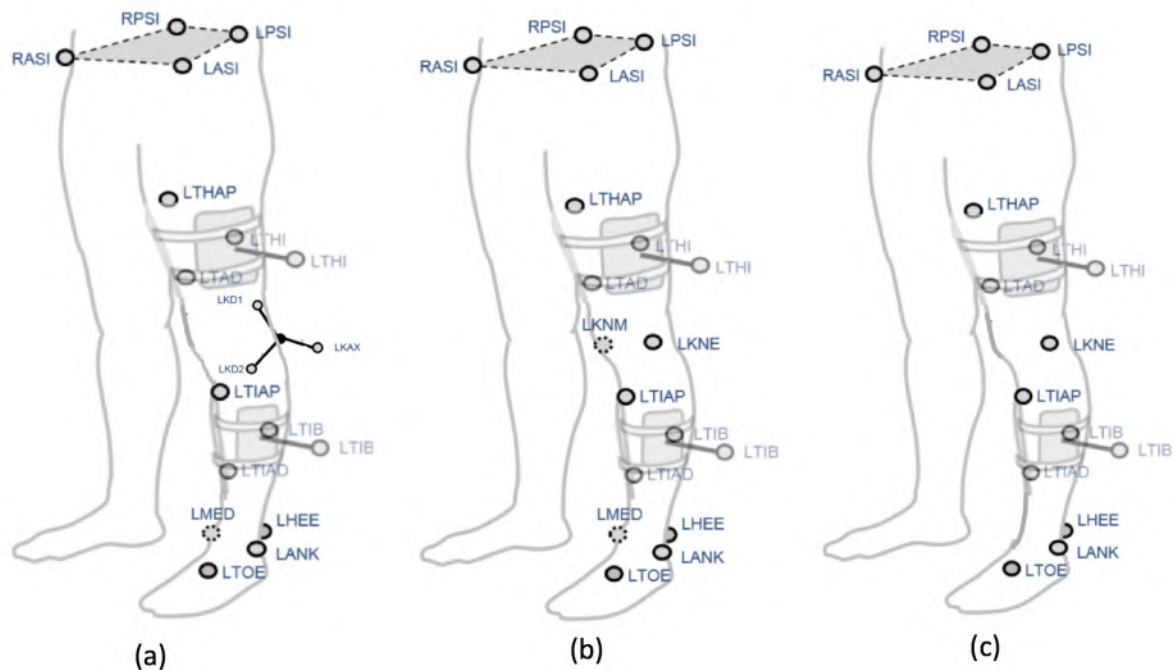


Figure III.3.1: The marker placement in the static trial with KAD (a), in the static trial with the lateral and medial knee marker (b) and in the dynamic trials (c)

The collected data is processed through 8 models: the CGM10Kad, CGM10Med, CGM11Kad, CGM11Med, CGM21, CGM22, CGM23 and PiG model. Per model, the appropriate static trial (the static trial with the KAD for the PiG, CGM10Kad and CGM11Kad model and the static trial with the two knee markers for the other five models) and all 10 dynamic trials are processed. For each model, the necessary markers are selected and the other markers are not taken into account. In this way, the exact same dynamic trials are processed through all eight models. Therefore, the difference in output is only related to the different processing of the models and not due to biological variability.

The aim of the study is to determine whether the CGM2.i model could form an appropriate alternative for the PiG model for clinical application. In order to answer this question, the dataset described above is analyzed focusing on 3 pillars: the pairwise comparison of the models, the repeatability and how well the models represent the real gait.

III.4 Data Analysis: Pairwise comparison of the models

In order to decide which model is best for clinical practice, it's necessary to fully understand how the models differ from each other in terms of processing and kinematic output. A good comprehension of the model is the basis for a correct interpretation of the model output. The CGM10Kad model is a clone of the 'VICON PiG model with medial ankle markers' and forms the basis for all the other models of the CGM2.i project. Each CGM2.i model is similar to another model but with one specific adaptation implemented. This structure of the CGM2.i project, allows comparison of the models in a pairwise manner. The pairs of models that are formed in this study and their corresponding theoretical difference, are listed below:

- **CGM10Kad & PiG** In the PiG the medial ankle markers are not applied and the CGM10Kad model is a clone of the PiG model but with medial ankle markers. In fact, the medial ankle markers can also be applied in the PiG model and then the malleolar axis is estimated in the same way in both models. Unfortunately, this is not the case in the dataset used in this study.
- **CGM11Kad & CGM10Kad** The CGM11Kad and CGM10Kad model differ in terms of rotation sequence of the pelvis angles and the definition of the tibia segment.
- **CGM11Kad & CGM11Med** Both models are the same except from the knee alignment method.
- **CGM21 & CGM11Med** Both models use different hip joint center locations.
- **CGM22 & CGM21** The CGM21 model uses the direct method whilst the CGM22 model uses inverse kinematics methods.
- **CGM23 & CGM22** The wand markers of the CGM22model are replaced by a non rigid cluster of 3 skin markers in the CGM23 model.

In the first part, a pairwise comparison between the models is done by plotting the segments of both models on the same plot (Matlab). An analysis of the differences between the axes systems of the models is done by checking if the differences are in agreement to what one would expect from the theoretical background (sections II.2 and II.3).

In the second step, the kinematic output of one model is subtracted from the kinematic output of the other model. The resulting kinematic differences are explained based on the difference in the axes systems or the theoretical background of the models. In order to fully understand how a change in the axes systems affects the kinematic output, some basic general principles are clarified in the following part.

The effect of changes in the axes system on the kinematic output

This part explains the effect of a change in the axes systems on the kinematic output. A joint angle is determined by the rotation axis and two segments axes which are projected onto the plane perpendicular to the rotation axis. A change in the segment axes or in the rotation axis, both have a different effect on the kinematic output.

A change in the segment axes system can cause an offset in the kinematics. When one of the segment axes is rotated in the plane perpendicular to the rotations axis, this causes an angle offset. To clarify this principle, the knee flexion/extension is given as example. The knee flexion/extension angle is defined as the angle between X_{Femur} and the projection of X_{Tibia} in the plane perpendicular to axis Knee1. The plane perpendicular to Knee1 is the sagittal plane of the femur segment. When one of the two segment axes (X_{Tibia} or X_{Femur}) undergo a rotation in a sagittal plane, this will cause an offset in the knee flexion/extension angle. For example, when the X_{Tibia} is downwards rotated in the sagittal plane, this will cause a flexion (positive) offset.

It needs to be noted that not all sagittal planes are aligned (sagittal plane tibia is not the same as sagittal plane femur and so on). Despite some misalignments between the planes allocated to the body, it can be assumed that a rotation of X_{Tibia} or X_{Femur} in any sagittal plane will result in a knee flexion/extension angle offset. The misalignment between the planes has only a small influence on the kinematic offsets. So, in order to conclude that it will induce an offset, it's not necessary to know in which sagittal plane exactly the rotation is.

When the segment axes are rotated in a plane parallel or almost parallel to the rotation axis, this change in orientation has no or only little influence on this specific rotation angle.

Beside the segment axes, there can also be a difference between the 2 models in the joint rotation axes themselves. These changes don't induce an angle offset but a change in the range of motion of the kinematic output. Another effect of a different orientation of the rotation axis is that in some specific cases, it can cause crosstalk between 2 rotation angles in different directions.

In the pairwise comparison the subtraction of the kinematic outputs of both models is examined and explained. In the subtraction of the kinematics, only an angle offset can be observed and a change in ROM or crosstalk between angles remain hidden. Therefore, only the rotations of the segment axes in the plane perpendicular to the rotation axis, which cause an angle offset, are of interest in the pairwise comparison of the models. This reasoning forms the basis for the discussion of the kinematic subtraction results of the experimental data.

III.5 Data Analysis: Repeatability

An important criteria a model needs to fulfill in order to be suitable for clinical practice, is the repeatability. When the gait of a subject hasn't changed between 2 tests, the model needs to generate the same output. The capacity of a model to generate the same result in different sessions is called the intersession repeatability. How consistent the output is, looking at the different trials in the same session, is represented through the intrasession repeatability. A high intersession repeatability is important as it allows differentiation between pre- and postoperative gait, walking with or without orthoses,... A high intrasession repeatability is indispensable since it ultimately limits intersession repeatability.

For the calculation of the repeatability both absolute (expressed in degrees) and relative measurements (unitless with a value between 0 and 1) exist, each taking into account the whole gait cycle or only a summary parameter. In this study both the intersession and intrasession repeatability are calculated through three parameters. Firstly, the averaged standard deviation (ASD) is calculated which is an absolute parameter that takes into account the whole gait cycle. The second parameter is the intraclass correlation coefficient (ICC), which represents the repeatability relatively to the homogeneity of the population. The ICC is calculated for 2 kinds of summary parameters: the peak and the range of motion of each of the kinematics of each trial. For the intersession repeatability, this results in 36 (9 angles x 2 summary parameters (Peak and ROM) x 2 sides (left and right)) ICC values for each model. The intrasession repeatability is represented by 108 (36 x 3 sessions) ICC values. Finally, the standard error of measurement (SEM) and thus the minimal detectable change (MDC) of the selected summary parameters are used to reflect the repeatability and the clinical value of each method and kinematic in a clinical setting.

III.5.1 Sources of variability

The intrasession variability is the variability between the trials of the same session. Sources of intrasession variability are [36]:

- Biological variability, which refers to the variability of the subject's intrinsic gait over the different cycles. This includes among others the walking speed and stride length variability.
- Soft tissue artefact.

The intersession variability is considered as the variability between the averaged output of the sessions. All the sources of intrasession variability also play a role in the intersession repeatability but their effect is generally swamped by other larger errors. Sources, only present in the intersession variability are [36]:

- Variability in the marker placement.
- Variability in walking speed from week to week is in theory greater than within the session. The knee flexion/extension angle, the knee rotation angle and the ankle dorsi/plantar flexion angle have a positive correlation with the walking speed [37]. The varus/valgus angle on the other hand is shown to be independent of the walking speed [38].
- Inconsistent anthropometric measurements. This variability is not present in this study as the same anthropometric measurements are used for the 3 sessions.

III.5.2 Averaged standard deviation (ASD)

The averaged standard deviation is an absolute parameter representing the variability in the kinematic output, which means that the parameter is expressed in degrees. It's a frequently used method to quantify both the intersession and intrasession variability of the kinematics [39] [40] [41].

Intersession Averaged Standard Deviation

The way of calculating the intersession averaged SD is schematized in figure III.5.1. For each model (8), subject (2), side (left and right) and relative angle (9), the mean of the 10 trials per session is calculated. This results in 3 mean waveforms corresponding to the 3 sessions. Next, the mean and standard deviation of these 3 mean waveforms are calculated for each timeframe. In the last step the average standard deviation over all the timeframes of a gait cycle is calculated. The whole process results in one value per model, subject, side and angle. The larger the value, the larger variability between the mean waveforms of the three sessions. A low intersession averaged standard deviation corresponds thus with a high intersession repeatability.

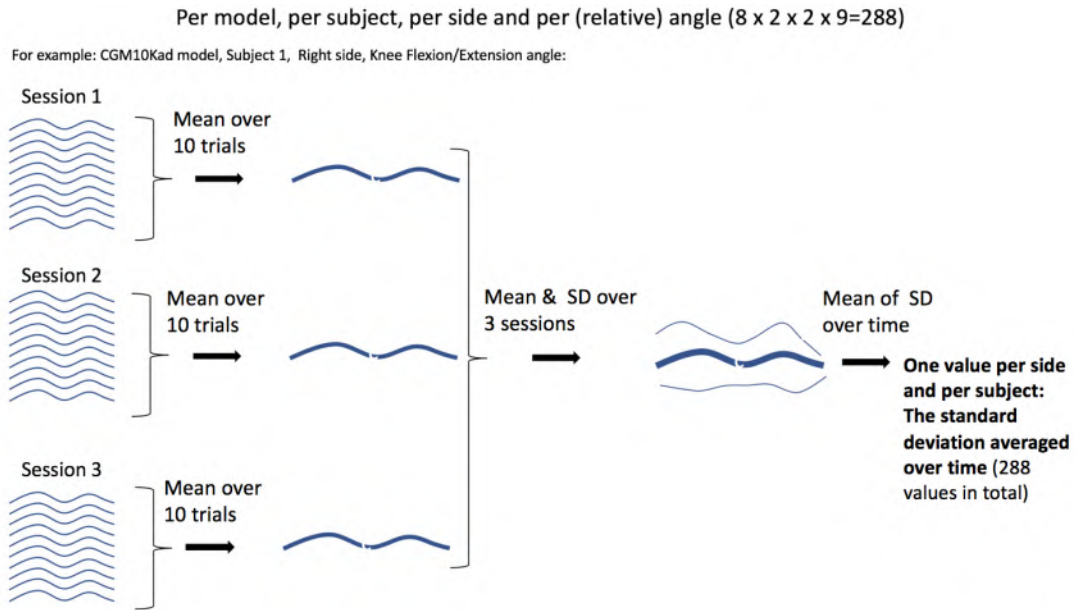


Figure III.5.1: Scheme of calculation of the intersession averaged SD

Intrasession Averaged Standard Deviation

How the intrasession averaged SD is calculated is shown in figure III.5.2. Per model (8), session (3), subject (2), side (2) and angle (9), the mean waveform and the corresponding standard deviation of the 10 trials is calculated. Next, the averaged standard variation over the gait cycle is calculated resulting in one intrasession averaged SD value. The lower the intrasession averaged SD, the lower the variability between the 10 trials of one session and thus the higher the intrasession repeatability.

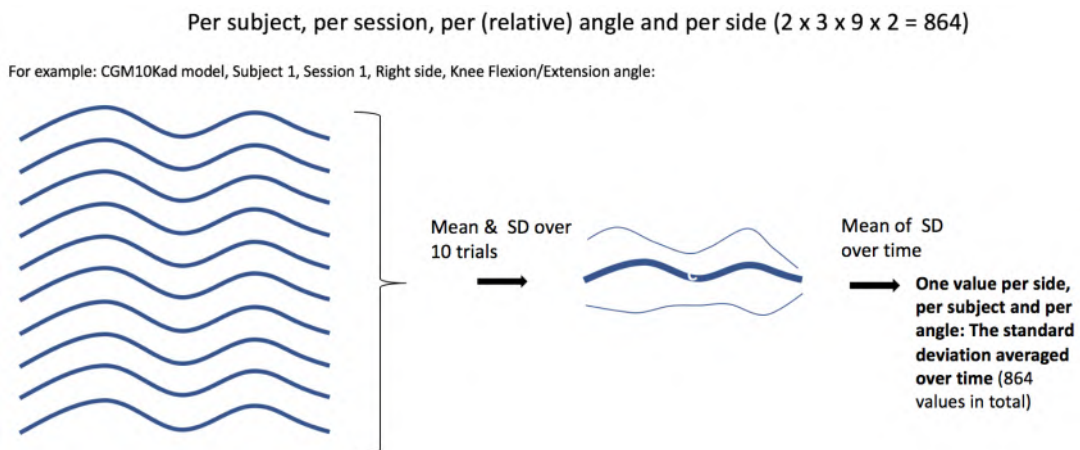


Figure III.5.2: Scheme of calculation of the intrasession averaged SD

The ASD parameter doesn't distinguish between different standard deviations at particular time moments in the gait cycle. Aside from this discussion point the averaged standard deviation provides useful insights into the repeatability.

III.5.3 Intraclass correlation coefficient (ICC)

The ICC is a relative (unitless) parameter representing how much of the total variance is due to 'error'. The ICC value lays in theory always between 0 and 1 and expresses the intersession/intrasession variability relative to the heterogeneity of the population. Although the ICC is the most common relative parameter used to express the repeatability of the model, confusion exists about where ICC values come from and how they should be interpreted. Therefore, this section provides a detailed explanation of the meaning and use of the intraclass correlation coefficient in this context.

The reliability coefficient is defined by

$$\frac{\textit{between subjects variance}}{\textit{between subjects variance} + \textit{variance due to error}} \quad (\text{III.1})$$

A value of one corresponds to no error and a value of zero indicates that the total observed variability is due to errors. A reliability coefficient of 0,95 means that an estimated 5% of the total variance is due to errors. Errors in this context are unknown sources of variability in a set of measurement data. In the ideal situation one subject has the same results over different trials/sessions and the reliability coefficient is 1. However, this is not realistic as multiple sources provoke errors between the different sessions/trials. The error sources can be typically divided into 2 types: (1) Random errors due to imprecisions, luck, alertness, ... and (2) systematic errors [42].

The intraclass correlation coefficient quantifies the reliability coefficient in equation III.1 based on the variances derived from between-subject-ANOVA. Different versions of ICC computational formulas exist, each based on different assumptions and corresponding to a different situation and interpretation. The system of McGraw and Fleiss, containing 10 different forms of the ICC, is the most recent and complete guide to correct use of ICC [43].

In this study 2 kinds of ICC's will be calculated, the intersession ICC and the intrasession ICC. Both types of ICC require the appropriate ICC formula and ANOVA.

Intersession ICC

Appropriate ANOVA

The ICC expresses the reliability of one summary parameter per gait cycle for each kinematic and does not represent the reliability across the whole gait cycle. In this study, both the range of motion and the peak value are chosen as summary parameters [44]. For the intersession ICC, the average of the summary parameters over the 10 cycles per session is calculated. This results in a matrix of 2 (subjects) x 3 (sessions) summary parameters, on which the ANOVA is executed.

The ANOVA analysis executed in Matlab outputs 3 sources of variability. The first source of variability is the variability between the subjects and MS_B is the mean square corresponding to this source of variability. The 'trial term', MS_T , corresponds to the variance due to systematic error and the 'error term', MS_E , corresponds to the variance due to random error.

Choice of ICC

The choice of the appropriate ICC addresses 4 different aspects using the system of McGraw and Fleiss : (1) a 1- or 2-way model, (2) a random- or mixed-effect model, (3) the type: are the values in the actual application a result from a single measurement or a 'mean of k measurements', and (4) the definition: consistency or absolute agreement between the measurements [45][42].

The choice between a 1-way model and a 2-way model depends on the differentiation between systematic and random errors. The study is designed in such a way that all the subjects are tested in all sessions [45], which allows to distinguish between variances due to systematic error ('trial term') and variances due to random error ('error term'). The 2-way model takes into account the difference between systematic and random errors and the 1-way model not. As the design of the study allows to differentiate between the error sources, a 2-way model is chosen. When the systematic error is small, the 1-way model ICC will have the same value as the 2-way model ICC.

With respect to choosing a random- or mixed-model in this case, the eventual generalization of the reliability results to a population of similar raters is important [45]. The aim of this repeatability study is to give an objective comparative review between the CGM2 model and the PiG model used in the gait analysis laboratory in UZ Ghent. As the majority of the actual clinical assessments are done by the same rater, the one who participated in this study, there is no need to generalize the results of this reliability study to a population of general raters. Consequently, a mixed-model is chosen.

The third aspect to address is the type, which depends on how the measurement protocol will be executed in the actual application [45]. The question if the summary parameters are based on one measurement or a mean of multiple measurements in actual practice, needs to be answered. Both in this study as in actual clinical practice, the parameters per session are an average of different cycles. Therefore the 'mean of multiple measurements' type is chosen instead of 'single measurement'.

The last choice to be made in order to obtain the appropriate ICC, is the definition of the relationship between the repeated sessions: consistency or absolute agreement? Due to the nature of this study, a repeatability study, it's evident the absolute agreement must be chosen as the repetitions are meaningless if there is no absolute agreement between them. Critically regarding these 4 aspects, the appropriate choice for the intersession

ICC in this case is the 'Two-way mixed effects model with absolute agreement and mean of multiple measurements'. The corresponding computational formula according to the system of McGraw and Fleiss is [43]:

$$ICC = \frac{MS_B - MS_E}{MS_B + (MS_T - MS_E)/n} \quad (III.2)$$

All the factors used in equation III.2 are results from the appropriate ANOVA analysis for this situation (see above). (n =number of subjects=2, MS_B = mean square for the between subject variability, MS_E = mean square for the 'error term', MS_T = mean square for the 'trial term').

Intrasession ICC

Although the reasoning for the intrasession ICC is quite similar to the one for the intersession ICC, the intrasession ICC requires another ANOVA and another ICC formula. In the case of the intrasession ICC the data exist of k (=10) trials (in the same session) collected from n (=2) subjects. The resulting 2(subjects) x 10(trials) matrix is used for the ANOVA analysis, which gives similar results but the interpretation is different.

MS_B represents the variance of all the group averages (average per subject over all his trials in one session) multiplied by the group number, $k=10$ (the number of trials). MS_T , the mean square of the 'trial term', and MS_E , the mean square of the 'error' term, correspond to the variability due to respectively the systematic and random error between the multiple trials. MS_W is the mean square of the variability of the trials within a subject.

The model (2-way mixed-effect model) and the definition (absolute agreement) are the same as for the intersession ICC. The only aspect that differs in choosing the suitable formula is the type of ICC. In actual application, each cycle consists of only one measurement. Therefore, the 'single measurement' is chosen instead of the 'mean of multiple measurements' type. According to the system of McGraw and Fleiss, the formula corresponding to the '2- way mixed-effect model with absolute agreement and single measurement' is [43]:

$$ICC = \frac{MS_B - MS_E}{MS_B + (k - 1)MS_E + k(MS_T - MS_E)/n} \quad (III.3)$$

The intraclass correlation coefficients are calculated in Matlab, using a script that gives results identical to the ones in SPSS [46]. The results consist of the ICC and its confidence interval.

Interpretation of ICC

The interpretation and comparison of multiple ICC's are complicated by several factors [42]. First of all, the value of the ICC depends on the heterogeneity of the population. Comparing 2 populations with the variability due to error but with a different MS_B

(between subject variability), the more homogeneous population will have a lower ICC value although both have the same variability due to error. This has 2 consequences.

Firstly, a low between subjects variability can mask a low variability due to measurement errors. Calculating the absolute error, such as the averaged standard deviation, in addition to the ICC is thus recommended. Secondly, only ICC's of populations with similar heterogeneity can be compared and therefore a publication of ICC values of a study is incomplete without mentioning the heterogeneity of the population.

Another factor complicating the interpretation of the ICC is that the ICC is a unitless parameter, which is more difficult to interpret intuitively than an absolute parameter, having the same dimensions as the measurements.

III.5.4 The Standard Error Measurement (SEM) and the Minimal Detectable Change (MDC)

The standard error measurement quantifies the precision with which the kinematic output can be determined in an individual test. This corresponds to the trial-to-trial noise when looking at the intrasession repeatability and the session-to-session noise in the case of the intersession repeatability. It's an absolute parameter that represents the magnitude of the noise due to measurement errors. Two frequently used formulas exist to estimate the standard error measurement in an individual test [42]. The first one, mentioned in most references is:

$$SEM = SD * \sqrt{1 - ICC} \quad (III.4)$$

As the ICC is shown to be meaningless and thus inappropriate in this study, it is excluded to use this definition for quantifying the SEM. The alternative definition is:

$$SEM = \sqrt{MS_E} \quad (III.5)$$

Using this definition makes the SEM independent of the population heterogeneity, which is highly desired.

Based on the SEM values, the minimal detectable change can be calculated. The minimal detectable change (MDC) is the difference that can be considered as a real physical change in the kinematics and not as a difference due to measurement errors between two tests. The formula for quantifying the minimal detectable change is [42]:

$$MDC = SEM * \sqrt{2} * 1,96 \quad (III.6)$$

The SEM is the measurement precision of a kinematic score on one individual test and 1,96 is the z-score corresponding to the 95% confidence interval of that score. However, the MDC doesn't talk about the kinematic output on one test, but about the detectable

difference between the scores on two tests. The scores contain the same level of uncertainty on both tests and thus the confidence intervals of both scores needs to be taken into account. $SEM * 1,96$ is multiplied by $\sqrt{2}$ to take into account the uncertainty of both scores [42]. Both the standard error measurement and the minimal detectable change are expressed in degrees.

III.6 Data Analysis: How realistically do the models represent the physical gait?

Another condition for a model in order to be suitable for clinical application, besides the repeatability, is the accuracy. The model needs to represent the physical gait as realistically as possible without errors. Possible errors are knee axis misalignment, soft tissue artefact,... The model least prone to these errors, is thus sought.

In the ideal situation the real kinematic output is known and it can be compared with the kinematics processed by the models. Unfortunately, knowing the real kinematic output requires other equipment and expertise which are not available for this study. Therefore, some other tests on the kinematic data are executed in order to estimate how realistically the eight models represent the subjects gait.

III.6.1 The crosstalk between the knee flexion/extension angle and the knee varus/valgus angle

The real knee joint functions somewhat as a hinge joint although not perfectly since the knee axis actually changes its orientation with flexion/extension [47]. The real varus/valgus angle should thus be relatively constant during normal gait. This more or less constant value is determined by the anatomy of the knee and therefore different for each subject. When there is a misalignment of the knee flexion/extension axis in the transverse plane, a physical knee flexion/extension movement is partially modelled as a varus/valgus angle. Hence, a correlation between the flexion/extension angle and the varus/valgus angle indicates a knee misalignment in the transverse plane. The model which generates the least correlation between both knee angles, is least prone to errors in the knee alignment.

Since it has not been demonstrated that the relationship between the flexion/extension and the varus/valgus angle is linear, it is more appropriate to use the Kendall's tau correlation coefficient than the Pearson's correlation coefficient.

The null hypothesis is $H_0 : \tau = 0$ and the alternative hypothesis is $H_1 : \tau \neq 0$. For each trial, the Kendall's tau value and the critical value corresponding to the 5% significance level are calculated. When the Kendall's tau exceeds the critical value, it can be said

that the correlation between the knee flexion/extension and the varus/valgus is different from zero with 95% confidence. The Kendall's tau value is then significantly different from zero in that specific trial.

Quantifying the correlation between the flexion/extension and varus/valgus angle over time for each trial is done in two ways:

- The average of the 10 Kendall's tau values per session, corresponding to the 10 trials, is calculated.
- Counting for each session how many of the 10 Kendall's tau coefficients differ significantly from zero.

III.6.2 The range of motion (ROM) of the knee varus/valgus angle

When there are no errors present, the range of motion of the varus/valgus angle is close to zero. A misalignment of the knee axis and soft tissue artefact are two types of errors that increase the ROM. The model with the lowest range of motion, is the model which is most robust for soft tissue artefact and knee alignment errors.

III.6.3 The distance between the hip joint centers

Another way of checking how realistically the model represents physical gait, is by looking at the distance between the hip joint centers. In reality, the hip joint centers are fixed to the pelvis and the distance between them thus remains constant during walking. It's expected that the CGM23 has the least variability on the HJC distance. Unfortunately, the OpenSim IK solver does not outputs the joint center positions. As the HJC of the CGM22 and CGM23 model are unknown and because it's irrelevant to compare only the first six models, this method won't be applied in this study.

Yet, it's mentioned in this report as it's recommended to execute the test, when the hip joint center positions of the CGM22 and CGM23 model would be available in any later versions. As this method is not related to the knee axis misalignment, this forms a interesting addition to the crosstalk and varus/valgus ROM calculations.

Chapter IV

Results and Discussion

IV.1 Pairwise comparison of the models

When positions and orientations of the axes are described, it's always the position/orientation of model, mentioned first in the title, relative to the second model in the title. The notations of the origins and axes in this chapter are illustrated in figure II.2.13.

IV.1.1 CGM10Kad & Plug-In-Gait

Difference in the segment axes systems

The body segment coordinate systems for both the 'CGM10 model with Kad' and the 'Plug-In-Gait model with Kad and without medial markers' are visualized in figure IV.1.1 (PiG in red and CGM10Kad in blue).

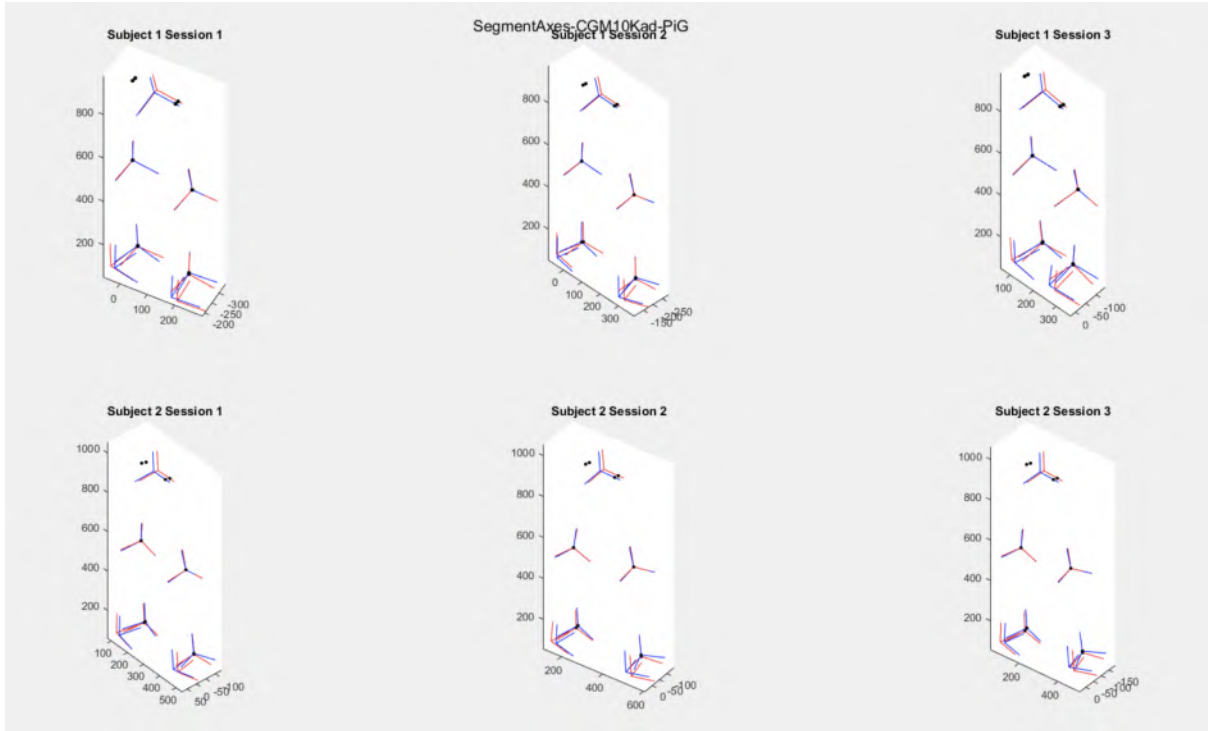


Figure IV.1.1: The segment axes systems of the PiG model (red) and the CGM10Kad model (blue) (Anterior-Superior view)

Pelvis

In all the subjects and sessions, the hip joint centers and thus the pelvis origin is positioned more anterior in the CGM10Kad (blue) than in the PiG model (red). Depending on the measurements entered in Nexus, slightly different hip models are used [5]. However, the same hip model, described in section II.2.2, should be used in all the models since the same measurements are entered in all the models. For the pelvic origin and HJC's, there is thus an unexpected discrepancy between the PiG model and it's 'clone' CGM10Kad. The mean distances between the HJC's are 14mm and 24mm for respectively the first and second subject.

The orientation of the pelvic axes on the other hand is the same for both models.

Femur

The origin of the femur is the same in both models. Relative to the axes system of the PiG model, the axes system of the CGM10Kad is rotated in the sagittal plane over about 2 degrees: X_{Femur} is tilted in the inferior direction and Z_{Femur} to the anterior side because the KJC is the same in both models and the HJC is positioned more anterior in the CGM10Kad.

Tibia

One can see in figure IV.1.1 that the tibia segment axes of the CGM10Kad model are

externally rotated in the transverse plane compared to the axes of the PiG model. This is because the tibia segment axes are defined in a different way in the 2 models. In the 'Plug-In-Gait model with KAD and without medial markers' the tibia segment axes are aligned with the femur segment axes in both the static and dynamic trials. The CGM10Kad model generates a torsioned and untorsioned tibia segment in the dynamic trials but not in the static trials (see section II.3.1). As figure IV.1.1 is based on the static trials, the torsioned tibia segment axes are shown for the CGM10Kad (blue) and for the PiG model (red) the untorsioned tibia segment axes are plotted.

There is also a small discrepancy visible between the origins of the tibial segments of the 2 models. The magnitude and direction of the differences in tibial origins vary over the sessions and subjects and are related to the definition of the ankle joint center (AJC) II.3.1.

In the 'Plug-In-Gait model with KAD and without medial markers' the tibial coronal plane is defined based knee axis and the tibial torsion value obtained from the anthropometric measurements. In the CGM10Kad model the tibial coronal plane is \langle Knee Joint Center, Medial Ankle marker, Lateral Ankle Marker \rangle . A different definition of tibial coronal plane leads to different AJC positions. The difference in AJC's varies a lot over the sessions and subjects. The mean difference in the origin positions of the tibia are 5.5mm(std=2.5mm) and 9.5mm(std=3mm) respectively for the first and second subject.

Foot

The orientation of the foot segment axes are the same but there is a difference in the origin of the foot coordinate system. The foot segment axes system of the CGM10Kad model is shifted towards the medial side compared to the PiG model (figure IV.1.2). The mean distance between the foot origins of both models are 24mm and 24.7mm for respectively the first and second subject.

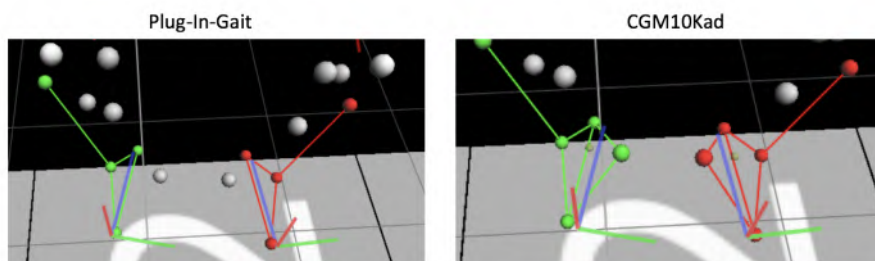


Figure IV.1.2: Comparison of foot segment position relative to HEE-TOE markers line

How do the differences in kinematics between PiG and CGM10Kad come about?

In the dynamic trials, each gait cycle is processed by the PiG and the CGM10Kad model. Afterwards for each gait cycle the PiG kinematic output is subtracted from the CGM10Kad kinematics. The difference between the 2 kinematic outputs is only due to differences in the models. Because the exact same gait cycles are used and in a pairwise manner subtracted, variation in the subjects walking is excluded. This subtraction is done for each gait cycle for all the sessions and subjects. The mean difference and the corresponding standard deviation over all the cycles is shown in figure IV.1.3. Only the relative angles (hip, knee and ankle) will be discussed.

Figure IV.1.4 presents a scheme clarifying the relationship between the kinematic offsets observed in the experimental data (Figure IV.1.3) and the observed difference in segment axes systems between the models. To understand the scheme the hip flexion/extension and the hip abduction/adduction are explained as an example.

The hip flexion/extension axis is called 'Hip1' and is perpendicular to the sagittal plane. The proximal segment axis and the distal segment axis are the segment axes that will be projected in the plane perpendicular to the rotation axis (sagittal in this case) in order to define the angles. The proximal segment axis is here the X_{Pelvis} , which is the same in both models. The distal segment axis is the X_{Femur} . As explained in section IV.1.1, the X_{Femur} of the CGM10Kad model is tilted downwards in the sagittal plane compared to the X_{Femur} of the PiG model. As mentioned in section III.4, a rotation of a segment axis in the plane perpendicular to the rotation axis (the sagittal plane) causes an offset. Because X_{Femur} is rotated downwards in the CGM10Kad, this gives the impression that there is more hip extension in the CGM10Kad model than in the PiG model. Therefore, subtracting the PiG kinematics from the CGM10Kad kinematics, results in a extension offset, which is a negative offset.

Hip 3 is the hip adduction/abduction axis, which is perpendicular to the coronal plane. The proximal segment axis, Z_{Pelvis} is the same in both models and the distal segment axis, Z_{Femur} is rotated in the sagittal plane to the anterior side when comparing the CGM10Kad to the PiG. The rotation of the distal segment axis is not in the plane perpendicular to the rotation axis (coronal) and thus it has no effect on the hip abduction/adduction angle.

The reasoning is similar for the other angles. The angles that are expected to be different in the 2 models based on the difference in axes systems, are indicated in gray in the scheme. When comparing those results to figure IV.1.3, one can see that there is a very good agreement: Hip Ab/Ad, Hip Rot, Knee Var/Val, Knee Rot, Ankle DorPla,

AnkleInvEv have a difference fluctuating around zero. The Hip Flex/Ext has a negative offset around -2 degrees and the Knee Flex/Ext has a negative offset around -3 degrees. The Ankle Rot experiences a large variability over the different cycles especially at the right side.

Conclusions

The results from the experimental data from the CGM10Kad and PiG model tend to be in agreement with those found in literature although, two additional differences were noted. An anterior/posterior shift of a few centimeters in the hip joint center position and the foot segment of the CGM10Kad model that is located medial to that of the PiG model.

Looking at the difference in kinematics during the dynamic trials, there is an extension offset in the Hip Flex/Ext (-2°) and the Knee Flex/Ext (-3°) in the CGM10Kad model compared to the PiG model. These extension offsets are due to an unexplained shift in the HJC. There differences between the 2 models in the Hip Ab/Ad, Hip Rot, Knee Var/Val, Knee Rot, Ankle DorPla and AnkleInvEv angles fluctuate around zero. The difference in Ankle Rotation differs from session to session.

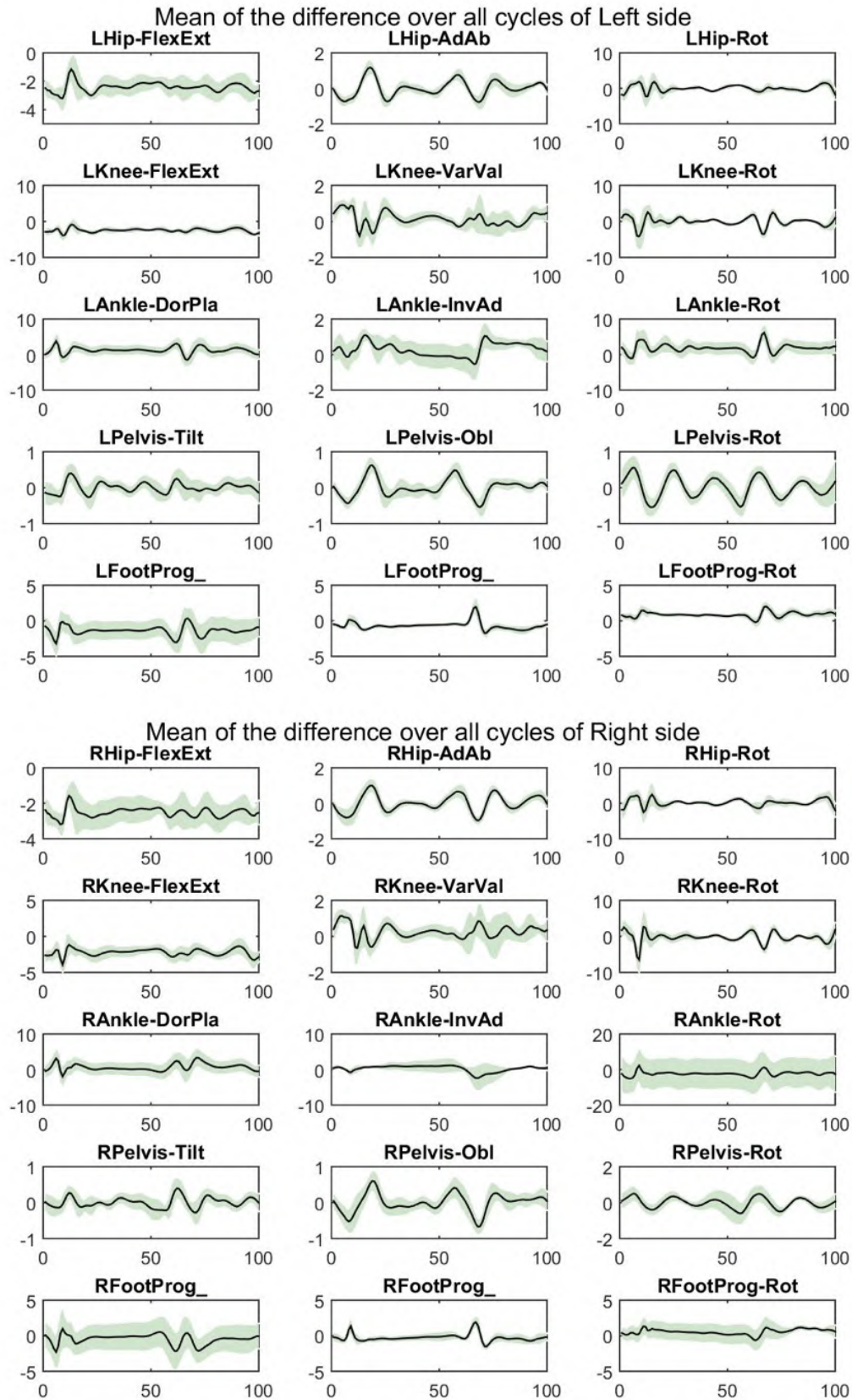


Figure IV.1.3: Subtraction of the PiG kinematics from the CGM10Kad kinematics: Mean and SD over all sessions and subjects (x-axis: % time in gait cycles, y-axis: degrees)

CGM10Kad-PiG

Angle	Joint Rotation Axis	Proximal Segment Axis	Distal Segment Axis	Effect on kinematics (CGM10Kad-PiG)
Hip Flex/Ext	Hip 1 (\perp sagittal)	\bar{X}_{Pelvis} Same	\bar{X}_{Femur} In <u>sagittal</u> plane to inferior	Extension offset (negative)
Hip Ab/Ad	Hip 3 (\perp coronal)	Z_{Pelvis} Same	Z_{Femur} In <u>sagittal</u> plane to anterior	Negligible
Hip Rot	Hip 2 (\perp transverse)	\bar{X}_{Pelvis} Same	\bar{X}_{Femur} In <u>sagittal</u> plane to inferior	Negligible
Knee Flex/Ext	Knee 1 (\perp sagittal)	\bar{X}_{Femur} In <u>sagittal</u> plane to inferior	\bar{X}_{Tibia} Static: In <u>transverse</u> plane to external Dynamic: Same	Extension offset (negative)
Knee Var/Val	Knee 3 (\perp coronal)	Z_{Femur} In <u>sagittal</u> plane to anterior	Z_{Tibia} Same	Negligible
Knee Rot	Knee 2 (\perp transverse)	\bar{X}_{Femur} In <u>sagittal</u> plane to inferior	\bar{X}_{Tibia} Static: In <u>transverse</u> plane to external Dynamic: Same	Static: External offset (neg) Dynamic: Negligible
Ankle DorPla	Ankle 1 (\perp sagittal)	\bar{X}_{Tibia} Static: In <u>transverse</u> plane to external Dynamic: Same	Y_{Foot} Same	Static: Negligible Dynamic: Negligible
Ankle InvEv	Ankle 2 (\perp coronal)	Z_{Tibia} Same	\bar{X}_{Foot} Same	Negligible
Ankle Rot	Ankle 3 (\perp transverse)	\bar{X}_{Tibia} Static: In <u>transverse</u> plane to external Dynamic: Same	Y_{Foot} Same	Large variation in offset values because the ankle rotation is dependent on the AJC position.

Figure IV.1.4: Scheme of the effect of change in axes system on kinematic data (PiG subtracted from CGM10Kad)

IV.1.2 CGM11Kad & CGM10Kad

As explained in section II.3.1 and II.3.2, there are two important differences between CGM11Kad and CGM10Kad. Firstly, the rotation sequence of the pelvic angles is Rotation-Obliquity-Tilt in the CGM11 model instead of Tilt-Obliquity-Rotation in the CGM10 model. This can have an influence on the pelvic kinematics but not on the segment axes system in the static trial. Secondly, in the dynamic trials the tibia is modelled as an untortioned and tortioned tibia in the CGM10 model and in the CGM11 model the tibia consists of only one (tortioned) segment. This induces no change in the axes systems of the static trial but only a twofold difference in the kinematic output of the dynamic trials: (1) ankle inversion/eversion and rotation error and (2) an offset in the knee rotation.

Difference in the segment axes systems

Figure IV.1.5 shows the segment axes systems of the CGM11Kad model (blue) and the CGM10Kad model (red) in the static trial.

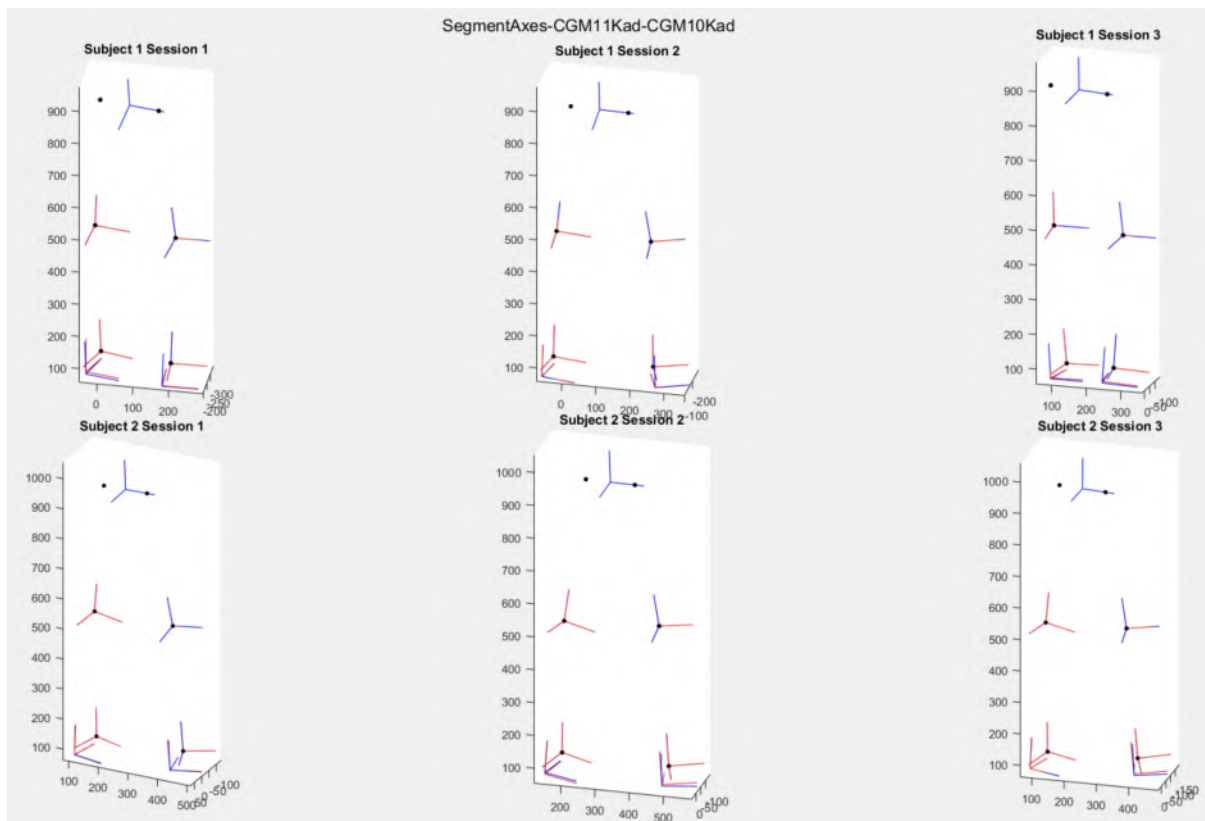


Figure IV.1.5: The segment axes systems of the CGM11Kad model (blue) and the CGM10Kad model (red) (Anterior view)

Pelvis, Femur and Tibia

The differences in the pelvis, femur and tibia segments between both models are negligible, regarding both the origins and the axes. This is in line with what is expected.

Foot

In some cases the foot origin undergoes a superior-interior shift. The direction and magnitude of the shift vary between the sessions and subjects. These superior-interior shifts are associated with a rotation in the sagittal plane of X_{Foot} and Z_{Foot} . Figure IV.1.6 shows a superior origin shift of the CGM11 model compared to the CGM10 model at the right foot and an inferior origin shift at the left foot. The corresponding rotations in the sagittal plane of X_{Foot} and Z_{Foot} are also visible. The cause of this superior-inferior shift in the foot origin is unknown and shouldn't be present according to the description models.

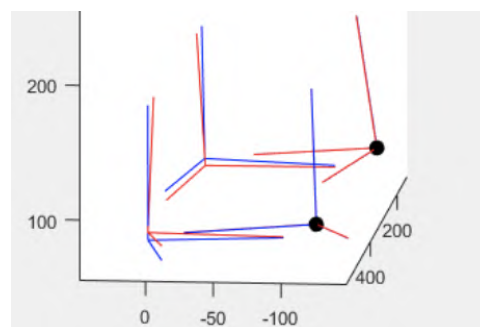


Figure IV.1.6: Expanded view in the sagittal plane of the foot segments (subject 2 session 2)

How do the differences in kinematics between CGM11Kad and CGM10Kad come about?

The kinematic output of CGM10Kad subtracted from the kinematic output of CGM11Kad, is shown in figure IV.1.7.

As the pelvis, femur and tibia segment axes are the same in both models in the static trial, one expects that there is no offset in the hip and knee angles. The offset values are indeed negligibly small for the Hip Flex/Ext, the Hip Ab/Ad, the Hip Rot, the Knee Flex/Ext and the Knee Var/Val. However, there is a large offset present in the knee rotation kinematics. In the CGM10 model the untortioned tibia segment is used for the knee angles in the dynamic trials and in the CGM11 model there is only one, tortioned, tibia segment. The knee rotation offset is thus equal to the tibial torsion value which is different for both sides and in the different sessions and subjects, which explains the different knee rotation offset values in figure IV.1.7.

The Ankle Dorsi/Plantar Flexion is the angle between the projections of X_{Tibia} and Z_{Foot} in the plane perpendicular to axis Ankle1. X_{Tibia} is the same in both models but Z_{Foot}

undergoes a rotation in the sagittal plane, in the cases where there is a superior-interior shift in the foot origin. The superior-inferior (SI) shift in the foot origin, causes an Ankle Dorsi/Plantar offset.

In the CGM10Kad model, there is an error present in the static plantarflexion offset, which induces an error in the Ankle Inversion/Eversion and the Ankle Rotation angles(see section II.3.2). This error is eliminated in the CGM11Kad model, which leads to differences in both ankle angles. The error in the CGM10Kad model is due to the fact that the static plantarflexion offset is considered relative to the proximal tibial segment instead of relative to the distal tibial segment. The difference between the distal and proximal tibial segment is the rotation in the transverse plane by the negative value of the tibial torsion. Therefore, the difference in the Ankle Inversion/Eversion angle and the Ankle Rotation angle between the 2 models should be related to the value of the tibial torsion. To check this relationship the Pearson's Correlation Coefficient is calculated between (1) the tibial torsion values and the ankle Inversion/Eversion offset values and (2) the tibial torsion values and the ankle rotation offset values over all the subjects and sessions. The correlation coefficients are respectively 0.89 and 0.82, which suggests that the static plantarflexion offset is causing the Ankle Inversion/Eversion offset and the Ankle Rotation offset between both models.

Conclusions

In general, the axes systems and the differences in kinematics are in line with the theory behind the CGM10Kad and CGM11Kad model: They are almost exactly the same except from the knee rotation angles and the Ankle Inversion/Eversion and Rotation angles.

There is only one unexplained difference in the experimental data, which is the superior-interior shift of the foot origin. This shift induces the sagittal rotation in the foot segment axes and ankle axes and the corresponding offsets in the ankle dorsiplantar flexion.

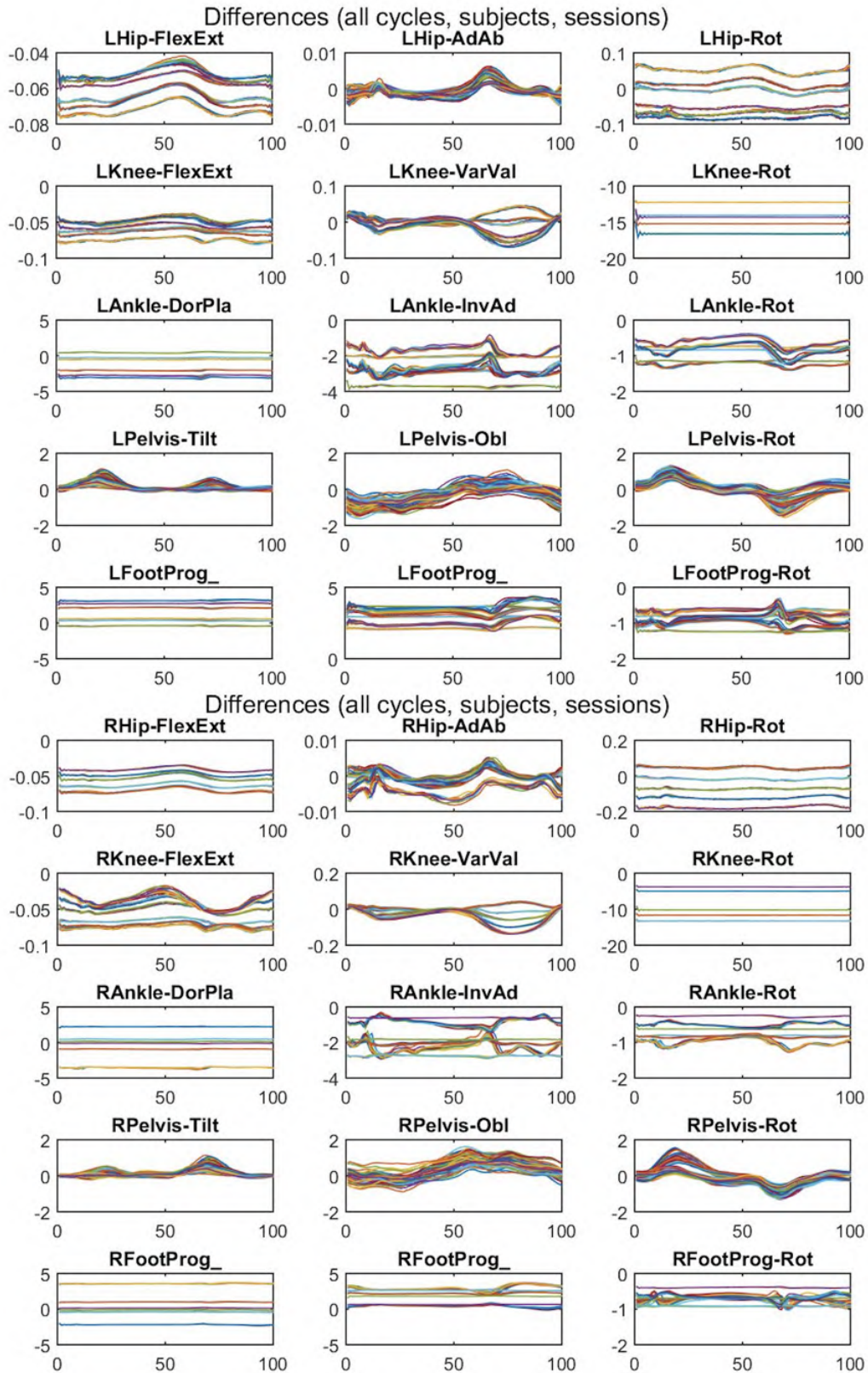


Figure IV.1.7: Subtraction of the CGM10Kad kinematics from the CGM11Kad kinematics for all sessions and subjects ($2 \times 3 \times 10 = 60$ trials) (x-axis: % time in gait cycles, y-axis: degrees)

IV.1.3 CGM11Kad & CGM11Med

The CGM11Kad and the CGM11Med model differ in terms of definition of the femoral coronal plane, which can be determined using the KAD device or a medial and lateral knee marker. As the axes and centers are determined through a top-down approach (from the pelvis to the foot), a change in the femoral coronal plane does not only affect the femur axes and knee joint center but also the tibia, ankle,...

Comparing the axes of the CGM11Kad model with the CGM11Med model in the static trial doesn't offer useful information. In the previous comparisons the exact same static trial is processed through 2 different methods. Consequently, the difference in axes and origins only depends on the used model. For the CGM11Kad model and the CGM11Med model a static trial with KAD and one with lateral and medial knee markers are compared. Between these 2 static trials the posture of the patient and the skin movement vary, leading to different origin positions and axes orientations. The differences in the axes system are thus only partially caused by the use of another model.

Therefore, it's better to look at the axes systems in the dynamic trials. For the dynamic trials, the exact same trials are processed through different models which leads to a difference in axes only dependent on the used model.

Difference the in segment axes systems

Figure IV.1.8 shows the body segments axes during the third session of subject 2. The position of the CGM11KAD axis system is described relative to the position of the CGM11Med axis system. Since, the difference between the 2 models is dependent on how the the KAD and the medial and lateral knee marker are placed relative to each other, the left and right side need to be considered separately. The reasoning is only explained for session 3 of subject 2 (right side) to not overload the report. Applying a similar reasoning to the other side, subjects and sessions, results in the same conclusions.

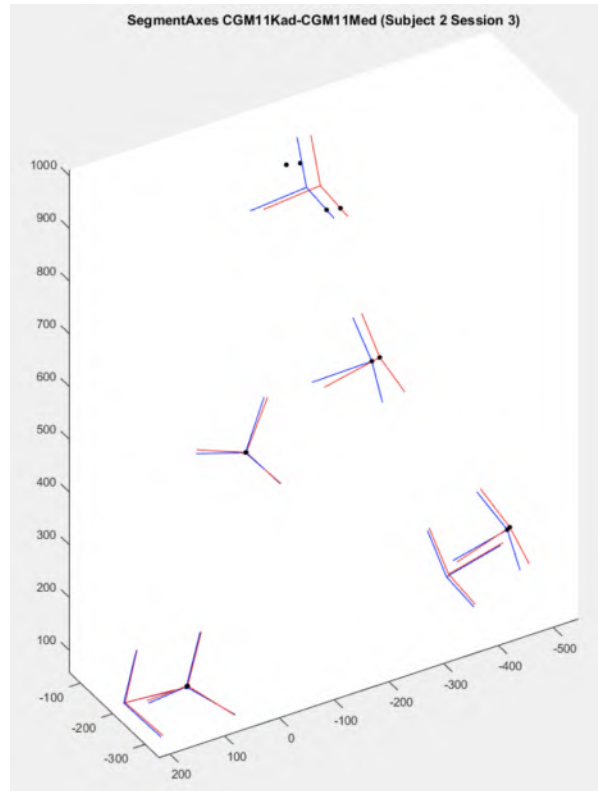


Figure IV.1.8: The segment axes systems of the CGM11Kad model (blue) and the CGM11Med model (red) (Anterior-superior view, left leg first and right leg behind)

Pelvis

In the CGM11Kad model the hip joint centers and thus also the pelvis origin are shifted anterior compared to the CGM11Med model (about 30mm). The expectation that the hip joint centers are the same in both models, is not confirmed by the experimental data, as depicted in figure IV.1.8.

The pelvic axes on the other hand are the same for both models, which is in line with the expectations.

Femur Right

The knee joint center in the CGM11Kad model has undergone a large anterior shift relative to KJC of the CGM11Med model. This could indicate that the KAD axis is positioned more anterior than the KNE-KNM line. The size of the anterior shift in the HJC is a little bit larger than the anterior shift in the KJC which leads to only a small rotation of the femur axes in the sagittal plane. Z_{Femur} tilted a little bit forwards and X_{Femur} tilted downwards.

In the transverse plane there is large external rotation visible on figure IV.1.8. From the anterior shift in the KJC, it could be known that the KNE-KNM line lies more posterior than the KAD axis. From the external rotation in the CGM11Kad model relative to the CGM11Med model, one could deduce that relative to the KAD axis the lateral

knee marker has undergone a small posterior shift and the medial knee marker a larger posterior shift (see figure IV.1.9).

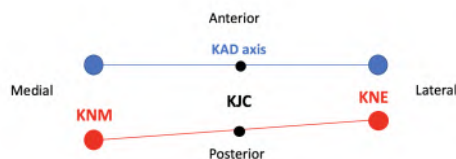


Figure IV.1.9: Effect of misaligned KNE-KNM line and KAD axis

This reasoning shows that the differences in the femur axes between the 2 models could be explained through a discrepancy between the KAD device and medial and lateral knee markers. In order to confirm that the changes in the axes are due to a discrepancy in the placement of the KAD and KNE-KNM markers, the position of the medial and lateral knee marker relative to the KAD device needs to be known and further investigation is thus needed.

Tibia Right

The origin of the tibia, which is by definition the same as the ankle joint center, is positioned more anterior in the CGM11Kad model than in the CGM11Med model. The question is now whether this anterior shift in the AJC can be caused by the replacement of the KAD device by a medial and lateral knee marker.

During the static trial the AJC is created in the tibial coronal plane: <Knee Joint Center, Lateral Ankle Marker, Medial Ankle Marker>. The replacement of the KAD device by 2 knee markers, caused a posterior shift in the KJC but has no influence on the position of the ANK and MED marker and can therefore not induce an AP shift in the ankle joint center in the static trial.

In the dynamic trials the AJC is determined in another and more complex way using the shank rotation value θ (see section II.2.2). In this more complex case, a shift in the KJC could induce an anterior-posterior shift in the AJC but a more detailed investigation is necessary, which can't be done using the collected data in this study.

An anterior shift in the ankle joint center while ANK remains at the same position, causes an external rotation of the tibia segment. This results in an external rotation in the transverse plane of Y_{Tibia} and X_{Tibia} . Y_{Tibia} is largely rotated to the anterior side and X_{Tibia} to the lateral side in the transverse plane.

Foot Right

The orientation of the foot axes is the same in both models. The foot origin undergoes an anterior shift from the CGM11Med model to the CGM11Kad model. From a theoretical

point of view, this AP shift can't be associated with the replacement of the KAD by two knee markers.

Looking at static trials separately

As already mentioned, showing the axes of the static trials of both the CGM11Kad and CGM11Med model on the same plot, does not offer useful information. However, it is interesting to look at how the KJC and knee axes are generated in the CGM11Kad and CGM11Med model separately in order to verify if the KJC and knee axes are generated in the same way in practice as is described in the theory.

CGM11Kad

The femoral coronal plane in the static trial is defined by 3 points: (1) the KAX marker, (2) a point equidistant from KAX, KD1 and KD2 and (3) the HJC. The knee joint center, Y_{Femur} and Z_{Femur} lie all by definition in this femoral coronal plane. Figure IV.1.10 indicates that this appear to be true for the static trial of the CGM11Kad model. It is checked for all sessions and subjects and it can be concluded that the the CGM11Kad model generated the knee joint center and axes in practice as described in the theoretical background.

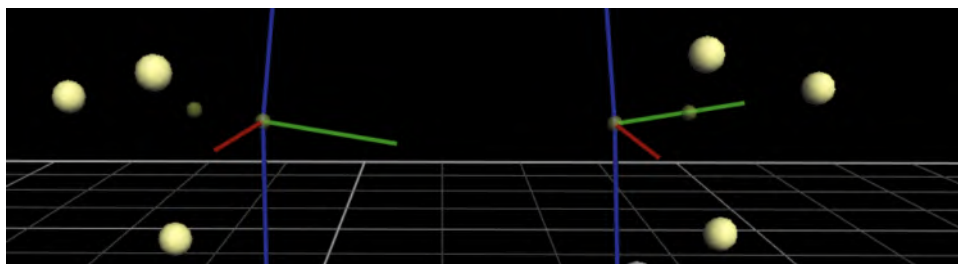


Figure IV.1.10: Anterior view of KAD (yellow) and the corresponding equidistant point (green), knee axes and knee joint center

CGM11Med

Leboeuf et al. describe that the CGM11 model with the medial knee marker is based on the same principle as when using the KAD device [16]. The femoral coronal plane in the static trial is thus defined by (1) the lateral knee markers, (2) the medial knee marker and (3) the hip joint center. In theory the KJC, Y_{Femur} and Z_{Femur} lie all in this plane. However, when looking at the experimental data in the static trial of the CGM11Med model of subject 2 in session 1, this contradicts the theoretical background (Figures IV.1.11 and IV.1.12). The knee joint centers don't lie in the $\langle KNE,KNM,HJC \rangle$ planes, but more posterior. This is also the case for the other sessions and subjects.

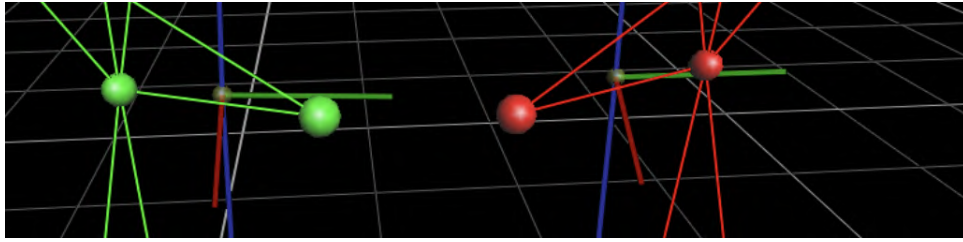


Figure IV.1.11: Anterior view of the medial and lateral knee marker, the knee axes and knee joint center in the CGM11Med model

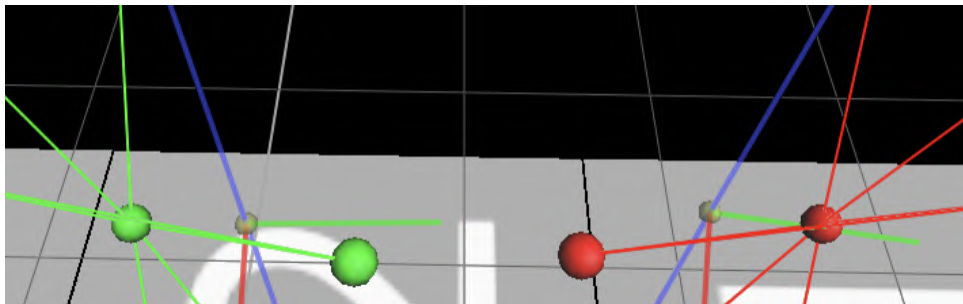


Figure IV.1.12: Superior view of the medial and lateral knee marker, the knee axes and knee joint center in the CGM11Med model

How do the difference in kinematics between CGM11Kad and CGM11Med come about?

Figure IV.1.13 shows the kinematics from the CGM11Med model are subtracted from the kinematic output of the CGM11Kad model (Subject 2 Session 3). An explanation of the difference in kinematics starting from the difference in axes systems is shown in figure IV.1.14 for the right side.

The gray colored rows in the scheme indicate an offset expected based on the change in segment axes. Only the relative angles are discussed (hip, knee, ankle), but it should be noted that the difference in pelvic angles is exactly zero. This is what is expected because the CGM11Kad and CGM11Med differ in how they define the femoral coronal plane and this has no effect on the pelvic angles.

There is a discrepancy between the measured kinematic data and the reasoning in the scheme for the Ankle Inversion/Eversion angle (warning sign in scheme IV.1.14). This is because the fact that the coronal plane of the tibia is not perfectly aligned with the coronal plane of the foot, has been neglected in the previous reasoning but does have a dominant effect in this particular case.

Conclusions

It's impossible to draw general conclusions as the differences in axes systems and kinematic output are highly dependent on how the medial and lateral knee marker are positioned relative to the KAD device. This is different for each session. Yet, it can be said that the anterior-posterior shift in the pelvis origin and foot origin can't be related to the replacement of the KAD by a medial and lateral knee marker. Why these shifts are present in the python code is thus unknown.

All the other differences in axes orientations and origins between the 2 models could be explained by a misalignment between the 2 knee markers and the KAD. However, this needs to be investigated in more detail. Especially since it's demonstrated that the CGM11Med model doesn't generate the KJC in the correct position. For the other sessions and subjects, similar conclusion can be drawn.

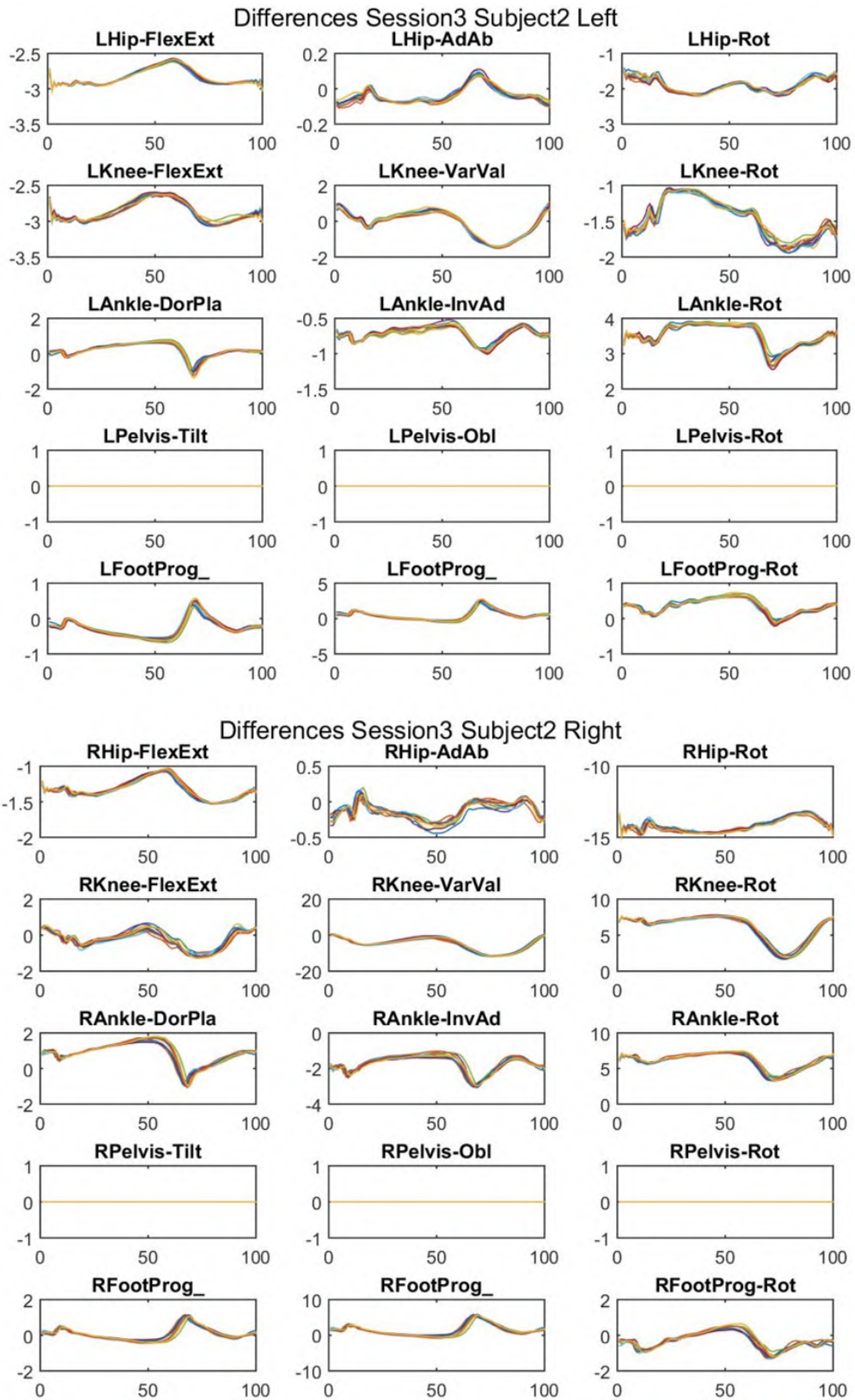


Figure IV.1.13: Subtraction of the CGM11Med kinematics from the CGM11Kad kinematics: Subject 2 Session 3 (10 trials) (x-axis: % time in gait cycles, y-axis: degrees)

CGM11Kad-CGM11Med (Session3 Subject 2 Right)


Angle	Joint Rotation Axis	Proximal Segment Axis	Distal Segment Axis	Effect on kinematics
Hip Flex/Ext	Hip 1 (\perp sagittal)	X_{Pelvis} Same	X_{Femur} In transverse plane to lateral (large) In sagittal plane to inferior (small)	Extension offset (negative & small)
Hip Ab/Ad	Hip 3 (\perp coronal)	Z_{Pelvis} Same	Z_{Femur} In sagittal plane to anterior (small)	Negligible
Hip Rot	Hip 2 (\perp transverse)	X_{Pelvis} Same	X_{Femur} In transverse plane to lateral (large) In sagittal plane to inferior (small)	External offset (negative & large)
Knee Flex/Ext	Knee 1 (\perp sagittal)	X_{Femur} In transverse plane to lateral (large)	X_{Tibia} In transverse plane to lateral (large)	Negligible
Knee Var/Val	Knee 3 (\perp coronal)	Z_{Femur} In sagittal plane to anterior (small)	Z_{Tibia} Same	Negligible
Knee Rot	Knee 2 (\perp transverse)	X_{Femur} In transverse plane to lateral (large)	X_{Tibia} In transverse plane to lateral (large)	Ext Rot a lot larger in femur: Internal offset (positive & large)
Ankle DorPla	Ankle 1 (\perp sagittal)	X_{Tibia} In transverse plane to lateral (large)	Y_{Foot} Same	Negligible
Ankle InvEv	Ankle 2 (\perp coronal)	Z_{Tibia} Same	X_{Foot} Same	Negligible 
Ankle Rot	Ankle 3 (\perp transverse)	X_{Tibia} In transverse plane to lateral (large)	Y_{Foot} Same	Internal offset (positive & large)

Figure IV.1.14: Scheme of the effect of change in axes system on kinematic data at the right side (CGM11Med subtracted from CGM11Kad)

IV.1.4 Software bug in CGM10Med

Figure IV.1.15 compares a static trial of the CGM11Med model and the CGM10Med model. As already mentioned, in the CGM11Med model the KJC is generated slightly outside the femoral coronal plane. When looking at figure IV.1.15, it is clear that the same error occurs for the CGM10Med, only worse. The KJC is generated that much posterior to the KNE-KNM line, that the KJC doesn't lie in the $\langle \text{KNE}, \text{KNM}, \text{HJC} \rangle$ plane. In order to know if the error is always present and if it is always larger in the CGM10Med model than in the CGM11Med model, more subjects needs to be investigated. However, in this study the error in the CGM10Med model is so large that the orientations of the knee axis and the kinematic output are useless.

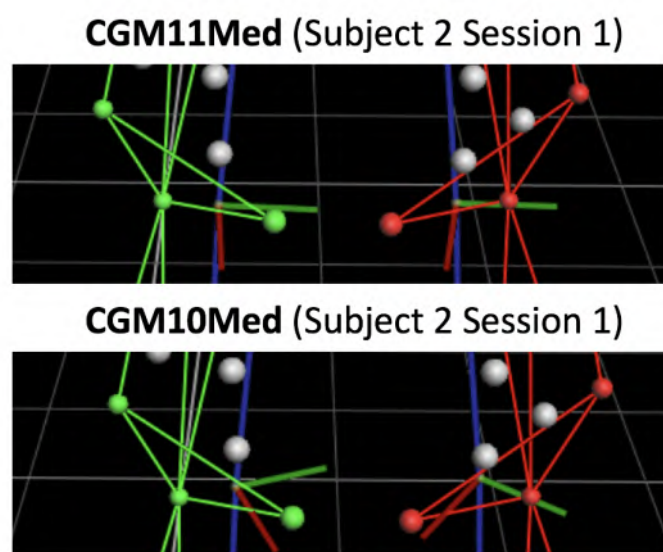


Figure IV.1.15: Comparison of the CGM10Med model and CGM11Med model knee joint center and axis generation in the first session of the second subject

The CGM10Med model is not valid for clinical practice as the error in the KJC position is too large. This is probably due to a software bug in the pyCGM2 package version 3.0.8. As the axes orientations and the corresponding kinematic output are useless, the CGM10Med model will be rejected in the rest of the study (Figure IV.1.16).

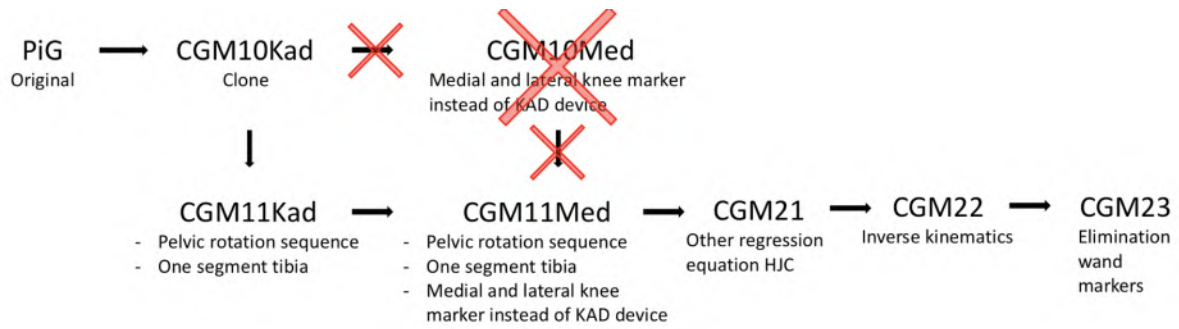


Figure IV.1.16: A scheme showing the effect of the elimination of the CGM10Med model in the study

IV.1.5 CGM21 & CGM11Med

The theoretical difference between the CGM21 and the CGM11Med model is the use of different equations for the hip joint center position (see section II.3.3).

Difference in the segment axes systems

Figure IV.1.17 shows the segment axes of the CGM2.1 model in red and those of the CGM11Med model in blue. The positions of the centers and orientation of the axes from the CGM21 model are described relative to the CGM11Med model.

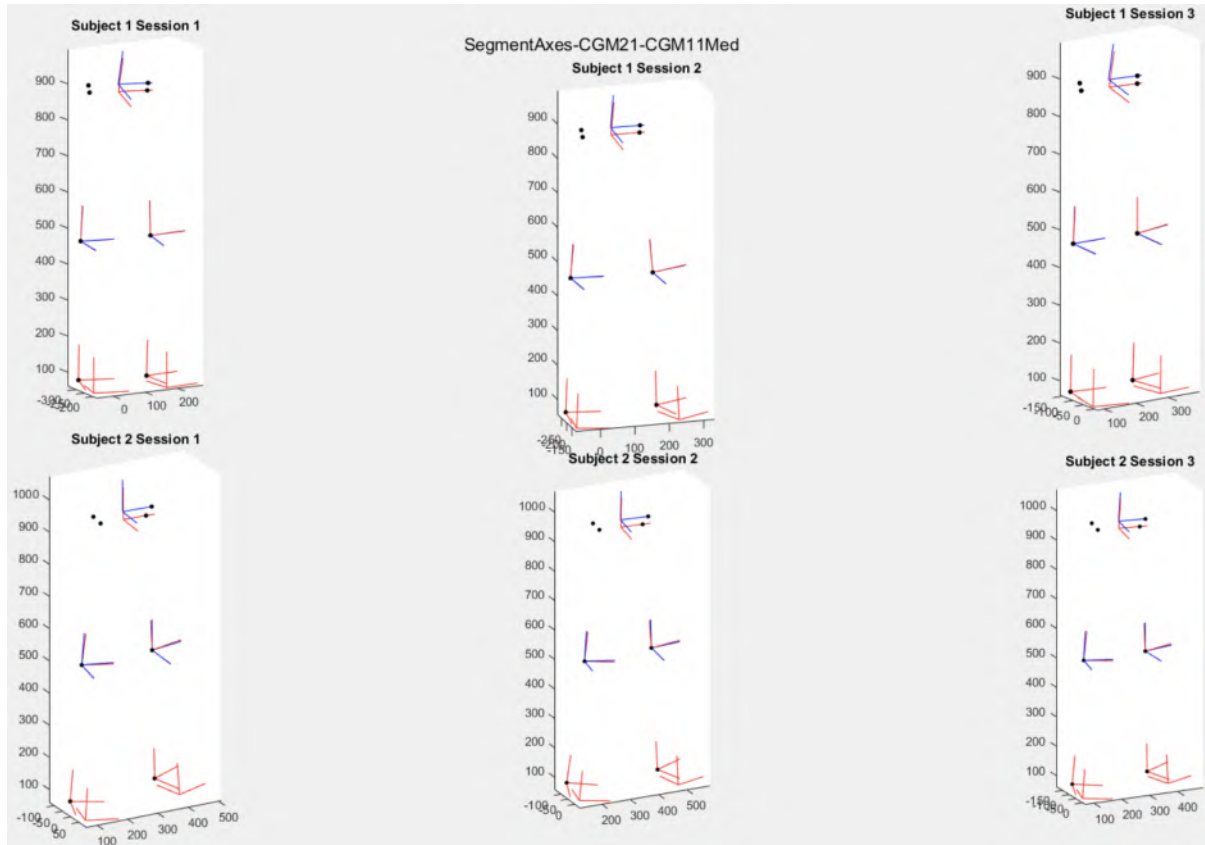


Figure IV.1.17: The segment axes systems of the CGM21 model (blue) and the CGM11Med model (red) (Anterior view)

The Pelvis

As expected one can see that the hip joint centers and therefore also the pelvic origin are positioned differently in both models. The position of hip joint centers of the CGM21 model (relative to the CGM11Med model) is more lateral and more superior. The pelvic origin lies by definition on the midpoint of the line between the left and right hip joint centers. The lateral shift in the hip joint centers has the same size at both sides and does thus not affect the medio-lateral position of pelvic origin. The shift in the pelvic origins is only superior. The orientation of the pelvic axes is the same.

The Femur

The origin of the femur, the knee joint center, is the same in both models. Z_{Femur} is externally rotated in the coronal plane because the hip joint center is shifted to the lateral side in the CGM21 model. This rotation in the coronal plane of Z_{Femur} leads to an upward tilt of Y_{Femur} at the right side in the coronal plane and to a downward tilt at the left side.

The Tibia and the Foot

The origins and the axes of both the tibia and the foot segment are the same in the CGM21 and CGM11Med model.

How do the difference in kinematics between CGM21 and CGM11Med come about?

Figure IV.1.18 shows the kinematic output of the CGM21 model from which the kinematic output of the CGM11Med is subtracted. The scheme in figure IV.1.19 shows how the differences in segment axes result in the different kinematic outputs between the 2 models. Based on the same reasoning as used in the previous comparisons, one can see that the last column 'effect on kinematics' corresponds with the results shown in figure IV.1.18.

It's clear that the Hip Ab/Ad and the Knee Var/Val offsets can be subdivided in 2 groups (figure IV.1.18). These 2 groups correspond to the 2 subjects in the study. In the second subject, the lateral shift in the HJC is much larger, leading to more rotation of Z_{Femur} in the coronal plane and thus larger offset values.

The total distance between the hip joint centers of the CGM21 and CGM11Med model are:

$$Subject1 : Mean = 20,00mm \quad and \quad SD = 0,13mm$$

$$Subject2 : Mean = 30,89mm \quad and \quad SD = 0,0018mm$$

Conclusions

It can be concluded that the data in this study matches with what is expected from the theory behind the CGM21 model. The hip joint center is positioned more lateral and superior in the CGM21 compared to the CGM11Med model. Although the direction of the shift is the same for both subjects, the size of the shift depends on the anthropometric measurements of the subject. In order to generalize this conclusion, more subjects and their HJC position need to be investigated.

The shift in hip joint center causes only a observable offset in the Hip Abduction/Adduction (subject1: about $0,5^\circ$, subject 2: about 3°) and the Knee Varus/Valgus angle (subject1: about -1° , subject 2: about $-3,5^\circ$).

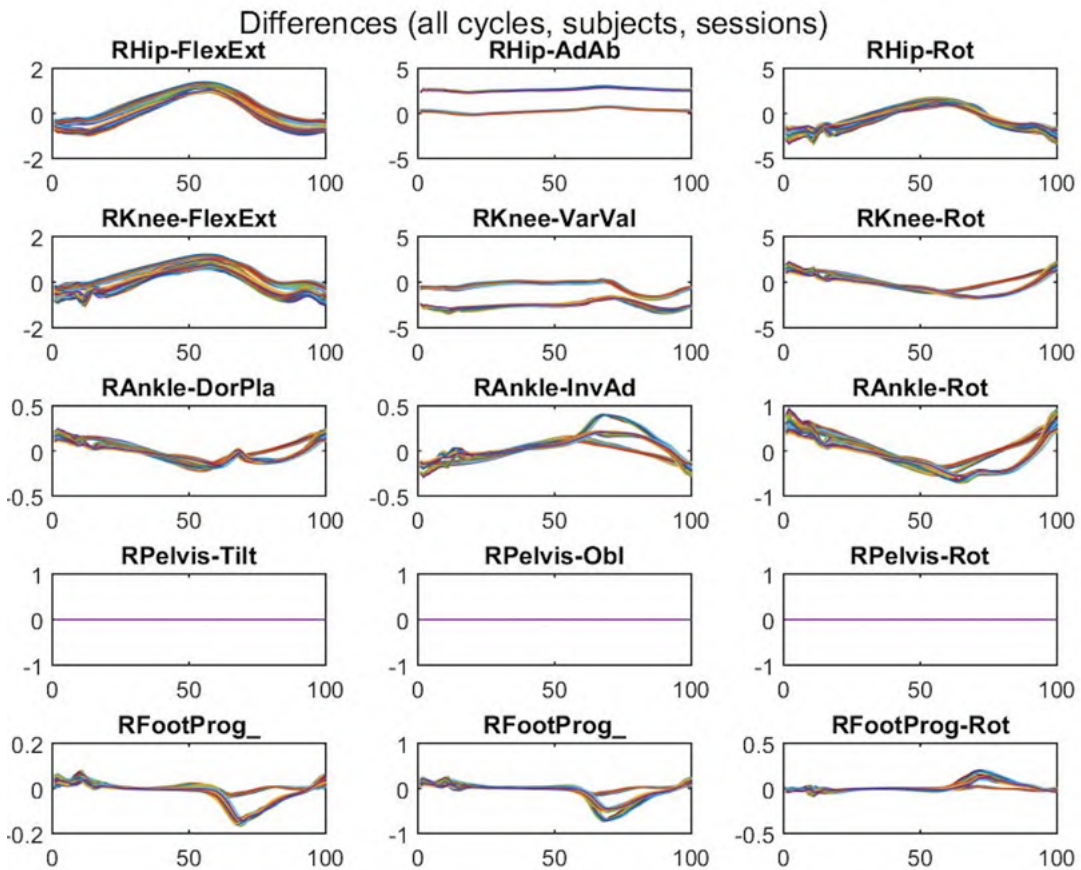
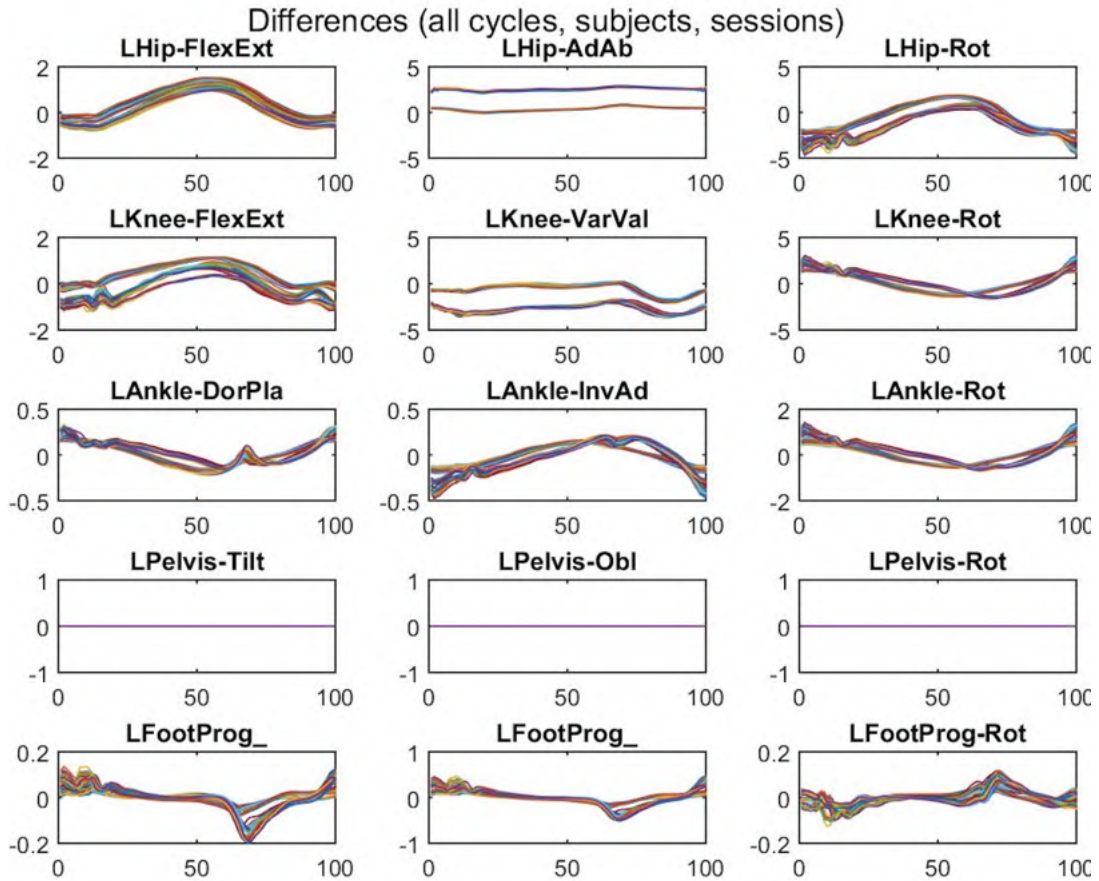


Figure IV.1.18: Subtraction of the CGM11Med kinematics from the CGM21 kinematics: All sessions and subjects ($2 \times 3 \times 10 = 60$ trials) (x-axis: % time in gait cycle, y-axis: degrees)

CGM21-CGM11Med

Angle	Joint Rotation Axis	Proximal Segment Axis	Distal Segment Axis	Effect on kinematics (CGM21-CGM11Med)
Hip Flex/Ext	Hip 1 (⊥ sagittal) Same	X_{Pelvis} Same	X_{Femur} Same	Negligible
Hip Ab/Ad	Hip 3 (⊥ coronal) Same	Z_{Pelvis} Same	Z_{Femur} In <u>coronal</u> plane, externally	Adduction offset (positive)
Hip Rot	Hip 2 (⊥ transverse) In coronal plane, externally	X_{Pelvis} Same	X_{Femur} Same	Negligible
Knee Flex/Ext	Knee 1 (⊥ sagittal) Right: In coronal plane, upward tilt Left: In coronal plane, downward tilt	X_{Femur} Same	X_{Tibia} Same	Negligible
Knee Var/Val	Knee 3 (⊥ coronal) Same	Z_{Femur} In <u>coronal</u> plane, externally	Z_{Tibia} Same	Valgus offset (negative)
Knee Rot	Knee 2 (⊥ transverse) Same	X_{Femur} Same	X_{Tibia} Same	Negligible
Ankle DorPla	Ankle 1 (⊥ sagittal) Same	X_{Tibia} Same	Y_{Foot} Same	Negligible
Ankle InvEv	Ankle 2 (⊥ coronal) Same	Z_{Tibia} Same	X_{Foot} Same	Negligible
Ankle Rot	Ankle 3 (⊥ transverse) Same	X_{Tibia} Same	Y_{Foot} Same	Negligible

Figure IV.1.19: Scheme of the effect of change in axes system on kinematic data (CGM11Med subtracted from CGM21)

IV.1.6 CGM22 & CGM21

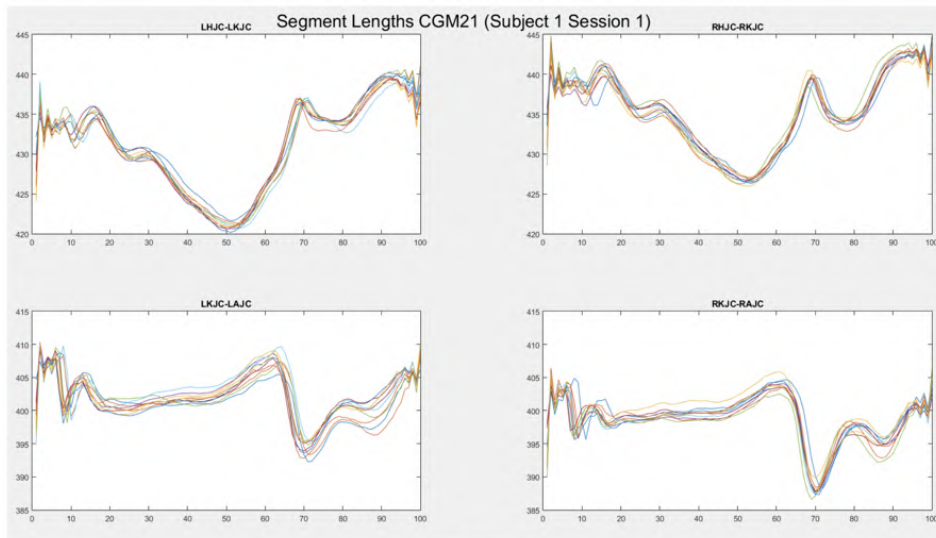
In the CGM22 model the dynamic processing is done using the 'inverse kinematics method' as explained in section II.3.4. This method assures a constant segment length throughout the dynamic trial, which was not the case in the CGM21 model.

The segment axes systems

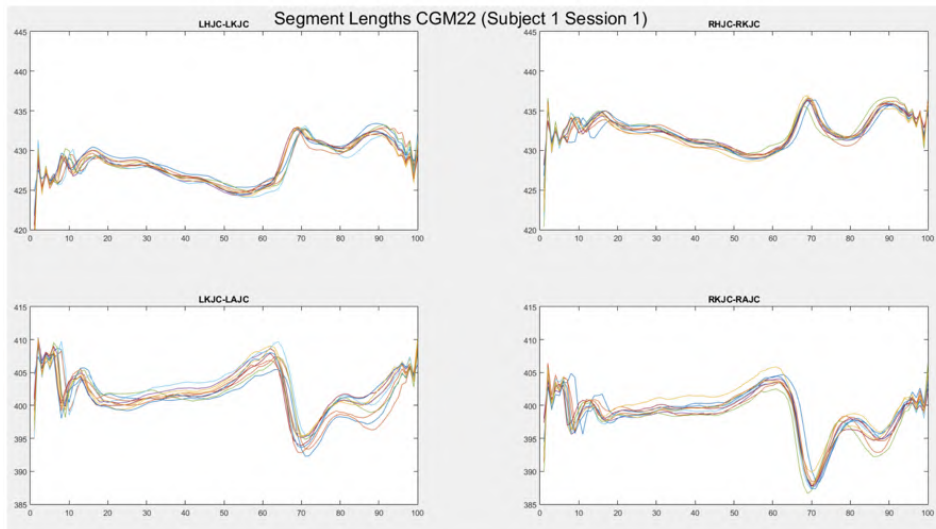
In the static trial of the CGM22 model, a segment model is created that is fitted to the measured markers, in the dynamic trials afterwards. The segment model in the CGM22 model is generated in the same way as it is done in the static trial of the CGM21 model. Therefore, the joint center positions and the segment axes of the CGM21 and CGM22 model are exactly the same in the static trial.

In the dynamic trials, the best match between the segment model with joint constraints and the measured markers is searched. This fitting is done by the OpenSim IK solver. This IK solver generates directly the joint angles which correspond to the minimal cost function. The intermediate steps such as generating axes, joint centers and segment origins in the dynamic trials, are not part of the OpenSim IK solver output. The CGM22 model in Vicon Nexus 2.8.1 consists of the CGM21 model with the addition of the OpenSim IK solver. Hence, the segment origins and axes shown in Nexus and presented in the corresponding c3d file are those of the CGM21 model as they are not overwritten by the OpenSim IK solver.

The fact that the segment origins of the CGM22 model are not represented in Nexus, is a large disadvantage. The segment lengths, as now shown in Nexus and the c3d file, have as a consequence a variable length in the CGM22 model, while the theoretical strength of the model is the constant segment length (figure IV.1.20).



(a)



(b)

Figure IV.1.20: The femur and tibia segment lengths for the CGM21 model (a) and the CGM22 model (b) (Subject 1 Session 1: 10 trials)(x-axis: % time in gait cycle, y-axis: segments length in mm)

Figure IV.1.20 shows that the segment length in the CGM22 model in Nexus is not constant over the gait cycle, and also reveals a contradiction between the theory and the experimental data. As one can see, the distance between the knee joint center and ankle joint center is exactly the same in the CGM21 and CGM22 model in all trials. This indicates that the KJC and AJC are generated in the same way in both models, which corresponds with the fact that the joint centers (=segment origins) are not overwritten by the OpenSim IK solver. However, the distance between the hip joint center and the knee joint center differs in both models. This is because the hip joint center in Nexus is positioned differently in the CGM21 and CGM22 model. For this, there is no reasonable

explanation. In the static trials of both models the same HJC's are generated, which suggests that the error is due to the remodelling in the dynamic trials. Figure IV.1.20 shows the issue for the first session of the first subject, but the error of the HJC is present in all subjects and sessions.

How do the difference in kinematics between CGM22 and CGM21 come about?

Figure IV.1.21 shows the kinematic output of the CGM22 model from which the CGM21 kinematic output is subtracted. Different than in the previous model comparisons, both models have the same axes systems in the static trial. As a consequence, the different kinematic output is not due to the differences in static axes systems. CGM22 and CGM21 differ in terms of knee axis alignment in the dynamic trials ('direct method' vs. 'inverse kinematics method') and in terms of soft tissue artefact. In the CGM21 model, each segment is modelled separately and a STA of a specific marker has an influence on the position of the segment to which the marker is applied. In the CGM22 model, an overall lower body segment model is subjected to a whole lower body optimization in each timeframe. The more markers there are prone to soft tissue artefact, the larger the marker error will be between the measured and the modelled markers. Are the differences in the kinematic output related to soft tissue artefact and knee axis misalignment? This question is addressed by analyzing the nature of the kinematic differences.

- For the right side, 2 groups, corresponding to the two subjects, can be clearly distinguished for some angles (Hip Rotation, Knee Varus/Valgus, Ankle Dorsi/Plantar Flexion, Ankle Rotation). As the soft tissue artefact is demonstrated to be subject dependent, this indicates that the difference in kinematics could be caused by the soft tissue artefact [11]. The knee axis misalignment is more session dependent than subject dependent.
- The difference in Knee Varus/Valgus is particularly high in the swing phase. This could indicate that differences are due to knee axis misalignment since the crosstalk between the knee flexion/extension and varus/valgus reaches its maximum in the swing phase. The pattern of the soft tissue artefact over the gait cycle is not exactly known and goes beyond the scope of this study.
- The relatively high offsets in the Hip Rotation, Knee Varus/Valgus, Knee Rotation and Ankle Rotation indicate also that knee axis misalignment in the transverse plane could be related to the differences in kinematics.
- For each subject, the difference in kinematics has the same pattern over the gait cycle and so do the crosstalk induced patterns and the soft tissue artefact patterns.

Hence, the differences in kinematics between the models could be related to soft tissue artefact and knee axis misalignment but further investigation is required. The effect of knee axis misalignment and soft tissue artefact on both models separately, rather than on the differences between them, is discussed later in this study.

Conclusions

The segment axes in the static trials are the same for both models, but in the dynamic trials there is a difference. The difference in kinematic output could be caused by soft tissue artefact or knee axis misalignment. However, from the subtraction of the kinematic output no conclusions can be taken and further investigation is required.

It also needs to be mentioned that caution is needed when working with the CGM22 model in Nexus. The segment axes and origins shown in Nexus in the dynamic trials are the ones of the CGM21 model and not of the CGM22 model itself.

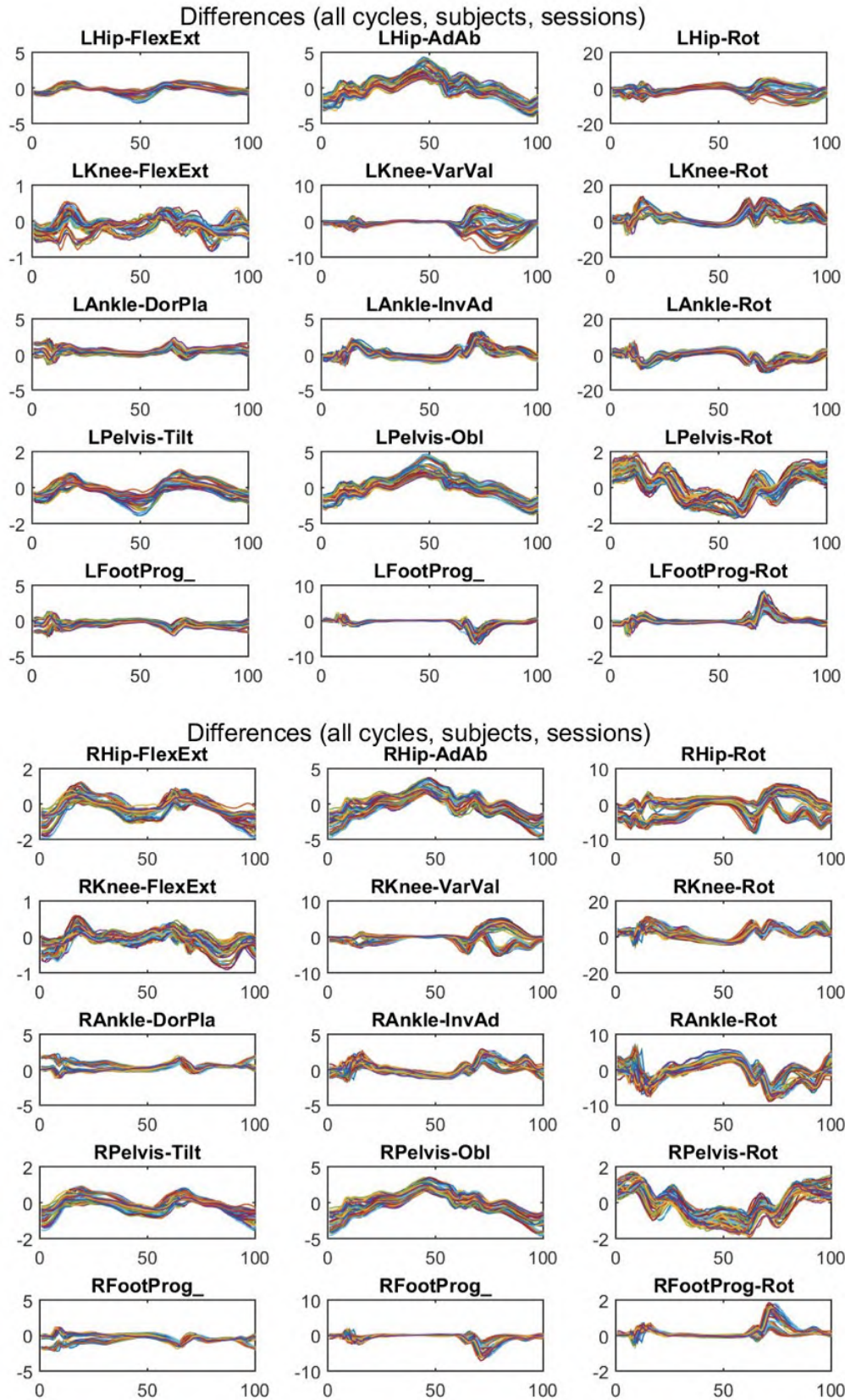


Figure IV.1.21: Subtraction of the CGM21 kinematics from the CGM22 kinematics: All sessions and subjects (x-axis: % time in gait cycle, y-axis: degrees)

IV.1.7 CGM23 & CGM22

The segment axes systems

The replacement of lateral thigh and tibia wand markers by three skin markers, does not affect the segment generation in the static trial since the lateral thigh and tibia markers, in combination with the thigh/tibia rotation offset parameter θ , are only used to define the segments in the dynamic trials and not in the static trial. Hence, the segment model which is generated in the static trial and fitted to the measured markers in the dynamic trials, is the same in CGM22 and CGM23.

Caution is needed when using the CGM23 model in Nexus2.8. The segments and joint centers shown in Nexus2.8 in the dynamic trials are not the ones corresponding to the CGM23 model. The OpenSim IK solver functions as black box which does not output the segments and the joint centers.

How do the difference in kinematics between CGM23 and CGM22 come about?

CGM23 is designed to be less susceptible to soft tissue artefact. Using the 'inverse kinematic method' with a larger number of markers, positioned on anatomical landmarks felt to be less prone to STA, reduces the importance of markers particularly prone to STA such as the lateral knee marker. The differences in kinematics between the models, shown in figure IV.1.22, could be related to soft tissue artefact and knee axis misalignment but further investigation is required. The effect of knee axis misalignment and soft tissue artefact on CGM22 and CGM23 separately, rather than on the differences between them, is discussed later in this study.

Moreover, the wand markers, which have inertia and appear to wobble in the anterior-posterior direction at the initial contact, are eliminated in the CGM23 model. This causes the differences in hip rotation between CGM22 and CGM23 shown in figure IV.1.22.

Conclusions

The segment axes in the static trials are the same for both models. The segment axes in the dynamic trials in Nexus are incorrect as they are not the segment axes corresponding to the CGM23 model. The CGM23 model is expected to be less prone to STA than the CGM22 model. However, from the subtraction of the kinematic output it can't demonstrate that the CGM23 model is less prone to STA. The difference in kinematics could be related to soft tissue artefact, the elimination of the wand markers prone to wobbling and knee axis misalignment. However, further investigation is required.

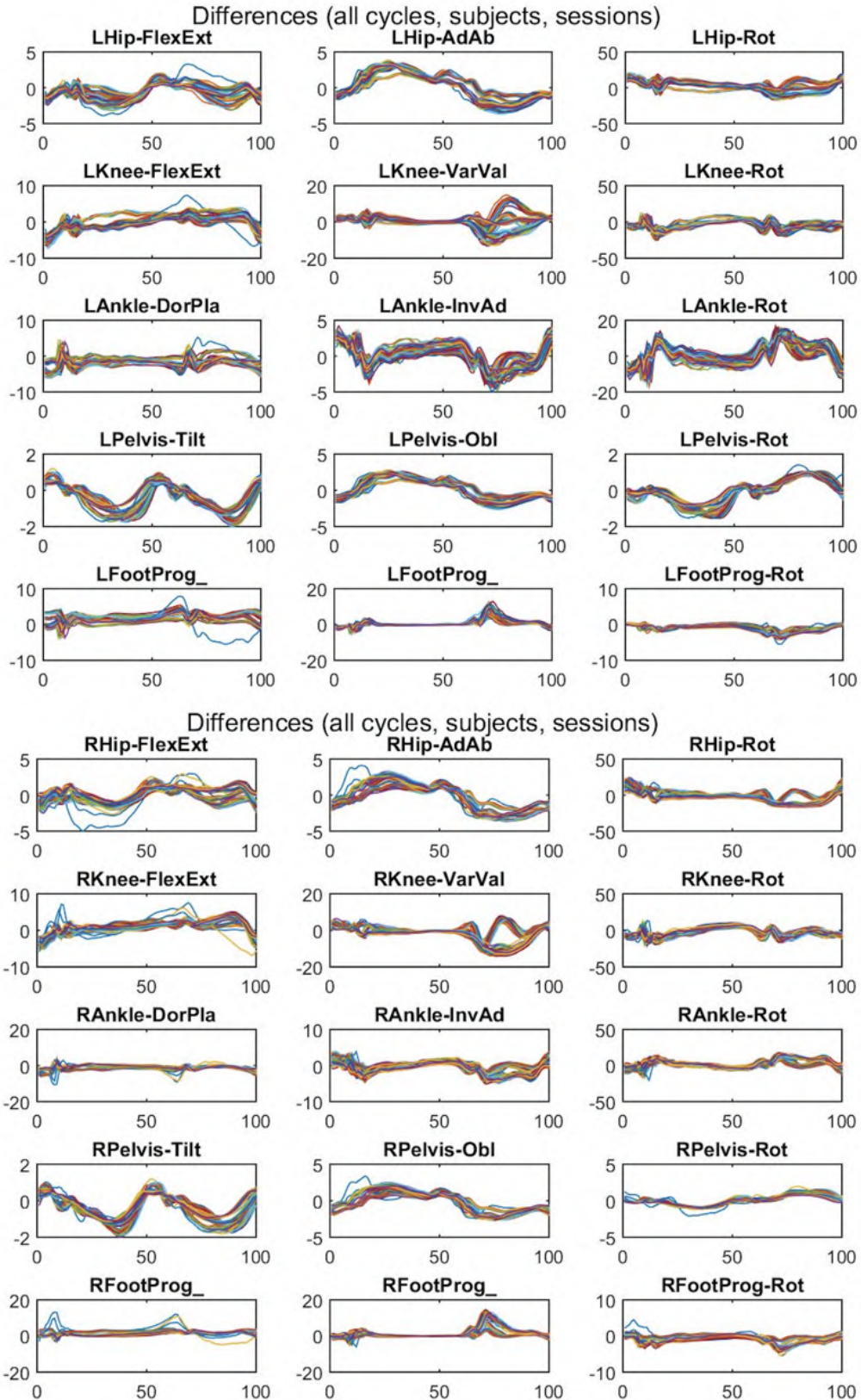


Figure IV.1.22: Subtraction of the CGM22 kinematics from the CGM23 kinematics: All sessions and subjects (x-axis: % time in gait cycle, y-axis: degrees)

IV.2 Repeatability

The aim of checking the repeatability in this study is twofold for both intersession and intrasession: (1) Comparing the repeatability of the 8 models and (2) giving an idea of the magnitude of the repeatability parameter values.

IV.2.1 The averaged standard deviation (ASD)

Intersession averaged standard deviation

For both subjects, the intersession averaged SD values can be found in table A.0.1 and A.0.2 in the appendix.

Comparing the intersession repeatability of the models

In order to compare the intersession repeatability of the different models, the models are ranked from low to high intersession averaged SD, thus from the best to the worst intersession repeatability. The results of this ranking are shown in table A.0.3 in the appendix. Although this table contains all the information necessary to compare the intersession repeatability of the 8 models, it's too unclear to derive direct conclusions from it.

Therefore, another more structured method to rank the intersession repeatability of the different models, is introduced. A value of 1 is assigned to the most repeatable model and a value of 8 to the least repeatable model for a certain angle, subject and side. This values represents the position of the model in the 'Repeatability Ranking'. The mean position of each model is calculated by taking the average of the values over all the sides, subjects and angles per model. This process results in 8 values, each representing 'the mean position in the repeatability ranking' of the corresponding model. The 'mean position' for each model is shown in table IV.2.1.

Table IV.2.1: 'Mean position' of the models in the ranking based on the intersession averaged SD calculation

Ranked Models	Mean position
CGM23	2,1667
CGM21	2,5278
CGM11Med	2,8333
CGM22	3,1944
CGM11Kad	4,0899
PiG	4,3056
CGM10Kad	4,4167
CGM10Med	5,4722

Looking at the 'mean position' of the 8 models in table IV.2.1, one can conclude that

the CGM23 model has the best intersession repeatability and the CGM10Med the worst. The conclusions concerning the intersession repeatability are:

- The CGM10Med model has the lowest intersession repeatability, which is caused by the the software bug in the pyCGM2 package of CGM10Med (see section IV.1.4).
- The models using the knee alignment device (KAD) have a rather bad intersession repeatability. The PiG, CGM10Kad and CGM11Kad model, score worse than the other models. This is in line with the expectations as the KAD is harder to handle and creates more soft tissue movement in the static trial than the medial and lateral knee marker.
- Implementing the inverse kinematics with the wand markers for the dynamic processing, makes the intersession repeatability worse. This can be seen by comparing the CGM21 and CGM22 model.
- When the kinematic fitting is executed without wand markers and with more skin mounted markers, there is a large improvement in the intersession repeatability. In total, over all the angles, subjects and sides, the CGM23 is shown to perform the best intersession repeatability and the CGM22 model only occupies the 4th place.

Some points of attention need to be mentioned concerning the 'mean position method' and the conclusions drawn from it. The strength of this method is that it's very understandable but it also contains some weaknesses.

Firstly, these conclusions are related to the intersession repeatability in general and not for the angles separately. Although, the intersession repeatability of the models varies a lot for the different angles, the choice of averaging over the angles is justified. In this study, the search is about the best model in clinical practice. This implies that the most repeatable model in general needs to be found, and not the most repeatable model for each angle separately. Therefore, the dependency of the intersession ASD of the different models on the angles can be seen in tables A.0.1 and A.0.2, but is not discussed in this report.

Secondly, this method is based on a ranking of the models but does not take into account the distribution of the ASD values between the models. The next section talks about size order of the intersession ASD values and shows how much the ASD values differ between the models.

The magnitude of the intersession averaged standard deviation

Table IV.2.2 shows the intersession ASD values averaged over both subjects and sides.

Table IV.2.2: Intersession averaged SD: Mean over both subjects and sides. Last 2 columns: the mean and standard deviation over all models (CGM10Med excluded)

	CGM10KAD	CGM10Med	CGM11KAD	CGM11Med	CGM21	CGM22	CGM23	PiG	Mean	SD
HipFlexExt	2,3983092	2,436086	2,398846	2,210829	2,117682	2,037435	1,990631	2,410379	2,223445	0,180939
HipAbAd	0,9210899	0,778273	0,920521	0,9479	0,903425	0,958984	1,035414	0,919313	0,943807	0,044587
HipRot	4,5966178	8,284616	4,622807	2,980065	3,051113	3,597417	1,839008	4,469561	3,593798	1,047373
KneeFlexExt	1,5385239	2,937485	1,538808	1,19036	1,141936	1,166381	1,080145	1,625848	1,326	0,230421
KneeVarVal	1,6438431	3,213657	1,64942	1,099571	1,101686	1,436274	0,794072	1,748479	1,353335	0,359531
KneeRot	2,9141495	4,908024	2,67254	2,684742	2,742645	3,247246	2,459074	2,845356	2,795107	0,246306
AnkleDorPla	1,9043478	2,01109	0,790576	0,760896	0,766238	0,83481	0,633847	0,7637	0,922059	0,437453
AnkleInvAd	0,9513513	1,502405	0,655641	0,62106	0,620279	0,679656	0,575981	0,935611	0,71994	0,156128
AnkleRot	1,5016433	8,064993	1,571414	1,481238	1,475396	1,898606	1,520242	4,29025	1,962684	1,037008

A different alignment of the knee axis in the transverse plane causes on the one hand an offset in the hip rotation angle and on the other hand a variation in the knee varus/valgus angle. Therefore, the distribution of the intersession ASD values of these angles offers an insight in the variability of the knee misalignment over the sessions. The mean and the standard deviation of the intersession ASD values over the models (CGM10Med excluded) are:

$$\text{Hip Rot} : \text{Mean} = 3,59^\circ \quad \text{and} \quad \text{SD} = 1,05^\circ$$

$$\text{Knee Var/Val} : \text{Mean} = 1,35^\circ \quad \text{and} \quad \text{SD} = 0,36^\circ$$

This rather high standard deviation indicates a large difference between the models in intersession variability due to knee misalignment. The ASD values of the hip rotation and the knee varus/valgus are remarkably lower in the CGM23 model, which has the highest overall intersession repeatability, than in the PiG model, which is widely used. The values are indicated in bold in table IV.2.2. This demonstrates that the knee axis (mis)alignment is more consistent between the sessions in the CGM23 model than in the PiG model.

Intrasession Averaged Standard Deviation

The intrasession averaged standard deviation values for the three sessions are shown in table A.0.4, A.0.5, A.0.6 and A.0.7 in the appendix (Subject 1 Left, Subject 1 Right, Subject 2 Left and Subject 2 Right respectively).

Comparing the intrasession repeatability of the models

The way of comparing the intrasession repeatability of the models is similar to how the intersession repeatability of the models is compared. The models are ranked from best to worst intrasession repeatability. This ranking is shown in table A.0.8 and A.0.9 in the appendix for the first and second subject respectively. A more structured and clear way of representing how well the intrasession repeatability of the different models scores, is through the 'mean position' method. The mean ranking position of the models is shown in table IV.2.3.

Table IV.2.3: 'Mean position' of the models in the ranking based on the intrasession averaged SD

Session1	Session1	Session2	Session2	Session3	Session3
PiG	1,6667	PiG	1,5556	PiG	1,3889
CGM23	1,8056	CGM23	1,66667	CGM23	1,6944
CGM21	2,6667	CGM10Med	2,75	CGM21	2,6111
CGM11Med	3	CGM21	2,8611	CGM11Kad	3
CGM10Med	3,0556	CGM11Med	3	CGM11Med	3,1111
CGM11Kad	3,0833	CGM11Kad	3,1944	CGM10Kad	3,2222
CGM10Kad	3,1944	CGM10Kad	3,4167	CGM10Med	3,3056
CGM22	3,5278	CGM22	3,5556	CGM22	3,6667

Table IV.2.3 shows the 'mean position' of the models in the intrasession repeatability ranking for the 3 sessions. When eliminating the CGM10Med model from table IV.2.3, the following conclusions can be taken:

- The intrasession repeatability is similar for the CGM11Med and CGM11Kad model.
- When eliminating the CGM10Med model and taking into account that the CGM11Med and CGM11Kad have a similar intrasession repeatability, the ranking of the models is the same for all three sessions: PiG, CGM23, CGM21, CGM11Med/CGM11Kad, CGM10Kad and CGM22.
- Although the PiG model and the CGM10Kad are clones in theory, the PiG has a much better intrasession repeatability than the CGM10Kad model.
- The implementation of the inverse kinematics causes a deterioration in the intrasession repeatability (from CGM21 to CGM22).
- On the other hand, using the inverse kinematics with more skin mounted markers on anatomical landmarks less sensible to STA, leads to a large improvement of the intrasession repeatability (compare CGM22 and CGM23). This is expected as CGM23 is designed to be less prone to STA, one of the sources of intrasession repeatability. This suggests that the main cause of the low CGM22 intrasession repeatability is the high sensibility to soft tissue artefact. Moreover, the wand markers have inertia and tend to wobble at the initial contact. Eliminating the wand markers also contributes to a better intrasession repeatability.

The magnitude of the intrasession averaged standard deviation

The intrasession ASD values averaged over the 2 subjects, the 2 sides and the 3 sessions are shown in table IV.2.4.

Table IV.2.4: Intrasession averaged SD: Mean over subjects, sides and sessions. Last 2 columns: the mean and standard deviation over all models (CGM10Med excluded)

	CGM10KAD	CGM10Med	CGM11KAD	CGM11Med	CGM21	CGM22	CGM23	PiG	Mean	SD
HipFlexExt	1,1706475	1,175844	1,170515	1,174771	1,130019	1,119134	1,105752	1,159206	1,150736	0,028079
HipAbAd	0,6875713	0,682519	0,687546	0,688524	0,658406	0,670752	0,696662	0,661386	0,679171	0,013958
HipRot	1,3193867	1,299736	1,319464	1,307096	1,356589	1,591054	1,158113	1,144462	1,311987	0,137266
KneeFlexExt	1,6597335	1,644752	1,659453	1,670713	1,652129	1,650469	1,715324	1,630824	1,660425	0,025103
KneeVarVal	0,5919713	0,755593	0,592302	0,578558	0,584279	0,774941	0,416178	0,527569	0,602674	0,116265
KneeRot	1,5446792	1,579095	1,544713	1,539946	1,544412	2,087441	1,274926	1,217659	1,541609	0,260612
AnkleDorPla	1,169525	1,121593	1,169879	1,145285	1,144338	1,133677	1,120651	1,135059	1,142501	0,019044
AnkleInvAd	0,40733	0,394932	0,391799	0,391918	0,393807	0,554589	0,325797	0,361082	0,402657	0,066668
AnkleRot	1,6116555	1,500757	1,615757	1,588506	1,593503	2,132236	1,316282	1,496698	1,606924	0,234358

The mean and the standard deviation of the intrasession ASD values indicate that the difference between the models in intrasession repeatability is not as distinct as for the intersession repeatability (table IV.2.4). Realistically, the ASD values of the hip rotations and knee varus/valgus all look similar (indicated in bold).

$$Hip\ Rot : Mean = 1,31^{\circ} \quad and \quad SD = 0,14^{\circ}$$

$$Knee\ Var/Val : Mean = 0,60^{\circ} \quad and \quad SD = 0,12^{\circ}$$

This indicates that the intrasession variability due to knee misalignment is similar in all models.

Comparing the intersession and intrasession ASD

A few interesting points of attention are revealed by the comparison of the intersession and intrasession ASD:

- Using the KAD results in worse intersession repeatability than using the medial and lateral knee marker. The intrasession repeatability on the other hand is not related to the use of knee alignment method.
- The CGM10Kad and PiG model, which are in theory clones, have a similar intersession repeatability but the PiG has a better intrasession repeatability.
- There are large differences observed in the intersession repeatability between the models. For the intrasession repeatability on the other hand, the differences between the models are less distinct.

For the use in clinical practice a high intersession repeatability is very valuable. This leads to a better evaluation of how the gait differs pre- and postoperative, with and without orthoses,... However, a good intrasession repeatability is also necessary in clinical practice. As the CGM23 model has the best intersession repeatability and the second best intrasession repeatability, it can be concluded that the CGM23 model is the most appropriate for clinical application.

Table IV.2.5 shows the average intersession ASD values from which the average intrasession ASD values are subtracted. A positive value corresponds to a larger intersession variability than intrasession variability.

Table IV.2.5: The intrasession ASD values subtracted from the intersession ASD values (averaged over all the subjects, sessions and sides)

Inter-Intra	CGM10KAD	CGM10Med	CGM11KAD	CGM11Med	CGM21	CGM22	CGM23	PiG
HipFlexExt	1,2276617	1,260243	1,228332	1,036058	0,987664	0,918301	0,884879	1,251174
HipAbAd	0,2335186	0,095754	0,232974	0,259377	0,245019	0,288232	0,338751	0,257927
HipRot	3,2772311	6,984881	3,303343	1,672969	1,694524	2,006363	0,680895	3,325099
KneeFlexExt	-0,1212097	1,292733	-0,12065	-0,48035	-0,51019	-0,48409	-0,63518	-0,00498
KneeVarVal	1,0518718	2,458065	1,057117	0,521013	0,517407	0,661333	0,377893	1,22091
KneeRot	1,3694703	3,328929	1,127827	1,144796	1,198233	1,159804	1,184148	1,627696
AnkleDorPla	0,7348227	0,889496	-0,3793	-0,38439	-0,3781	-0,29887	-0,4868	-0,37136
AnkleInvAd	0,5440213	1,107473	0,263842	0,229141	0,226471	0,125068	0,250185	0,574529
AnkleRot	-0,1100122	6,564236	-0,04434	-0,10727	-0,11811	-0,23363	0,203961	2,793551

For the hip rotation and the knee varus/valgus the values are positive for all models. This indicates that the variability due to knee misalignment is larger intersession than intrasession, which is in line with the expectations. The angles that show for most models a larger intrasession than intersession variability are the knee flexion/extension, the ankle dorsi/plantar flexion and the ankle rotation. In order to explain why the intersession repeatability is higher than the intrasession repeatability for these angles, a more detailed study is necessary.

IV.2.2 Intraclass Correlation Coefficient (ICC)

Intersession ICC

The values of the intersession intraclass correlation coefficient can be found in table B.0.1 in the appendix.

ICC values out of range

Although in theory the ICC always has a value between 0 and 1, one can see that in practice this is not true: values greater than one and less than zero are found in table B.0.1. Based on the computational formula of the intersession ICC in equation III.2, it can be derived that:

$$ICC < 0 \Leftrightarrow \begin{cases} MS_B < MS_E \\ MS_B > \frac{MS_E - MS_T}{n} \end{cases} \quad (IV.1)$$

$$ICC > 1 \Leftrightarrow \begin{cases} MS_B < MS_E \\ MS_B < \frac{MS_E - MS_T}{n} \end{cases} \quad (IV.2)$$

Combining equations IV.1 and IV.2 makes clear that the intersession ICC value always is out of range when $MS_B < MS_E$. When the variability between the subjects is smaller than the variability due to error, the ICC is thus meaningless.

Table B.0.1 in the appendix shows the intersession ICC values for all relative angles and for all 8 models. When for a specific angle, one of the eight ICC values is out of range, a meaningful comparison of the 8 models is impossible. The angles for which a valuable comparison of the 8 models can be done, thus with 8 ICC values between 0 and 1, are indicated in bold in table B.0.1.

Dependency of the ICC on MS_B and MS_E

The ICC value is a measurement of the variability due to error relative to the heterogeneity of the population. The heterogeneity of the population is represented by the between subjects variability, MS_B . As the intersession variability is mainly caused by an inconsistent marker placement, it is assumed that the variability due to error is mainly caused by random error. Therefore the variability due to error is represented by MS_E . It is known that the ICC depends on both the MS_E and MS_B value. For a good interpretation of the ICC it is desired that the ICC value is more dependent on the MS_E value than on the MS_B value. Therefore, further analysis of the effect of both MS_B and MS_E on the ICC value is required.

As the relationship between the ICC and MS_B is not linear, the Pearson correlation coefficient is not appropriate. An alternative correlation coefficient, the Kendall's tau, should be used in this case [48]. Kendall's tau represents how monotone the relationship between ICC and MS_B is. In the same way, the Kendall's tau is calculated for the relationship between ICC and MS_E .

Table IV.2.6 shows the Kendall's tau values. The values indicated in bold are the ones for which the ICC values of all models lie between 0 and 1 and thus a meaningful comparison of ICC values between the 8 models can be done. The Kendall's tau averaged over all the bold and thus meaningful values is also shown.

Table IV.2.6: Kendall's tau values of the relationship intersession ICC-MSB (left) and intersession ICC-MSE (right)

Kendall's tau MSB	PeakL	PeakR	RomL	RomR	Kendall's tau MSE	PeakL	PeakR	RomL	RomR
HipFlexExt	0,36	1,00	0,86	0,71	HipFlexExt	-0,29	-0,36	-0,57	0,07
HipAbAd	1,00	0,64	-0,29	-0,07	HipAbAd	0,21	-0,07	-0,36	-0,64
HipRot	0,57	0,57	0,71	0,71	HipRot	0,14	0,00	0,29	0,50
KneeFlexExt	0,57	0,29	0,36	0,86	KneeFlexExt	-0,14	-0,21	0,71	0,00
KneeVarVal	0,71	0,50	0,64	0,50	KneeVarVal	-0,21	-0,07	0,29	0,14
KneeRot	0,86	0,29	0,36	0,64	KneeRot	0,14	-0,21	0,14	0,29
AnkleDorPla	0,07	0,79	0,36	1,00	AnkleDorPla	-0,29	-0,07	-0,36	-0,93
AnkleInvAd	0,29	0,79	-0,29	0,71	AnkleInvAd	0,21	0,07	-0,50	-0,57
AnkleRot	0,29	0,57	-0,21	-0,14	AnkleRot	0,14	-0,29	-0,07	-0,50
			Mean	0,42				Mean	-0,15

A value equal to 1 means, when comparing two models, the model with the highest ICC value always has the highest corresponding MS_B value. A value of -0,93 means that in the majority of the pairs made out of the 8 models, an increase in ICC corresponds to a decrease in the MS_E value, but for a few model pairs there is a concordant relationship.

The average Kendall's tau is equal to 0,42 for the ICC- MS_B relationship. The positive value means that in the majority of the cases, a higher ICC value corresponds to a higher MS_B value. For the intersession ICC- MS_E relationship, the mean Kendall's tau value is -0,15. The negative value indicates that for most cases, a higher ICC value corresponds to a lower variability due to random error. Because $|-0,15| < |0,42|$, the relationship between the ICC and the MS_E is not as strong as between the ICC and the MS_B . A higher ICC corresponds thus often to a higher between subject variability and less often to a variability due to error.

Intrasession ICC

The intrasession ICC values are shown in tables B.0.2, B.0.3 and B.0.4 for session 1, 2 and 3 respectively.

Intrasession ICC values out of range

In theory the ICC values lay between 0 and 1 but in this study also negative intrasession ICC values are found in the results. Based on equation III.3, using $k = 10$ and $n = 2$, one can derive for the intrasession ICC:

$$ICC < 0 \Leftrightarrow MS_B < MS_E \quad (IV.3)$$

When the between subjects variability is smaller than the variability due to random error, the ICC will always be negative. With $k = 10$ and $n = 2$, the intrasession ICC value can never be larger than 1.

The cases in which all 8 models have an intrasession ICC between 0 and 1 are indicated

in bold in table B.0.2, B.0.3 and B.0.4.

Dependency of the intrasession ICC on MS_B and MS_E

As in the case of the intersession ICC, the intrasession ICC also depends on both MS_B and MS_E . The main sources of intrasession variability are STA and biological variability. It is assumed that, because of their nature, all both sources can be categorized under the random error term and therefore, the variability due to error is represented by MS_E . Also for the intrasession ICC it needs to be investigated how its value is influenced by MS_B and MS_E . The Kendall's tau values are shown in table IV.2.7.

Table IV.2.7: Kendall's tau values of relationship intrasession ICC- MS_B (left) and intrasession ICC- MS_E (right)

Kendall's tau MS_B Session 1	Peak L	Peak R	RomL	RomR	Kendall's tau MS_E Session 1	Peak L	Peak R	RomL	RomR
HipFlexExt	1	0,785714	0,642857	0,785714	HipFlexExt	0,142857	-0,35714	-0,21429	-0,28571
HipAbAd	0,857143	0,5	0,142857	0,571429	HipAbAd	0,5	0,071429	-0,28571	-0,35714
HipRot	0,571429	1	0,857143	1	HipRot	-0,5	0	-0,28571	0,214286
KneeFlexExt	0,928571	0,928571	0,428571	1	KneeFlexExt	0,571429	0,071429	-0,07143	-0,07143
KneeVarVal	0,857143	0,642857	0,928571	0,928571	KneeVarVal	-0,57143	0,071429	0	0,642857
KneeRot	0,857143	0,785714	0,714286	0,5	KneeRot	0,285714	-0,35714	0	0,142857
AnkleDorPla	0,714286	1	0,785714	0,714286	AnkleDorPla	-0,07143	0,214286	0,428571	-0,21429
AnkleInvAd	0,857143	0,928571	0,714286	0,642857	AnkleInvAd	-0,07143	-0,14286	0,214286	-0,28571
AnkleRot	1	0,928571	0,785714	0,642857	AnkleRot	-0,28571	-0,07143	0,5	-0,28571
			Mean	0,758242				Mean	-0,07418

Kendall's tau MS_B Session 2	Peak L	Peak R	RomL	RomR	Kendall's tau MS_E Session 2	Peak L	Peak R	RomL	RomR
HipFlexExt	0,785714	1	0,5	0,571429	HipFlexExt	-0,28571	0,142857	0	0,285714
HipAbAd	1	0,857143	0,785714	0,785714	HipAbAd	-0,07143	0,142857	-1	-0,28571
HipRot	0,857143	1	0,857143	0,571429	HipRot	-0,35714	-0,07143	-0,28571	0,142857
KneeFlexExt	1	1	0,785714	1	KneeFlexExt	0,428571	0,714286	-0,35714	0,142857
KneeVarVal	0,785714	0,714286	1	0,571429	KneeVarVal	-0,14286	-0,35714	0,5	0
KneeRot	0,785714	0,857143	0,714286	0,785714	KneeRot	0,142857	0	0,357143	0,214286
AnkleDorPla	0,928571	1	0,642857	0,714286	AnkleDorPla	0,071429	-0,07143	-0,21429	0,357143
AnkleInvAd	0,785714	0,928571	0,642857	1	AnkleInvAd	0	0,5	0,428571	-0,14286
AnkleRot	0,857143	1	0,642857	0,857143	AnkleRot	0,071429	0,214286	-0,57143	-0,35714
			Mean	0,801948				Mean	-0,03571

Kendall's tau MS_B Session 3	Peak L	Peak R	RomL	RomR	Kendall's tau MS_E Session 3	Peak L	Peak R	RomL	RomR
HipFlexExt	1	1	0,285714	0,857143	HipFlexExt	0,071429	0,428571	-0,71429	0,071429
HipAbAd	1	0,785714	0,5	0,357143	HipAbAd	-0,07143	0,357143	-0,78571	0
HipRot	0,857143	1	0,928571	0,928571	HipRot	-0,21429	0,285714	0	0
KneeFlexExt	0,928571	0,928571	1	1	KneeFlexExt	-0,35714	0,285714	0,5	-0,21429
KneeVarVal	0,642857	0,785714	0,928571	0,928571	KneeVarVal	0,142857	-0,5	0,357143	0,357143
KneeRot	0,785714	0,857143	0,857143	0,857143	KneeRot	0,142857	-0,42857	0,285714	0,071429
AnkleDorPla	0,785714	1	0,428571	1	AnkleDorPla	0,071429	0,214286	-0,07143	0,428571
AnkleInvAd	0,928571	0,857143	0,785714	1	AnkleInvAd	-0,5	0,5	-0,35714	0,785714
AnkleRot	0,928571	1	0,928571	0,857143	AnkleRot	-0,35714	-0,42857	0,214286	0,071429
			Mean	0,812169				mean	0,005291

The average Kendall's tau values for the ICC- MS_B relationship are positive and quite close to 1 for all three sessions. This indicates that almost always, when comparing the ICC values of 2 models, a higher ICC corresponds to a higher MS_B value. The average Kendall's tau value for the ICC- MS_E relationship is negative for the first two sessions and positive for the third session. All 3 values lie so close to zero that it can be approximately said that there is no correlation between the ICC and MS_E value. It can be concluded that the ICC value is mainly determined by the MS_B value and almost not by the MS_E

value.

Evaluating the utility of the ICC

A comparison of repeatability of the models can't be done using the ICC. Based on the previous, quite thorough analysis of the ICC, it can be concluded that the ICC is inappropriate to represent the repeatability in this study for several reasons:

- For both the intersession and intrasession ICC, many values lay outside the range and are therefore not interpretable. When the ICC value isn't between 0 and 1 for one of the 8 models, a meaningful comparison of the ICC values for that specific angle and summary parameter is not possible.
- The value of the ICC value is more determined by the between subjects variability than by the variability due to error. As this leads to a misinterpretation, it's better not to represent the repeatability of the models by the ICC.
- In the case of the intersession repeatability the power of the ANOVA test is too low as the group number is only 3. The intrasession ANOVA test has a higher power because of the higher group number ($k=10$). However, both ANOVA tests and as well the corresponding ICC's are only valid for the 2 subjects in the study. In any case, more subjects are required for more valuable ANOVA tests and ICC calculations.

IV.2.3 The Standard Error Measurement (SEM) and the Minimal Detectable Change (MDC)

Intersession SEM and MDC

Table C.0.1 in the appendix shows the intersession standard error measurement values. This gives an idea with what precision the mean peak and the mean range of motion can be measured in an individual session. In table D.0.1 in the appendix, the minimal detectable change values are shown. These represent the smallest difference that can be considered as a real change between the mean peak and the mean range of motion in two separate sessions. The smallest MDC value is underlined for each angle in table D.0.1.

As is done for the averaged standard deviation, the 'mean position method' is also applied on the intersession MDC values. The results are shown in table IV.2.8. The CGM23 and the CGM21 model share the first position in the intersession repeatability ranking based on the MDC values.

Table IV.2.8: 'Mean position' of the models in the ranking based on the intersession minimal detectable change values

Ranked Models	Mean Position
CGM23 / CGM21	2,8889
CGM11Med	3,3611
PiG	3,4167
CGM22	3,8333
CGM11Kad	3,8611
CGM10Kad	3,9444
CGM10Med	4,8065

The intersession repeatability of the eight models is ranked based on the 'mean position' method using both the intersession averaged standard deviation (table IV.2.1) and the intersession minimal detectable change (table IV.2.8). When comparing the corresponding tables, one can see that, the intersession repeatability ranking of the models is similar but not exactly the same. This is due to the fact that different error sources are taken into account. When calculating the minimal detectable change, only the random errors are considered, while in the ASD calculation, all the errors are included.

Intrasession SEM and MDC

Tables C.0.2, C.0.3 and C.0.4 in the appendix show the intrasession standard error measurement values of respectively session 1, 2 and 3. These intrasession SEM values represent the precision with which a peak or range of motion can be measured in one trial. In tables D.0.2, D.0.3, D.0.4 the values of the minimal detectable changes are shown. The lowest value is underlined for each angle. These values indicate the minimal difference that can be distinguished between the peaks or range of motions from 2 trials in the same session.

The intrasession repeatability ranking based on the MDC values, set up using the 'mean position' method, is shown in table IV.2.9.

Table IV.2.9: 'Mean position' of the models in the ranking based on the intrasession minimal detectable change values

Session 1	Session 1	Session2	Session2	Session 3	Session 3
CGM23	1,9167	CGM23	2,7222	CGM23	2,8333
CGM21	3,3056	PiG	2,9442	PiG	2,8611
PiG	3,3333	CGM21	3,1944	CGM21	2,8889
CGM11Med	3,4444	CGM10Kad	3,7778	CGM22	3,7222
CGM10Med	4,0278	CGM10Med/CGM11Med	3,8611	CGM11Med	4,0833
CGM22	4,25	CGM11Kad	3,9722	CGM11Kad	4,1389
CGM11Kad	4,3333	CGM22	4,6667	CGM10Med	4,1667
CGM10Kad	4,3889			CGM10Kad	4,3056

The CGM23 shows the best intrasession repeatability which corresponds to the lowest MDC values. The CGM21 and PiG model occupy the second and third places in the intrasession MDC ranking, as expected. Apart from the 3 models that scores the best (CGM23, PiG and CGM21) there is no consistency over the three sessions in the ranking of the subsequent models. This is in contradiction with the intrasession repeatability ranking based on the averaged standard deviation parameter (table IV.2.3). A possible explanation is that the calculation of the MDC value is only based on the random error. It is assumed that due to the nature of the intrasession errors, the random error is the main error source. The inconsistency between the sessions themselves and between the model ranking for the ASD and MDC parameter could suggest that the assumption that the random error is the main error, is wrong. In order to know for sure whether the neglect of the systematic error is the cause of the inconsistency, a more detailed investigation is required. This investigation is beyond the scope of this study.

The magnitude of the minimal detectable change

Knowing the magnitude of the intersession minimal detectable change is very valuable in clinical practice. It allows for example to evaluate the differences between pre- and postoperative gait. Also having an idea of the size order of the intrasession MDC is important. The magnitude of the minimal detectable change values can be consulted in tables D.0.1, D.0.2, D.0.3, D.0.4 in the appendix. However, taking general conclusions about the magnitude of the minimal detectable change is not possible because the MDC is highly dependent on the specific angle and summary parameter that is considered.

IV.2.4 Conclusions

The intersession and intrasession repeatability are tested through 3 parameters: the averaged standard deviation (absolute), the intraclass correlation coefficient (relative) and the minimal detectable change (absolute).

The ICC is shown to be inappropriate to represent the repeatability of the models in this study for three reasons. Firstly, the small between subject variability in this study leads to many ICC values which are meaningless because they don't lie between 0 and 1. Secondly, the ICC value is more determined by the between subject variability than by the variability due to error, which could lead to misinterpretation. Thirdly, the number of sessions and trials is too low which leads to insufficient power of the ANOVA on which the ICC calculation is based.

Hence, the conclusions concerning the repeatability are only based on absolute parameters (ASD and MDC). Looking at both parameters separately results in the unambiguous conclusion that the CGM23 model shows the best intersession repeatability. Also for the intrasession repeatability the CGM23 scores the best, although the intrasession repeatability

bility of the CGM23 model is comparable with the CGM21 and PiG model. The results show that the repeatability is highly dependent on the angle, however the repeatability is analyzed in general and not for all angles separately. The reason is that for clinical practice, this study is searching for the model with the best overall repeatability.

IV.3 How realistically is the physical gait represented?

IV.3.1 The crosstalk between the knee flexion/extension and the varus/valgus angle

Table IV.3.1 shows the absolute values of the average Kendall's tau value for each session, subject, model and side. The sign of the Kendall's tau value is related to the direction of the knee axis misalignment and is irrelevant in this discussion.

Table IV.3.1: The absolute value of the Kendall's tau averaged over 10 trials per session for the left and the right side

Averaged Kendall's tau Left	CGM10KAD	CGM10Med	CGM11KAD	CGM11Med	CGM21	CGM22	CGM23	PiG
Subject 1 Session 1	0,341172	0,762263	0,34703	0,118384	0,038545	0,161616	0,175434	0,429859
Subject 1 Session 2	0,548727	0,031313	0,550545	0,314465	0,376485	0,634465	0,422828	0,503273
Subject 1 Session 3	0,035192	0,250869	0,033818	0,652727	0,64598	0,791354	0,679838	0,005051
Subject 2 Session 1	0,301737	0,885576	0,29798	0,24404	0,208242	0,292727	0,53996	0,397899
Subject 2 Session 2	0,016808	0,891717	0,026384	0,353414	0,331596	0,347071	0,162182	0,079475
Subject 2 Session 3	0,289616	0,816929	0,296768	0,017091	0,022828	0,292929	0,398505	0,18998
Mean Subject 1	0,308364	0,348148	0,310465	0,361859	0,35367	0,529145	0,426034	0,312727
Mean Subject 2	0,202721	0,864741	0,207044	0,204848	0,187556	0,310909	0,366882	0,222451

Averaged Kendall's tau Right	CGM10KAD	CGM10Med	CGM11KAD	CGM11Med	CGM21	CGM22	CGM23	PiG
Subject 1 Session 1	0,252808	0,533495	0,255879	0,097212	0,022909	0,223919	0,024525	0,364889
Subject 1 Session 2	0,211152	0,398303	0,212525	0,081818	0,138545	0,349899	0,376727	0,156242
Subject 1 Session 3	0,010384	0,557455	0,012606	0,041778	0,006303	0,243798	0,175152	0,107919
Subject 2 Session 1	0,176364	0,875636	0,183111	0,176646	0,189818	0,194061	0,543879	0,192081
Subject 2 Session 2	0,383636	0,922222	0,390626	0,095434	0,171556	0,263758	0,731111	0,451636
Subject 2 Session 3	0,670384	0,903919	0,676121	0,342788	0,351556	0,433455	0,584889	0,68703
Mean Subject 1	0,158114	0,496418	0,160337	0,073603	0,055919	0,272539	0,192135	0,209684
Mean Subject 2	0,410128	0,900593	0,41662	0,204956	0,237643	0,297091	0,61996	0,443582

The crosstalk between the knee flexion/extension and varus/valgus angle is caused by a misalignment of the knee flexion/extension axis in the transverse plane. The question addressed in this section is: 'Which model results in the best alignment of the knee axis averaged over the three sessions?' The knee alignment is done in two ways: through the KAD (PiG, CGM10Kad and CGM11Kad) and through a medial and lateral knee marker (CGM10Med, CGM11Med, CGM21, CGM22 and CGM23). Answering the question separately for both groups, allows to conclude which model is least prone to knee misalignment per knee alignment method (KAD or medial and lateral knee marker).

First, the crosstalk between the flexion/extension and varus/valgus angle is analyzed in the models using the 2 knee markers for the knee alignment. The model which produces the lowest crosstalk between the knee flexion/extension and varus/valgus angle is most capable of generating a realistic kinematic output when errors in the knee marker placement are present. The models with a medial knee marker are the CGM11Med, CGM21, CGM22 and CGM23 model, as the CGM10Med model is not included in the discussion. As can be seen in table IV.3.1, the Kendall's tau values are very similar in the CGM11Med and CGM21 model; The difference is never larger than 0,10. This is in

line with the expectations as a shift in the HJC cannot affect the orientation of the knee flexion/extension axis in the transverse plane.

The lowest Kendall's tau value averaged over the three session is underlined per group. For the group 'Med models', the CGM11Med and CGM21 model show for both subjects and sides the lowest Kendall's tau value and thus the best knee axis alignment.

The models using the KAD device for the knee alignment are the PiG, CGM10Kad and CGM11Kad model. When looking at table IV.3.1, it's clear that the difference in average Kendall's tau values between the three models is always lower than 0,10. The CGM10Kad model has for all subjects and sessions the lowest Kendall's tau value averaged over the session but it can be said that the PiG, CGM10Kad and CGM11Kad model have a similar knee axis alignment.

When comparing both knee alignment methods, there can't be drawn conclusions about whether the medial and lateral knee marker or the KAD is the best knee alignment method. In some cases the KAD method provides a more realistic knee alignment, which corresponds to lower Kendall's tau values, and in some cases the two knee markers do. The intrasession ASD values of the knee varus/valgus and hip rotation angles, suggest that using the medial and lateral knee marker leads to more consistent knee alignment than using the KAD, but does also not indicate which alignment method is the most realistic one. Using the two knee markers leads thus to less intersession variability of the knee alignment, but no statements can be made about which knee alignment method leads to the most realistic knee alignment.

The numbers of correlation coefficients that significantly differ from zero are shown in table IV.3.2.

Table IV.3.2: Kendall's tau values significant different from zero (%)

Percent of Significant Kendall's tau Left	CGM10KAD	CGM10Med	CGM11KAD	CGM11Med	CGM21	CGM22	CGM23	PiG
Subject 1 Session 1	1	1	1	0,3	0,1	0,7	0,7	1
Subject 1 Session 2	1	0	1	1	1	1	1	1
Subject 1 Session 3	0	1	0	1	1	1	1	0,1
Subject 2 Session 1	1	1	1	1	0,9	1	1	1
Subject 2 Session 2	0,2	1	0,2	1	1	1	0,7	0,3
Subject 2 Session 3	1	1	1	0,1	0	0,9	1	0,7

Percent of Kendall's tau Right	CGM10KAD	CGM10Med	CGM11KAD	CGM11Med	CGM21	CGM22	CGM23	PiG
Subject 1 Session 1	1	1	1	0,2	0	1	0	1
Subject 1 Session 2	1	1	1	0	0,7	1	1	0,8
Subject 1 Session 3	0	1	0	0	0	1	0,7	0,3
Subject 2 Session 1	0,6	1	0,6	0,9	0,9	1	1	0,6
Subject 2 Session 2	1	1	1	0,2	0,9	1	1	1
Subject 2 Session 3	1	1	1	1	1	1	1	1

The less trials with a correlation significantly different from zero, the lower the correlation

is between the knee angles in that session. When looking at table IV.3.2, one can see that the number of significant correlations is indeed similar for the PiG, CGM10Kad and CGM11Kad model in all sessions.

Also for the CGM11Med and the CGM21 model the number of significant correlations is the same, except for the sessions indicated with a frame. However, in general it can be said that also based on the number of significant correlations, the CGM21 and CGM11Med model deal with a knee misalignment in the same way. The CGM21 and CGM11Med model also have for each session a lower number of significant correlations than the CGM22 and CGM23 model. Therefore, searching for the model with the least significant correlations, confirms the conclusion that when using a medial and lateral knee marker, the CGM21 and CGM11Med model result in the best knee alignment.

IV.3.2 The range of motion of the knee varus/valgus

A larger range of motion of the knee varus/valgus is related to a more extreme knee misalignment or more soft tissue artefact. Even if the modelled knee axis is perfectly aligned with the real physical axis, the STA ensures a non constant knee varus/valgus. The question that is addressed in this section is: 'Which model is least prone to the combination of knee misalignment and soft tissue artefact errors?'

Table IV.3.3: The varus/valgus range of motion averaged over the 10 trials per session

Average ROM Left	CGM10KAD	CGM10Med	CGM11KAD	CGM11Med	CGM21	CGM22	CGM23	PiG
Subject 1 Session1	10,06256	16,87141	10,06123	9,978653	11,27157	14,82916	5,711699	9,36266
Subject 1 Session 2	11,5641	10,46712	11,5626	10,98618	12,67407	18,15877	4,685826	9,36336
Subject 1 Session 3	10,54588	11,09165	10,53989	13,15628	14,40013	21,17221	8,536081	9,029058
Subject 2 Session 1	9,668835	30,0785	9,65082	9,353473	9,337508	13,24025	6,562841	9,34614
Subject 2 Session 2	9,108725	31,29209	9,088075	10,40066	10,33129	13,4502	4,944384	8,637857
Subject 2 Session 3	7,230074	18,72558	7,213296	7,897801	7,746825	7,800465	4,773564	6,521525
Mean Subject 1	10,72418	12,81006	10,72124	11,3737	12,78192	18,05338	6,311202	9,251692
Mean Subject 2	8,669211	26,69872	8,65073	9,21731	9,138541	11,49697	<u>5,42693</u>	8,168507

Average ROM Right	CGM10KAD	CGM10Med	CGM11KAD	CGM11Med	CGM21	CGM22	CGM23	PiG
Subject 1 Session1	11,97671	14,46659	11,96143	12,5688	14,22791	19,96275	6,460892	10,2084
Subject 1 Session 2	12,64982	13,96832	12,64411	12,51275	13,77988	17,84656	6,387463	11,87576
Subject 1 Session 3	13,99532	16,80097	13,97716	14,18388	15,52614	21,39324	7,837511	12,62157
Subject 2 Session 1	8,634259	24,55451	8,617211	9,705199	9,746469	12,52143	7,405557	7,592252
Subject 2 Session 2	7,363886	37,50256	7,369051	8,031547	7,999123	11,57214	7,349689	6,239522
Subject 2 Session 3	9,755856	41,13023	9,886246	8,620159	8,217537	11,5948	7,530481	8,732926
Mean Subject 1	12,87395	15,07863	12,8609	13,08848	14,51131	19,73418	6,895289	11,56858
Mean Subject 2	8,584667	34,39577	8,624169	8,785635	8,654376	11,89612	<u>7,428576</u>	7,521567

Table IV.3.3 shows the range of motion of the varus/valgus angle averaged over the 10 trials per session. The mean ROM over all the sessions is also presented. The lowest range of motion is for both subjects and sides found in the CGM23 model (underlined in table IV.3.3). This indicates that the CGM23 model is least prone to the combination of knee misalignment and soft tissue artefact errors. Analyzing the crosstalk between the knee flexion/ extension and varus/valgus angle, demonstrated that the CGM21 and CGM11Med models are less prone to knee axis misalignment than the CGM23 model.

The fact that the varus/valgus ROM of the CGM23 model is in all cases the smallest, suggests that the CGM23 model is less sensible to soft tissue artefact and that the STA overshadows the effect of the knee misalignment on the varus/valgus ROM. This is in agreement with the high intrasession repeatability of the CGM23 model.

IV.3.3 Conclusions

The model which represents the real physical gait the best is in fact the model which is least prone to errors. The two types of errors that are considered, are the knee misalignment and the soft tissue artefact.

When analyzing the crosstalk between the knee flexion/extension and varus/valgus only the knee alignment error is considered. This analysis demonstrated that all the models using the KAD result in a similar knee misalignment. From all the models using the lateral and medial knee marker, the CGM21 and CGM11Med model result in a similar knee alignment which is more realistic than the knee alignment in the CGM22 and CGM23 model.

On the other hand, when considering both the knee alignment error and the soft tissue artefact, the CGM23 model performs the best. This is due to the low soft tissue artefact present in the CGM23 model.

Chapter V

Additional remarks

V.1 The ease of use of the pyCGM2 package

A criteria that is not discussed in this report but which is also important in order to be appropriate for clinical practice, is the ease of use. No matter how repeatable, comprehensible and accurate the model is, if it's not easy to work with, it can't be used in clinical practice. In general, the main problem of the pyCGM2 package version 3.0.8 is that it is too sensitive to errors of the user. For example, when the marker labelling and the event detection are done, it's impossible to change the model template of the subject. If an incorrect VST workflow is chosen in the beginning, it's impossible to undo this error. In the PiG model, the error can be undone which saves a lot of time. A high concentration is needed when working with the pyCGM2 package, as one small error can lead to for example ankle axes which rotate 360° during walking. If this is the case, the user needs to restart from the very beginning. Therefore, the PiG is felt to be more user friendly.

V.2 Future work

In this study, the appropriateness for clinical application is checked on a small sample of normal subjects. Firstly, the normative database needs to be expanded to a wider range of ages and BMIs. Secondly, for each pathology the data analysis needs to be done again because the results of this study can't be generalized for the wide range of pathologies.

That the kinematic output is dependent on the spatial-temporal parameters, such as stride length and walking speed is well known [37],[38]. For example the knee flexion/extension peak, the knee rotation angle and the ankle dorsi/plantar flexion angle increase with the increasing walking speed [37]. The varus/valgus angle on the other hand has been shown to be independent of the walking speed [38]. Although the walking speed is one of the most important sources of variability in the kinematic output, it is not

taken into account in this study. It is recommended that further study of the impact of spatial-temporal parameter variation is made in future studies.

In this study no distinction has been made (although alluded in the context of STA) between the different phases of the gait cycle. When using for example the averaged standard deviation, the difference between the variability at the initial contact and in the swing phase is not considered, although this could give interesting insights. Furthermore, the crosstalk between the knee flexion/extension and varus valgus is expected to be largest in the swing phase but this was not checked in the data analysis of this study. More attention to the different phases of the gait cycle is desired in future studies.

The CGM2.i project has recently started-off and is still ongoing. Whether the CGM2.4, CGM2.5, CGM2.6 and any other future models offer an improvement to the CGM2.3 model still needs to be checked.

Chapter VI

Conclusions

The research question of this master thesis is: 'Do the lower limb kinematic CGM2.i models form a suitable alternative to the PiG model in a clinical setting?'. The CGM2.i models that are investigated in this study are the CGM10Kad, CGM10Med, CGM11Kad, CGM11Med, CGM21, CGM22 and CGM23 model. The 3 pillars on which the data analysis focuses, in order to address the question, are: a pairwise comparison of the underlying segment definitions and the kinematic output, the repeatability and how well the physical gait is represented.

Pairwise comparison of the segment axes and kinematic output

In order to be suitable for clinical practice, the derivation of the kinematic output and the relationship with the defined segments needs to be transparent and in this context any changes from the current clinical standard needs to be understood. This issue is addressed by ascertaining that the differences between 2 models are conform with the theory behind the models. An overview of the pairwise comparison is shown in table VI.0.1. The CGM10Med is eliminated since version 3.0.8 of the pyCGM2 package appears to contain a software bug for this particular model. The segment definitions and kinematic output are found to be understandable for CGM10Kad, CGM10Med, CGM11Kad, CGM11Med and CGM21, except from some shifts in the HJC and foot origin. For the CGM22 and CGM23 model, the joint centers and segment axes can't be seen in Nexus, which results in a lower transparency these 2 models.

Table VI.0.1: Overview pairwise comparison of the models

		Segments axes	Kinematics
CGM10Kad-PiG	Expected	Variable AJC position	Variable change in Ankle Rotation
	Errors	AP shift in HJC ML shift in foot origin	Hip Flexion/Extension offset Knee Flexion/Extension offset /
CGM11Kad-CGM10Kad	Expected	untortioned vs. tortioned tibia segment	Knee Rotation offset = τ
	Errors	SI shift in foot origin	Ankle Dorsi/Plantar offset
CGM11Kad-CGM11Med	Expected	Different knee alignment	Offsets in Hip/Knee and Ankle angles ! Further investigation needed !
	Errors	AP shift in HJC	Hip Flexion/Extension offset
		AP shift in foot origin	Knee Flexion/Extension offset /
CGM21-CGM11Med	Expected	SI and ML shift in HJC	Hip Abduction/Adduction offset Knee Varus/Valgus offset
	Errors	/	/
CGM22-CGM21	Expected	Exact same static segment axes	Related to soft tissue artefact
	Errors	Dynamic segments not overwritten by OpenSim IK solver	Kinematics can't be fully interpreted
CGM23-CGM22	Expected	Exact same static segment axes	Related to soft tissue artefact
	Errors	Dynamic segments not overwritten by OpenSim IK solver	Kinematics can't be fully interpreted

Repeatability

Both the intersession and intrasession repeatability are investigated using 3 parameters: the average standard deviation (ASD), the intraclass correlation coefficient (ICC) and the minimal detectable change (MDC). The ICC is demonstrated to be inappropriate to compare the repeatability of the eight models in this study. Firstly, many ICC values are meaningless as they didn't lie between 0 and 1 due to the low between subject variability. Secondly the ICC value is more dependent on the between subject variability than on the variability due to error, which leads to misinterpretation. Therefore, the repeatability of the models is compared only based on the ASD and MDC parameters. Both parameters conclude that CGM23 scores the best in terms of intersession repeatability and also for the intrasession repeatability CGM23 scores very well, similar to CGM21 and PiG .

How well is the real physical gait represented?

The model which represents the real physical gait the best is in fact the model which is least prone to errors. The two types of errors that are considered, are knee axis misalignment and soft tissue artefact. When analyzing the crosstalk between the knee flexion/extension and varus/valgus only the knee alignment error is considered. This analysis demonstrated that all the models using the KAD result in a similar knee misalignment. From all the models using the lateral and medial knee marker, the CGM21 and CGM11Med model result in a similar knee alignment which is more realistic than

the knee alignment in CGM22 and CGM23. On the other hand, when considering both the knee alignment error and the soft tissue artefact by analyzing the varus/valgus ROM, CGM23 performs the best. This is probably due to the low soft tissue artefact present in the CGM23 model.

Is CGM23 a suitable alternative to PiG in a clinical setting?

CGM23 is designed to be less susceptible to soft tissue artefact than the PiG model. Using the 'inverse kinematic method' with a larger number of markers, positioned on anatomical landmarks felt to be less prone to STA, reduces the importance of markers particularly prone to STA such as the lateral knee marker.

The intersession repeatability is higher for the CGM23 than for the PiG model and the intrasession repeatability is comparable. The CGM23 model is demonstrated to be least sensitive to soft tissue artefact and least susceptible to knee axis misalignment when both error types are considered together. When only taking into account the knee axis misalignment, by an analysis of the crosstalk between the knee flexion/extension and varus/valgus, CGM23 is not shown to be less prone to errors than the PiG model. The overall intersession ASD value of the knee varus/valgus and hip rotation are lower for the CGM23 model than for the PiG model which indicates a more consistent knee (mis)alignment over the session in the CGM23 model (section IV.2.1). It is thus suggested that the knee axis alignment is more consistent over the session in the CGM23 model but more correct in the PiG model.

In terms of underlying segment definitions and kinematic output the PiG model is more understandable since CGM23 is a black box with unknown (at least unseen) joint centers and segments. Besides the 3 pillars on which the data analysis focuses, there is also a fourth important criteria: the ease of use. The pyCGM2 packages are very sensitive to human errors and therefore the PiG is felt to be more user friendly.

Leading to the conclusion that the CGM23 will be more appropriate for clinical practice than the PiG model once the following points are addressed:

1. Although the unexpected shifts in HJC's and foot origins in the CGM2.i models are found to have a predictable impact on the kinematics in a range of patient pathologies, an explanation of the shifts is desired as the previous CGM2.i models form the basis for CGM23.
2. The joint centers and segment axes of the CGM23 model need to be available in Nexus. This allows to confirm that the segment length is constant and that the CGM23 model is compatible with other biomechanical models.
3. The knee axis misalignment leading to a large crosstalk between the knee flex-

ion/extension and varus/valgus.

4. For all the CGM2.i models, the pyCGM2 package must become more user friendly.

Bibliography

- [1] R. B. Davis, S. Öunpuu, D. Tyburski, and J. R. Gage, “A gait analysis data collection and reduction technique,” *Human Movement Science*, vol. 10, pp. 575–587, 1991.
- [2] “Vicon Nexus User Guide.”
- [3] M. W. Whittle, “Clinical gait analysis: A review,” tech. rep., 1996.
- [4] G. Paolini, “Plug in Gait WebEx Training Session 3 Interpreting PiG results: PiG biomechanical modelling,” tech. rep.
- [5] Vicon Motion Systemd Ltd., *Plug-in Gait Reference Guide*. 2016.
- [6] F. Leboeuf, “CGM2.4 Extended-Foot-Model,” 2018.
- [7] Vicon Motion Systems, “Plug-In-Gait Kinematic Variables,” in *Plug-in Gait Reference Guide*, pp. 72–80, 2016.
- [8] F. Leboeuf, “Weaknesses of the Conventional Gait Model,” 2018.
- [9] A. Leardini, A. Cappozzo, F. Catani, S. Toksvig-Larsen, A. Petitto, V. Sforza, G. Cassanelli, and S. Giannini, “Validation of a functional method for the estimation of hip joint centre location,” tech. rep., 1999.
- [10] M. Sangeux, H. Pillet, and W. Skalli, “Which method of hip joint centre localisation should be used in gait analysis?,” *Gait and Posture*, vol. 40, no. 1, pp. 20–25, 2014.
- [11] A. Peters, B. Galna, M. Sangeux, M. Morris, and R. Baker, “Quantification of soft tissue artifact in lower limb human motion analysis: A systematic review,” 1 2010.
- [12] M. C. Carson, M. E. Harrington, N. Thompson, J. J. O’Connor, and T. N. Theologis, “Kinematic analysis of a multi-segment foot model for research and clinical applications: a repeatability analysis.,” *Journal of biomechanics*, vol. 34, pp. 1299–307, 10 2001.
- [13] F. Leboeuf, “CGM2.i Project: Design Criteria,” 2018.
- [14] F. Leboeuf, “The CGM2.i project,” 2018.

- [15] F. Leboeuf, “CGM2.i Project: Future Requirements,” 2018.
- [16] F. Leboeuf, R. Baker, A. Barré, J. Reay, R. Jones, and M. Sangeux, “The conventional gait model, an open-source implementation that reproduces the past but prepares for the future,” *Gait and Posture*, vol. 69, pp. 126–129, 3 2019.
- [17] “Tibia,” in *Plug-In-Gait Reference Guide*, p. 52, 2016.
- [18] A. G. Schache and R. Baker, “On the expression of joint moments during gait,” *Gait and Posture*, vol. 25, pp. 440–452, 3 2007.
- [19] A. G. Schache, R. Baker, and C. L. Vaughan, “Differences in lower limb transverse plane joint moments during gait when expressed in two alternative reference frames,” *Journal of Biomechanics*, vol. 40, no. 1, pp. 9–19, 2007.
- [20] Vicon Motion Systems, “PiG output specification,” in *Plug-in Gait Reference Guide*, p. 93, 2016.
- [21] R. Baker, “Pelvic angles: A mathematically rigorous definition which is consistent with a conventional clinical understanding of the terms,” *Gait and Posture*, vol. 13, no. 1, pp. 1–6, 2001.
- [22] J. L. Hicks and J. G. Richards, “Clinical applicability of using spherical fitting to find hip joint centers,” *Gait and Posture*, vol. 22, pp. 138–145, 10 2005.
- [23] R. M. Ehrig, W. R. Taylor, G. N. Duda, and M. O. Heller, “A survey of formal methods for determining the centre of rotation of ball joints.,” *Journal of biomechanics*, vol. 39, no. 15, pp. 2798–809, 2006.
- [24] R. Hara, J. McGinley, C. Briggs, R. Baker, and M. Sangeux, “Predicting the location of the hip joint centres, impact of age group and sex,” *Scientific Reports*, vol. 6, 11 2016.
- [25] F. Leboeuf, “CGM2.1 Overview,” 2018.
- [26] T.-W. Lu, D. Phil, T.-W. Lu, and J. J. O’connor, “Bone position estimation from skin marker co-ordinates using global optimisation with joint constraints,” tech. rep., 1999.
- [27] F. Leboeuf, M. Sangeux, and R. Baker, “Direct kinematics and kinematic fitting provide very similar outputs when using the conventional gait model,” *Gait & Posture*, vol. 57, p. 196, 7 2017.
- [28] Open Sim Documentation, “How Inverse Kinematics Work,” 2017.
- [29] Open Sim Documentation, “Getting Started with Inverse Kinematics,” 2017.

- [30] F. Leboeuf, “CGM2.2 Overview,” 2018.
- [31] “Inverse Kinematics.”
- [32] F. Leboeuf, “CGM2.3 Removal of Thigh Wands,” 2018.
- [33] A. Peters, M. Sangeux, M. E. Morris, and R. Baker, “Determination of the optimal locations of surface-mounted markers on the tibial segment,” *Gait and Posture*, vol. 29, pp. 42–48, 1 2009.
- [34] J. Cockcroft, Q. Louw, and R. Baker, “Proximal placement of lateral thigh skin markers reduces soft tissue artefact during normal gait using the Conventional Gait Model,” *Computer Methods in Biomechanics and Biomedical Engineering*, vol. 19, pp. 1497–1504, 10 2016.
- [35] F. Leboeuf, “CGM2.6 Knee Calibration,” 2018.
- [36] J. L. McGinley, R. Baker, R. Wolfe, and M. E. Morris, “The reliability of three-dimensional kinematic gait measurements: A systematic review,” 4 2009.
- [37] J. W. Kwon, S. M. Son, and N. K. Lee, “Changes of kinematic parameters of lower extremities with gait speed: a 3D motion analysis study,” *Journal of Physical Therapy Science*, vol. 27, pp. 477–479, 2 2015.
- [38] C. Kirtley, M. W. Whittle, and R. J. Jefferson, “INFLUENCE OF WALKING SPEED ON GAIT PARAMETERS,” tech. rep.
- [39] A. Leardini, Z. Sawacha, G. Paolini, S. Ingrosso, R. Nativo, and M. G. Benedetti, “A new anatomically based protocol for gait analysis in children,” *Gait and Posture*, 2007.
- [40] J. L. McGinley, R. Baker, R. Wolfe, and M. E. Morris, “The reliability of three-dimensional kinematic gait measurements: A systematic review,” 4 2009.
- [41] I. W. Charlton, P. Tate, P. Smyth, and L. Roren, “Repeatability of an optimised lower body model,” *Gait and Posture*, vol. 20, pp. 213–221, 10 2004.
- [42] J. P. Weir, “QUANTIFYING TEST-RETEST RELIABILITY USING THE INTRACLASS CORRELATION COEFFICIENT AND THE SEM,” Tech. Rep. 1, 2005.
- [43] K. O. McGraw, “Forming Inferences About Some Intraclass Correlation Coefficients Intrinsic motivation View project,” 1996.
- [44] R. Ferber, I. McClay Davis, D. S. Williams, and C. Laughton, “A comparison of within- and between-day reliability of discrete 3D lower extremity variables in runners,” *Journal of Orthopaedic Research*, 2002.

- [45] T. K. Koo and M. Y. Li, “A Guideline of Selecting and Reporting Intraclass Correlation Coefficients for Reliability Research,” *Journal of Chiropractic Medicine*, 2016.
- [46] Arash Salarian, “Mathworks: Intraclass Correlation Coefficient.”
- [47] F. Colle, D. Bruni, F. Iacono, A. Visani, S. Zaffagnini, M. Marcacci, and N. Lopomo, “Changes in the orientation of knee functional flexion axis during passive flexion and extension movements in navigated total knee arthroplasty,” *Knee Surgery, Sports Traumatology, Arthroscopy*, vol. 24, pp. 2461–2469, 8 2016.
- [48] J. Prof. dr. De Neve, “Cursus Statistiek 1.” 2016.

Appendices

Appendix A

Averaged Standard Deviation

Table A.0.1: Subject 1: Intersession averaged SD (Left and Right side)

Subject 1 Left	CGM10KAD	CGM10Med	CGM11KAD	CGM11Med	CGM21	CGM22	CGM23	PiG
HipFlexExt	3,03670806	3,54733751	3,03576944	2,47032115	2,366252	2,228523	2,291102	3,032676
HipAbAd	0,72417455	0,659071021	0,72394871	0,7581346	0,728266	0,551495	0,462793	0,714737
HipRot	5,57289558	6,71580513	5,59955662	5,15671092	5,193894	5,277962	2,626005	5,528096
KneeFlexExt	1,87875746	2,53315979	1,87919765	0,95446861	0,956037	0,970264	1,074422	1,834301
KneeVar Val	1,73075182	3,321933766	1,73590299	1,54658932	1,561595	1,888433	0,859195	1,845839
KneeRot	5,09634539	4,695304242	4,39936491	4,76765985	4,787795	5,880476	2,950132	5,027482
AnkleDorPla	0,9634066	0,791176428	0,55069982	0,54358292	0,551744	0,536997	0,393978	0,596859
AnkleInvAd	0,52189041	1,684517531	0,3451378	0,3656144	0,368854	0,602469	0,408795	0,565779
AnkleRot	1,03728839	10,54127746	0,95334382	1,80048085	1,786577	2,690611	1,891291	1,683634

Subject 1 Right	CGM10KAD	CGM10Med	CGM11KAD	CGM11Med	CGM21	CGM22	CGM23	PiG
HipFlexExt	2,0440089	2,014484478	2,04615104	2,08937731	2,011201	1,967497	1,772084	2,081684
HipAbAd	1,07184169	1,073630347	1,07163516	1,07004116	1,024932	0,853204	1,05961	1,048986
HipRot	3,78725071	8,439190071	3,82226865	2,11426158	2,216232	2,674075	1,739578	3,584667
KneeFlexExt	1,11295974	1,81609448	1,11510626	0,97290513	0,962945	0,953273	0,809829	1,544515
KneeVar Val	1,38681439	3,973066063	1,39359776	0,64943322	0,63291	0,97505	0,772184	1,484128
KneeRot	2,41148782	4,467544171	2,62843573	1,40264167	1,467839	1,882141	2,292744	2,326939
AnkleDorPla	2,26920829	2,335240239	0,6474077	0,57310639	0,583956	0,578954	0,536952	0,596806
AnkleInvAd	0,31898993	2,07857753	0,47406915	0,31632547	0,32434	0,312894	0,456406	0,878719
AnkleRot	1,47703444	11,92952295	1,45955756	1,04900805	1,053022	1,174392	1,826127	7,605454

Table A.0.2: Subject 2: Intersession averaged SD (Left and Right side)

Subject 2	CGM10KAD	CGM10Med	CGM11KAD	CGM11Med	CGM21	CGM22	CGM23	PiG
Left								
HipFlexExt	2,43997	2,20098	2,44020	2,01564	1,92352	1,91312	1,95737	2,42604
HipAbAd	0,77016	0,60935	0,77007	0,78242	0,73747	0,99670	1,08806	0,79535
HipRot	4,46650	7,82642	4,46370	3,37719	3,32771	4,57903	2,02544	4,35264
KneeFlexExt	1,82081	2,91856	1,81935	1,07222	0,98460	1,05205	1,03955	1,78041
KneeVar Val	1,76832	2,90151	1,76426	1,55608	1,52943	2,15769	0,87799	1,89423
KneeRot	1,46881	4,42445	1,58706	3,56826	3,59653	3,45562	3,35969	1,55265
AnkleDorPla	2,86823	3,20443	1,06772	0,82509	0,82244	1,07036	0,70055	0,99675
AnkleInvAd	2,16968	1,20824	1,25051	1,16417	1,14587	1,07652	0,99498	1,58969
AnkleRot	2,46803	4,19959	2,73294	1,65209	1,61945	1,97135	1,42471	3,92508
Subject 2 Right								
HipFlexExt	2,07256	1,98154	2,07326	2,26798	2,16976	2,04060	1,94197	2,10112
HipAbAd	1,11818	0,77104	1,11643	1,18100	1,12303	1,43453	1,53120	1,11818
HipRot	4,55983	10,15705	4,60570	1,27209	1,46662	1,85860	0,96501	4,41284
KneeFlexExt	1,34157	4,48213	1,34157	1,76184	1,66416	1,68994	1,39678	1,34417
KneeVar Val	1,68948	2,65812	1,70392	0,64618	0,68281	0,72392	0,66691	1,76972
KneeRot	2,67995	6,04480	2,07530	1,00041	1,11841	1,77075	1,23373	2,47435
AnkleDorPla	1,51655	1,71351	0,89647	1,10180	1,10681	1,15293	0,90391	0,86439
AnkleInvAd	0,79485	1,03828	0,55285	0,63813	0,64205	0,72675	0,44374	0,70825
AnkleRot	1,02422	5,58959	1,13981	1,42337	1,44253	1,75807	0,93884	3,94683

Table A.0.3: Ranking of the different models from best to worst intersession repeatability (based on the intersession averaged SD value)

Subject 1 Left	Best							Worst
HipFlexExt	CGM22	CGM23	CGM21	CGM11Med	PiG	CGM11KAD	CGM10KAD	CGM10Med
HipAbAd	CGM23	CGM22	CGM10Med	PiG	CGM11KAD	CGM10KAD	CGM21	CGM11Med
HipRot	CGM23	CGM11Med	CGM21	CGM22	PiG	CGM10KAD	CGM11KAD	CGM10Med
KneeFlexExt	CGM11Med	CGM21	CGM22	CGM23	PiG	CGM10KAD	CGM11KAD	CGM10Med
KneeVarVal	CGM23	CGM11Med	CGM21	CGM10KAD	CGM11KAD	PiG	CGM22	CGM10Med
KneeRot	CGM23	CGM11KAD	CGM10Med	CGM11Med	CGM21	PiG	CGM10KAD	CGM22
AnkleDorPla	CGM23	CGM22	CGM11Med	CGM11KAD	CGM21	PiG	CGM10Med	CGM10KAD
AnkleInvAd	CGM11KAD	CGM11Med	CGM21	CGM23	CGM10KAD	PiG	CGM22	CGM10Med
AnkleRot	CGM11KAD	CGM10KAD	PiG	CGM21	CGM11Med	CGM23	CGM22	CGM10Med

Subject 1 Right	Best							Worst
HipFlexExt	CGM23	CGM22	CGM21	CGM10Med	CGM10KAD	CGM11KAD	PiG	CGM11Med
HipAbAd	CGM22	CGM21	PiG	CGM23	CGM11Med	CGM11KAD	CGM10KAD	CGM10Med
HipRot	CGM23	CGM11Med	CGM21	CGM22	PiG	CGM10KAD	CGM11KAD	CGM10Med
KneeFlexExt	CGM23	CGM22	CGM21	CGM11Med	CGM10KAD	CGM11KAD	PiG	CGM10Med
KneeVarVal	CGM21	CGM11Med	CGM23	CGM22	CGM10KAD	CGM11KAD	PiG	CGM10Med
KneeRot	CGM11Med	CGM21	CGM22	CGM23	PiG	CGM10KAD	CGM11KAD	CGM10Med
AnkleDorPla	CGM23	CGM11Med	CGM22	CGM21	PiG	CGM11KAD	CGM10KAD	CGM10Med
AnkleInvAd	CGM22	CGM11Med	CGM10KAD	CGM21	CGM23	CGM11KAD	PiG	CGM10Med
AnkleRot	CGM11Med	CGM21	CGM22	CGM11KAD	CGM10KAD	CGM23	PiG	CGM10Med

Subject 2 Left	Best							Worst
HipFlexExt	CGM22	CGM21	CGM23	CGM11Med	CGM10Med	PiG	CGM10KAD	CGM11KAD
HipAbAd	CGM10Med	CGM21	CGM11KAD	CGM10KAD	CGM11Med	PiG	CGM22	CGM23
HipRot	CGM23	CGM21	CGM11Med	PiG	CGM11KAD	CGM10KAD	CGM22	CGM10Med
KneeFlexExt	CGM21	CGM23	CGM22	CGM11Med	PiG	CGM11KAD	CGM10KAD	CGM10Med
KneeVarVal	CGM23	CGM21	CGM11Med	CGM11KAD	CGM10KAD	PiG	CGM22	CGM10Med
KneeRot	CGM10KAD	PiG	CGM11KAD	CGM23	CGM22	CGM11Med	CGM21	CGM10Med
AnkleDorPla	CGM23	CGM21	CGM11Med	PiG	CGM11KAD	CGM22	CGM10KAD	CGM10Med
AnkleInvAd	CGM23	CGM22	CGM21	CGM11Med	CGM10Med	CGM11KAD	PiG	CGM10KAD
AnkleRot	CGM23	CGM21	CGM11Med	CGM22	CGM10KAD	CGM11KAD	PiG	CGM10Med

Subject 2 Right	Best							Worst
HipFlexExt	CGM23	CGM10Med	CGM22	CGM10KAD	CGM11KAD	PiG	CGM21	CGM11Med
HipAbAd	CGM10Med	CGM11KAD	PiG	CGM10KAD	CGM21	CGM11Med	CGM22	CGM23
HipRot	CGM23	CGM11Med	CGM21	CGM22	PiG	CGM10KAD	CGM11KAD	CGM10Med
KneeFlexExt	CGM10KAD	CGM11KAD	PiG	CGM23	CGM21	CGM22	CGM11Med	CGM10Med
KneeVarVal	CGM11Med	CGM23	CGM21	CGM22	CGM10KAD	CGM11KAD	PiG	CGM10Med
KneeRot	CGM11Med	CGM21	CGM23	CGM22	CGM11KAD	PiG	CGM10KAD	CGM10Med
AnkleDorPla	PiG	CGM11KAD	CGM23	CGM11Med	CGM21	CGM22	CGM10KAD	CGM10Med
AnkleInvAd	CGM23	CGM11KAD	CGM11Med	CGM21	PiG	CGM22	CGM10KAD	CGM10Med
AnkleRot	CGM23	CGM10KAD	CGM11KAD	CGM11Med	CGM21	CGM22	PiG	CGM10Med

Table A.0.4: Subject 1 Left: Intrasession averaged SD for the 3 sessions

Subject 1 Left Session 1	CGM10KAD	CGM10Med	CGM11KAD	CGM11Med	CGM21	CGM22	CGM23	PiG
HipFlexExt	1,247594	1,248369	1,247484	1,249285	1,204416	1,227077	1,169944	1,217684
HipAbAd	0,624928	0,637222	0,624829	0,628104	0,601734	0,63142	0,664246	0,6435
HipRot	1,318589	1,330655	1,317866	1,337283	1,365076	1,633104	1,08152	1,180263
KneeFlexExt	1,914932	1,856776	1,915003	1,911243	1,898672	1,912668	1,948328	1,883724
KneeVarVal	0,644455	0,711276	0,644027	0,657523	0,666016	0,884548	0,440752	0,60817
KneeRot	1,662413	1,606569	1,662432	1,652505	1,661576	2,391918	1,327083	1,292014
AnkleDorPla	1,070171	1,181986	1,069318	1,06553	1,067608	1,059193	1,070359	1,047119
AnkleInvAd	0,295261	0,289609	0,284469	0,287466	0,288203	0,414972	0,239469	0,254885
AnkleRot	1,602908	1,731914	1,604173	1,601467	1,599687	2,166924	1,362545	1,429905

Subject 1 Left Session 2	CGM10KAD	CGM10Med	CGM11KAD	CGM11Med	CGM21	CGM22	CGM23	PiG
HipFlexExt	1,19583	1,198349	1,195717	1,198226	1,156582	1,166214	1,130714	1,201185
HipAbAd	0,654563	0,652446	0,654523	0,653991	0,626457	0,646373	0,676765	0,591809
HipRot	1,223226	1,225403	1,223002	1,225728	1,252008	1,631544	1,095806	1,024457
KneeFlexExt	1,774762	1,805782	1,77472	1,789613	1,769782	1,77052	1,792459	1,765709
KneeVarVal	0,715823	0,689341	0,715542	0,701654	0,713476	1,049504	0,42991	0,664164
KneeRot	1,762122	1,777457	1,762315	1,766381	1,775621	2,509743	1,408134	1,529352
AnkleDorPla	0,989503	0,959709	0,986761	0,972718	0,974086	0,974855	0,924757	0,9378
AnkleInvAd	0,438245	0,360382	0,430868	0,415974	0,416237	0,571583	0,315593	0,356997
AnkleRot	1,756074	1,703116	1,757646	1,731963	1,728771	2,357531	1,376102	1,714351

Subject 1 Left Session 3	CGM10KAD	CGM10Med	CGM11KAD	CGM11Med	CGM21	CGM22	CGM23	PiG
HipFlexExt	1,085524	1,090195	1,085328	1,08996	1,052148	1,061089	1,026141	1,059316
HipAbAd	0,615636	0,619648	0,615519	0,622265	0,596031	0,656977	0,70098	0,588047
HipRot	1,087865	1,092112	1,087589	1,090194	1,111747	1,276057	1,135283	0,905372
KneeFlexExt	1,578682	1,572521	1,578701	1,546511	1,536577	1,548085	1,558015	1,525017
KneeVarVal	0,475801	0,4966	0,475647	0,557604	0,558287	0,750191	0,41626	0,432415
KneeRot	1,525941	1,518214	1,525569	1,496523	1,504772	2,139846	1,263888	1,246445
AnkleDorPla	0,77192	0,772456	0,772453	0,752361	0,751997	0,748933	0,717469	0,668305
AnkleInvAd	0,367107	0,301179	0,324274	0,318952	0,319481	0,513038	0,267964	0,271047
AnkleRot	1,432208	1,455604	1,441907	1,416624	1,419473	2,098707	1,185445	1,312421

Table A.0.5: Subject 1 Right: Intrasession averaged SD for the 3 sessions

Subject 1 Right Session 1	CGM10KAD	CGM10Med	CGM11KAD	CGM11Med	CGM21	CGM22	CGM23	PiG
HipFlexExt	1,213044	1,210538	1,213051	1,211746	1,169857	1,164045	1,099316	1,190429
HipAbAd	0,691439	0,701965	0,691416	0,692725	0,664161	0,68372	0,727449	0,691228
HipRot	1,193665	1,197956	1,193246	1,203312	1,227036	1,516213	1,093064	1,050314
KneeFlexExt	1,560487	1,503143	1,56067	1,551378	1,538032	1,53948	1,306002	1,337455
KneeVarVal	0,552628	0,666431	0,552162	0,573007	0,580802	0,800441	0,346859	0,475864
KneeRot	1,541816	1,506034	1,541906	1,538067	1,543442	2,255682	0,999533	1,10361
AnkleDorPla	0,902717	0,883742	0,907378	0,897801	0,898446	0,89362	0,698145	0,726329
AnkleInvAd	0,465862	0,41497	0,370339	0,367669	0,365779	0,517004	0,27393	0,309726
AnkleRot	1,748769	1,747649	1,770499	1,756092	1,75174	2,393072	1,353993	1,535018

Subject 1 Right Session 2	CGM10KAD	CGM10Med	CGM11KAD	CGM11Med	CGM21	CGM22	CGM23	PiG
HipFlexExt	1,056768	1,054328	1,056789	1,055139	1,016677	0,990434	0,938885	1,027281
HipAbAd	0,683156	0,679125	0,683145	0,682373	0,653467	0,688274	0,700096	0,615849
HipRot	1,249269	1,240314	1,249385	1,243707	1,25657	1,470069	0,987066	1,123645
KneeFlexExt	1,337176	1,374015	1,337068	1,346621	1,325185	1,316299	1,312948	1,245749
KneeVarVal	0,580483	0,569315	0,580261	0,577395	0,595239	0,804294	0,397821	0,515481
KneeRot	1,469426	1,501961	1,46887	1,476242	1,483516	1,891245	1,074371	1,171708
AnkleDorPla	0,896154	0,857963	0,895536	0,882326	0,883844	0,848959	0,835764	0,718924
AnkleInvAd	0,409685	0,339362	0,423917	0,434945	0,435511	0,574432	0,338085	0,306002
AnkleRot	1,992378	1,796305	1,990108	1,951516	1,952778	2,444802	1,579038	1,66315

Subject 1 Right Session 3	CGM10KAD	CGM10Med	CGM11KAD	CGM11Med	CGM21	CGM22	CGM23	PiG
HipFlexExt	1,163864	1,165651	1,163747	1,166171	1,124411	1,11342	1,070098	1,145365
HipAbAd	0,793368	0,805094	0,793257	0,794938	0,761616	0,797352	0,784648	0,769569
HipRot	1,546593	1,54955	1,546284	1,552952	1,566024	1,881162	1,068546	1,370858
KneeFlexExt	1,696996	1,65166	1,69713	1,698089	1,683131	1,680765	1,671061	1,663646
KneeVarVal	0,661637	0,744283	0,660888	0,682854	0,682693	0,897431	0,430467	0,592709
KneeRot	1,581103	1,541248	1,580888	1,583567	1,589375	2,198249	1,310133	1,250737
AnkleDorPla	0,993237	1,033498	0,992804	0,987795	0,98805	0,956796	0,948506	0,93546
AnkleInvAd	0,402469	0,368087	0,37681	0,369841	0,368655	0,504811	0,301133	0,334155
AnkleRot	1,737052	1,812416	1,742036	1,734902	1,731666	2,283832	1,545742	1,620665

Table A.0.6: Subject 2 Left: Intrasession averaged SD for the 3 sessions

Subject 2 Left Session 1	CGM10KAD	CGM10Med	CGM11KAD	CGM11Med	CGM21	CGM22	CGM23	PiG
HipFlexExt	1,62965	1,645817	1,629229	1,648058	1,584858	1,536163	1,638394	1,70169
HipAbAd	1,049126	1,016213	1,049093	1,057897	1,008755	0,935561	0,964961	1,033164
HipRot	1,75029	1,708103	1,750914	1,713338	1,826094	2,144776	1,563921	1,555225
KneeFlexExt	1,844688	1,787879	1,844267	1,851344	1,813275	1,811783	2,241487	2,027996
KneeVarVal	0,562702	0,99049	0,562552	0,575999	0,585323	0,744725	0,417742	0,531176
KneeRot	1,939792	1,986023	1,940631	1,909446	1,934555	2,380606	1,690531	1,580298
AnkleDorPla	1,364489	1,283885	1,360903	1,348409	1,346072	1,346972	1,532105	1,361667
AnkleInvAd	0,511268	0,467983	0,521142	0,518193	0,523242	0,703414	0,451179	0,422186
AnkleRot	1,921095	1,663274	1,918917	1,906424	1,923791	2,426753	1,582476	1,780366

Subject 2 Left Session 2	CGM10KAD	CGM10Med	CGM11KAD	CGM11Med	CGM21	CGM22	CGM23	PiG
HipFlexExt	0,972166	0,977543	0,972038	0,976808	0,93633	0,918836	0,934937	0,949759
HipAbAd	0,667294	0,659062	0,667304	0,666345	0,63592	0,613495	0,640226	0,650562
HipRot	1,207671	1,183688	1,207646	1,197599	1,275522	1,451949	1,115226	1,068257
KneeFlexExt	1,587866	1,648857	1,587591	1,596628	1,575184	1,569132	1,638899	1,555549
KneeVar Val	0,579361	0,605045	0,57973	0,572108	0,578461	0,707834	0,439844	0,526017
KneeRot	1,362397	1,375691	1,362451	1,353059	1,359427	1,794856	1,22826	1,101688
AnkleDorPla	1,400825	1,232349	1,40486	1,353925	1,351467	1,336354	1,312264	1,359818
AnkleInvAd	0,42471	0,334236	0,382946	0,386579	0,392832	0,548095	0,346069	0,322312
AnkleRot	1,302115	1,101085	1,314427	1,288818	1,306673	1,746704	1,093478	1,204257

Subject 2 Left Session 3	CGM10KAD	CGM10Med	CGM11KAD	CGM11Med	CGM21	CGM22	CGM23	PiG
HipFlexExt	0,972166	0,977543	0,972038	0,976808	0,93633	0,918836	0,934937	0,949759
HipAbAd	0,667294	0,659062	0,667304	0,666345	0,63592	0,613495	0,640226	0,650562
HipRot	1,207671	1,183688	1,207646	1,197599	1,275522	1,451949	1,115226	1,068257
KneeFlexExt	1,587866	1,648857	1,587591	1,596628	1,575184	1,569132	1,638899	1,555549
KneeVar Val	0,579361	0,605045	0,57973	0,572108	0,578461	0,707834	0,439844	0,526017
KneeRot	1,362397	1,375691	1,362451	1,353059	1,359427	1,794856	1,22826	1,101688
AnkleDorPla	1,400825	1,232349	1,40486	1,353925	1,351467	1,336354	1,312264	1,359818
AnkleInvAd	0,42471	0,334236	0,382946	0,386579	0,392832	0,548095	0,346069	0,322312
AnkleRot	1,302115	1,101085	1,314427	1,288818	1,306673	1,746704	1,093478	1,204257

Table A.0.7: Subject 2 Right: Intrasession averaged SD for the 3 sessions

Subject 2 Right Session 1	CGM10KAD	CGM10Med	CGM11KAD	CGM11Med	CGM21	CGM22	CGM23	PiG
HipFlexExt	1,301405	1,312311	1,301209	1,308626	1,254896	1,235924	1,216044	1,286128
HipAbAd	0,727989	0,706475	0,727975	0,726976	0,696078	0,749639	0,754268	0,689497
HipRot	1,493528	1,438093	1,494169	1,455913	1,537055	1,773877	1,33773	1,295255
KneeFlexExt	1,677695	1,726816	1,677185	1,703614	1,684301	1,670441	1,861768	1,716266
KneeVarVal	0,643061	0,801162	0,643848	0,602124	0,616132	0,828894	0,455133	0,539694
KneeRot	1,572394	1,684042	1,57254	1,573659	1,571075	2,022429	1,447065	1,187986
AnkleDorPla	1,206171	1,12906	1,205506	1,184071	1,179891	1,166955	1,20405	1,226611
AnkleInvAd	0,415927	0,461737	0,419158	0,427461	0,426026	0,610391	0,337522	0,456591
AnkleRot	1,671901	1,467854	1,671826	1,637214	1,637261	2,197648	1,220288	1,645027
Subject 2 Right Session 2	CGM10KAD	CGM10Med	CGM11KAD	CGM11Med	CGM21	CGM22	CGM23	PiG
HipFlexExt	0,962289	0,96577	0,962251	0,962447	0,923348	0,907585	0,893381	0,942269
HipAbAd	0,570451	0,539727	0,57055	0,565988	0,540414	0,554949	0,579457	0,538143
HipRot	1,171667	1,130117	1,172415	1,132196	1,19941	1,359225	1,139468	0,975103
KneeFlexExt	1,503138	1,430302	1,502516	1,526216	1,515229	1,516186	1,629624	1,469365
KneeVarVal	0,46241	0,92627	0,463958	0,408518	0,40672	0,518916	0,339173	0,37078
KneeRot	1,218495	1,369426	1,218575	1,225052	1,21835	1,602704	1,046937	0,919013
AnkleDorPla	1,48087	1,425329	1,479128	1,458403	1,455095	1,456686	1,453716	1,578078
AnkleInvAd	0,345028	0,481045	0,39946	0,394646	0,397932	0,55482	0,356943	0,453863
AnkleRot	1,473341	1,304808	1,460576	1,438709	1,447394	1,83287	1,312573	1,476615
Subject 2 Right Session 3	CGM10KAD	CGM10Med	CGM11KAD	CGM11Med	CGM21	CGM22	CGM23	PiG
HipFlexExt	1,247468	1,26371	1,247292	1,253977	1,200372	1,189983	1,216234	1,239606
HipAbAd	0,505611	0,514184	0,50564	0,504337	0,480324	0,477774	0,526627	0,474701
HipRot	1,382604	1,317148	1,383401	1,335332	1,387006	1,502725	1,164498	1,116532
KneeFlexExt	1,852515	1,730417	1,851	1,93067	1,910998	1,901134	1,984399	1,823864
KneeVarVal	0,645934	1,261853	0,64928	0,461799	0,449741	0,604673	0,440336	0,548341
KneeRot	1,537852	1,706778	1,537926	1,551793	1,531803	2,067162	1,274921	1,127374
AnkleDorPla	1,557418	1,466794	1,559043	1,48616	1,484036	1,478447	1,438412	1,70078
AnkleInvAd	0,387689	0,586362	0,385258	0,394717	0,398956	0,594409	0,335603	0,522903
AnkleRot	1,39991	1,123975	1,402538	1,30953	1,316132	1,891279	1,090225	1,374345

Table A.0.8: Subject 1: Ranking of the different models from best to worst intrasession repeatability (based on the intrasession averaged standard deviation values)

Subject 1 Left Session 1	Best							Worst
HipFlexExt	CGM23	CGM21	PiG	CGM22	CGM11KAD	CGM10KAD	CGM10Med	CGM11Med
HipAbAd	CGM21	CGM11KAD	CGM10KAD	CGM11Med	CGM22	CGM10Med	PiG	CGM23
HipRot	CGM23	PiG	CGM11KAD	CGM10KAD	CGM10Med	CGM11Med	CGM21	CGM22
KneeFlexExt	CGM10Med	PiG	CGM21	CGM11Med	CGM22	CGM10KAD	CGM11KAD	CGM23
KneeVarVal	CGM23	PiG	CGM11KAD	CGM10KAD	CGM11Med	CGM21	CGM10Med	CGM22
KneeRot	PiG	CGM23	CGM10Med	CGM11Med	CGM21	CGM10KAD	CGM11KAD	CGM22
AnkleDorPla	PiG	CGM22	CGM11Med	CGM21	CGM11KAD	CGM10KAD	CGM23	CGM10Med
AnkleInvAd	CGM23	PiG	CGM11KAD	CGM11Med	CGM21	CGM10Med	CGM10KAD	CGM22
AnkleRot	CGM23	PiG	CGM21	CGM11Med	CGM10KAD	CGM11KAD	CGM10Med	CGM22

Subject 1 Left Session 2	Best							Worst
HipFlexExt	CGM23	CGM21	CGM22	CGM11KAD	CGM10KAD	CGM11Med	CGM10Med	PiG
HipAbAd	PiG	CGM21	CGM22	CGM10Med	CGM11Med	CGM11KAD	CGM10KAD	CGM23
HipRot	PiG	CGM23	CGM11KAD	CGM10KAD	CGM10Med	CGM11Med	CGM21	CGM22
KneeFlexExt	PiG	CGM21	CGM22	CGM11KAD	CGM10KAD	CGM11Med	CGM23	CGM10Med
KneeVarVal	CGM23	PiG	CGM10Med	CGM11Med	CGM21	CGM11KAD	CGM10KAD	CGM22
KneeRot	CGM23	PiG	CGM10KAD	CGM11KAD	CGM11Med	CGM21	CGM10Med	CGM22
AnkleDorPla	CGM23	PiG	CGM10Med	CGM11Med	CGM21	CGM22	CGM11KAD	CGM10KAD
AnkleInvAd	CGM23	PiG	CGM10Med	CGM11Med	CGM21	CGM11KAD	CGM10KAD	CGM22
AnkleRot	CGM23	CGM10Med	PiG	CGM21	CGM11Med	CGM10KAD	CGM11KAD	CGM22

Subject 1 Left Session 3	Best							Worst
HipFlexExt	CGM23	CGM21	PiG	CGM22	CGM11KAD	CGM10KAD	CGM11Med	CGM10Med
HipAbAd	PiG	CGM21	CGM11KAD	CGM10KAD	CGM10Med	CGM11Med	CGM22	CGM23
HipRot	PiG	CGM11KAD	CGM10KAD	CGM11Med	CGM10Med	CGM21	CGM23	CGM22
KneeFlexExt	PiG	CGM21	CGM11Med	CGM22	CGM23	CGM10Med	CGM10KAD	CGM11KAD
KneeVarVal	CGM23	PiG	CGM11KAD	CGM10KAD	CGM10Med	CGM11Med	CGM21	CGM22
KneeRot	PiG	CGM23	CGM11Med	CGM21	CGM10Med	CGM11KAD	CGM10KAD	CGM22
AnkleDorPla	PiG	CGM23	CGM22	CGM21	CGM11Med	CGM10KAD	CGM11KAD	CGM10Med
AnkleInvAd	CGM23	PiG	CGM10Med	CGM11Med	CGM21	CGM11KAD	CGM10KAD	CGM22
AnkleRot	CGM23	PiG	CGM11Med	CGM21	CGM10KAD	CGM11KAD	CGM10Med	CGM22

Subject 1 Right Session 1	Best							Worst
HipFlexExt	CGM23	CGM22	CGM21	PiG	CGM10Med	CGM11Med	CGM10KAD	CGM11KAD
HipAbAd	CGM21	CGM22	PiG	CGM11KAD	CGM10KAD	CGM11Med	CGM10Med	CGM23
HipRot	PiG	CGM23	CGM11KAD	CGM10KAD	CGM10Med	CGM11Med	CGM21	CGM22
KneeFlexExt	CGM23	PiG	CGM10Med	CGM21	CGM22	CGM11Med	CGM10KAD	CGM11KAD
KneeVarVal	CGM23	PiG	CGM11KAD	CGM10KAD	CGM11Med	CGM21	CGM10Med	CGM22
KneeRot	CGM23	PiG	CGM10Med	CGM11Med	CGM10KAD	CGM11KAD	CGM21	CGM22
AnkleDorPla	CGM23	PiG	CGM10Med	CGM22	CGM11Med	CGM21	CGM10KAD	CGM11KAD
AnkleInvAd	CGM23	PiG	CGM21	CGM11Med	CGM11KAD	CGM10Med	CGM10KAD	CGM22
AnkleRot	CGM23	PiG	CGM10Med	CGM10KAD	CGM21	CGM11Med	CGM11KAD	CGM22

Subject 1 Right Session 2	Best							Worst
HipFlexExt	CGM23	CGM22	CGM21	PiG	CGM10Med	CGM11Med	CGM10KAD	CGM11KAD
HipAbAd	PiG	CGM21	CGM10Med	CGM11Med	CGM11KAD	CGM10KAD	CGM22	CGM23
HipRot	CGM23	PiG	CGM10Med	CGM11Med	CGM10KAD	CGM11KAD	CGM21	CGM22
KneeFlexExt	PiG	CGM23	CGM22	CGM21	CGM11KAD	CGM10KAD	CGM11Med	CGM10Med
KneeVarVal	CGM23	PiG	CGM10Med	CGM11Med	CGM11KAD	CGM10KAD	CGM21	CGM22
KneeRot	CGM23	PiG	CGM11KAD	CGM10KAD	CGM11Med	CGM21	CGM10Med	CGM22
AnkleDorPla	PiG	CGM23	CGM22	CGM10Med	CGM11Med	CGM21	CGM11KAD	CGM10KAD
AnkleInvAd	PiG	CGM23	CGM10Med	CGM10KAD	CGM11KAD	CGM11Med	CGM21	CGM22
AnkleRot	CGM23	PiG	CGM10Med	CGM11Med	CGM21	CGM11KAD	CGM10KAD	CGM22

Subject 1 Right Session 3	Best							Worst
HipFlexExt	CGM23	CGM22	CGM21	PiG	CGM11KAD	CGM10KAD	CGM10Med	CGM11Med
HipAbAd	CGM21	PiG	CGM23	CGM11KAD	CGM10KAD	CGM11Med	CGM22	CGM10Med
HipRot	CGM23	PiG	CGM11KAD	CGM10KAD	CGM10Med	CGM11Med	CGM21	CGM22
KneeFlexExt	CGM10Med	PiG	CGM23	CGM22	CGM21	CGM10KAD	CGM11KAD	CGM11Med
KneeVarVal	CGM23	PiG	CGM11KAD	CGM10KAD	CGM21	CGM11Med	CGM10Med	CGM22
KneeRot	PiG	CGM23	CGM10Med	CGM11KAD	CGM10KAD	CGM11Med	CGM21	CGM22
AnkleDorPla	PiG	CGM23	CGM22	CGM11Med	CGM21	CGM11KAD	CGM10KAD	CGM10Med
AnkleInvAd	CGM23	PiG	CGM10Med	CGM21	CGM11Med	CGM11KAD	CGM10KAD	CGM22
AnkleRot	CGM23	PiG	CGM21	CGM11Med	CGM10KAD	CGM11KAD	CGM10Med	CGM22

Table A.0.9: Subject 2: Ranking of the different models from best to worst intrasession repeatability (based on the intrasession averaged standard deviation values)

Subject 2 Left Session 1	Best							Worst
HipFlexExt	CGM22	CGM21	CGM11KAD	CGM10KAD	CGM23	CGM10Med	CGM11Med	PiG
HipAbAd	CGM22	CGM23	CGM21	CGM10Med	PiG	CGM11KAD	CGM10KAD	CGM11Med
HipRot	PiG	CGM23	CGM10Med	CGM11Med	CGM10KAD	CGM11KAD	CGM21	CGM22
KneeFlexExt	CGM10Med	CGM22	CGM21	CGM11KAD	CGM10KAD	CGM11Med	PiG	CGM23
KneeVarVal	CGM23	PiG	CGM11KAD	CGM10KAD	CGM11Med	CGM21	CGM22	CGM10Med
KneeRot	PiG	CGM23	CGM11Med	CGM21	CGM10KAD	CGM11KAD	CGM10Med	CGM22
AnkleDorPla	CGM10Med	CGM21	CGM22	CGM11Med	CGM11KAD	PiG	CGM10KAD	CGM23
AnkleInvAd	PiG	CGM23	CGM10Med	CGM10KAD	CGM11Med	CGM11KAD	CGM21	CGM22
AnkleRot	CGM23	CGM10Med	PiG	CGM11Med	CGM11KAD	CGM10KAD	CGM21	CGM22

Subject 2 Left Session 2	Best							Worst
HipFlexExt	CGM22	CGM23	CGM21	PiG	CGM11KAD	CGM10KAD	CGM11Med	CGM10Med
HipAbAd	CGM22	CGM21	CGM23	PiG	CGM10Med	CGM11Med	CGM10KAD	CGM11KAD
HipRot	PiG	CGM23	CGM10Med	CGM11Med	CGM11KAD	CGM10KAD	CGM21	CGM22
KneeFlexExt	PiG	CGM22	CGM21	CGM11KAD	CGM10KAD	CGM11Med	CGM23	CGM10Med
KneeVarVal	CGM23	PiG	CGM11Med	CGM21	CGM10KAD	CGM11KAD	CGM10Med	CGM22
KneeRot	PiG	CGM23	CGM11Med	CGM21	CGM10KAD	CGM11KAD	CGM10Med	CGM22
AnkleDorPla	CGM10Med	CGM23	CGM22	CGM21	CGM11Med	PiG	CGM10KAD	CGM11KAD
AnkleInvAd	PiG	CGM10Med	CGM23	CGM11KAD	CGM11Med	CGM21	CGM10KAD	CGM22
AnkleRot	CGM23	CGM10Med	PiG	CGM11Med	CGM10KAD	CGM21	CGM11KAD	CGM22

Subject 2 Left Session 3	Best							Worst
HipFlexExt	CGM22	CGM23	CGM21	PiG	CGM11KAD	CGM10KAD	CGM11Med	CGM10Med
HipAbAd	CGM22	CGM21	CGM23	PiG	CGM10Med	CGM11Med	CGM10KAD	CGM11KAD
HipRot	PiG	CGM23	CGM10Med	CGM11Med	CGM11KAD	CGM10KAD	CGM21	CGM22
KneeFlexExt	PiG	CGM22	CGM21	CGM11KAD	CGM10KAD	CGM11Med	CGM23	CGM10Med
KneeVarVal	CGM23	PiG	CGM11Med	CGM21	CGM10KAD	CGM11KAD	CGM10Med	CGM22
KneeRot	PiG	CGM23	CGM11Med	CGM21	CGM10KAD	CGM11KAD	CGM10Med	CGM22
AnkleDorPla	CGM10Med	CGM23	CGM22	CGM21	CGM11Med	PiG	CGM10KAD	CGM11KAD
AnkleInvAd	PiG	CGM10Med	CGM23	CGM11KAD	CGM11Med	CGM21	CGM10KAD	CGM22
AnkleRot	CGM23	CGM10Med	PiG	CGM11Med	CGM10KAD	CGM21	CGM11KAD	CGM22

Subject 2 Right Session 1	Best							Worst
HipFlexExt	CGM23	CGM22	CGM21	PiG	CGM11KAD	CGM10KAD	CGM11Med	CGM10Med
HipAbAd	PiG	CGM21	CGM10Med	CGM11Med	CGM11KAD	CGM10KAD	CGM22	CGM23
HipRot	PiG	CGM23	CGM10Med	CGM11Med	CGM10KAD	CGM11KAD	CGM21	CGM22
KneeFlexExt	CGM22	CGM11KAD	CGM10KAD	CGM21	CGM11Med	PiG	CGM10Med	CGM23
KneeVarVal	CGM23	PiG	CGM11Med	CGM21	CGM10KAD	CGM11KAD	CGM10Med	CGM22
KneeRot	PiG	CGM23	CGM21	CGM10KAD	CGM11KAD	CGM11Med	CGM10Med	CGM22
AnkleDorPla	CGM10Med	CGM22	CGM21	CGM10Med	CGM11Med	CGM23	CGM10KAD	PiG
AnkleInvAd	CGM23	CGM10KAD	CGM11KAD	CGM21	CGM11Med	PiG	CGM10Med	CGM22
AnkleRot	CGM23	CGM10Med	CGM11Med	CGM21	PiG	CGM11KAD	CGM10KAD	CGM22

Subject 2 Right Session 2	Best							Worst
HipFlexExt	CGM23	CGM22	CGM21	PiG	CGM11KAD	CGM10KAD	CGM11Med	CGM10Med
HipAbAd	PiG	CGM10Med	CGM21	CGM22	CGM11Med	CGM10KAD	CGM11KAD	CGM23
HipRot	PiG	CGM10Med	CGM11Med	CGM23	CGM10KAD	CGM11KAD	CGM21	CGM22
KneeFlexExt	CGM10Med	PiG	CGM11KAD	CGM10KAD	CGM21	CGM22	CGM11Med	CGM23
KneeVarVal	CGM23	PiG	CGM21	CGM11Med	CGM10KAD	CGM11KAD	CGM22	CGM10Med
KneeRot	PiG	CGM23	CGM21	CGM10KAD	CGM11KAD	CGM11Med	CGM10Med	CGM22
AnkleDorPla	CGM10Med	CGM23	CGM21	CGM22	CGM11Med	CGM11KAD	CGM10KAD	PiG
AnkleInvAd	CGM10KAD	CGM23	CGM11Med	CGM21	CGM11KAD	PiG	CGM10Med	CGM22
AnkleRot	CGM10Med	CGM23	CGM11Med	CGM21	CGM11KAD	CGM10KAD	PiG	CGM22

Subject 2 Right Session 3	Best							Worst
HipFlexExt	CGM22	CGM21	CGM23	PiG	CGM11KAD	CGM10KAD	CGM11Med	CGM10Med
HipAbAd	PiG	CGM22	CGM21	CGM11Med	CGM10KAD	CGM11KAD	CGM10Med	CGM23
HipRot	PiG	CGM23	CGM10Med	CGM11Med	CGM10KAD	CGM11KAD	CGM21	CGM22
KneeFlexExt	CGM10Med	PiG	CGM11KAD	CGM10KAD	CGM22	CGM21	CGM11Med	CGM23
KneeVarVal	CGM23	CGM21	CGM11Med	PiG	CGM22	CGM10KAD	CGM11KAD	CGM10Med
KneeRot	PiG	CGM23	CGM21	CGM10KAD	CGM11KAD	CGM11Med	CGM10Med	CGM22
AnkleDorPla	CGM23	CGM10Med	CGM22	CGM21	CGM11Med	CGM10KAD	CGM11KAD	PiG
AnkleInvAd	CGM23	CGM11KAD	CGM10KAD	CGM11Med	CGM21	PiG	CGM10Med	CGM22
AnkleRot	CGM23	CGM10Med	CGM11Med	CGM21	PiG	CGM10KAD	CGM11KAD	CGM22

Appendix B

Intraclass Correlation Coefficient

Table B.0.1: Intersession ICC (Peak Left, Peak Right, Range of Motion Left, Range of Motion Right)

Peak Left	CGM10KAD	CGM10Med	CGM11KAD	CGM11Med	CGM21	CGM22	CGM23	PiG
HipFlexExt	-0,40394	0,677498	-0,41358	-0,72445	-0,3688	-0,022	-0,21296	-2,40815
HipAbAd	0,755721	0,860619	0,755857	0,751696	-2,01933	-0,20843	-1,5753	0,866382
HipRot	0,610301	0,933038	0,616982	0,198137	0,649042	0,248036	0,806229	0,692881
KneeFlexExt	0,859312	0,944882	0,858917	0,922885	0,948501	0,944078	0,909862	0,768879
KneeVarVal	0,741328	0,94718	0,745648	0,395031	0,837398	0,447547	0,981181	0,404104
KneeRot	-3,66664	-6,42148	0,652465	0,776202	0,694229	0,856495	0,805813	-6,37642
AnkleDorPla	0,953273	0,918258	0,986063	0,965558	0,966175	0,973317	0,963551	0,985693
AnkleInvAd	10,39282	0,967605	-0,24047	0,869014	0,886856	0,887636	0,902839	-1,37078
AnkleRot	0,960482	0,931769	0,9579	0,965309	0,963098	0,916464	0,816404	0,541226

Peak Right	CGM10KAD	CGM10Med	CGM11KAD	CGM11Med	CGM21	CGM22	CGM23	PiG
HipFlexExt	0,654337	0,930554	0,64893	0,564971	0,658936	0,208412	-0,76548	0,430266
HipAbAd	0,986121	0,991216	0,986133	0,986139	0,9692	0,933588	0,801948	0,986608
HipRot	0,823288	0,961889	0,825	0,817075	0,962162	0,87009	-4,85424	0,913227
KneeFlexExt	0,885597	0,933281	0,883862	0,775946	0,849788	0,840599	0,565246	0,898925
KneeVarVal	0,891997	0,961096	0,893647	0,717353	0,970522	0,78166	0,950266	0,855407
KneeRot	-0,49031	0,05098	0,981733	0,955869	0,900071	0,731263	-14,556	2,204645
AnkleDorPla	-0,059	0,773119	0,75803	0,173785	0,213313	0,257491	0,828986	0,902812
AnkleInvAd	0,43703	0,976991	-2,94641	0,888282	0,915756	0,92048	-9,64328	0,963963
AnkleRot	0,603674	0,870346	-0,04167	0,926668	0,948064	0,964386	0,632259	0,86447

ROM Left	CGM10KAD	CGM10Med	CGM11KAD	CGM11Med	CGM21	CGM22	CGM23	PiG
HipFlexExt	0,866765	0,865533	0,86681	0,857189	0,862946	0,875003	0,850209	0,909142
HipAbAd	0,968967	0,968364	0,968951	0,969633	0,970123	0,975264	0,975309	0,973789
HipRot	-0,39928	-0,1809	-0,40079	-0,2397	-0,03228	-0,12167	-2,85799	-0,59729
KneeFlexExt	0,983501	0,97159	0,983505	0,985074	0,982941	0,979993	0,597357	0,983852
KneeVarVal	0,824329	0,898354	0,827194	0,614872	0,888124	0,818543	-3,97312	0,460147
KneeRot	0,457045	-1,46374	0,447118	0,609642	-25,4322	0,849834	0,432498	2,369562
AnkleDorPla	0,994469	0,947202	0,995047	0,989809	0,989618	0,987248	0,990848	0,993646
AnkleInvAd	0,981511	0,981634	0,977583	0,965264	0,969253	0,97419	0,897457	0,998494
AnkleRot	5,448139	-7,15873	4,875021	-17,9806	22,46857	0,91163	0,798511	0,93864

ROM Right	CGM10KAD	CGM10Med	CGM11KAD	CGM11Med	CGM21	CGM22	CGM23	PiG
HipFlexExt	0,691224	0,674049	0,691446	0,664209	0,692477	0,472591	-0,35778	0,76445
HipAbAd	0,960278	0,962734	0,960284	0,959878	0,960427	0,979618	0,983219	0,963498
HipRot	0,860863	0,90016	0,859576	0,900388	0,903063	0,938148	0,61319	0,953187
KneeFlexExt	0,887057	0,888624	0,887426	0,869197	0,484667	0,538021	0,976782	0,938443
KneeVarVal	0,956138	0,931005	0,952551	0,970687	0,983154	0,981159	0,323748	0,938209
KneeRot	0,139059	0,985959	0,176173	0,349792	0,646712	-0,29045	0,152859	-0,48212
AnkleDorPla	0,983807	0,961356	0,984552	0,976087	0,976383	0,97658	0,989466	0,999271
AnkleInvAd	-0,47251	0,984097	-0,57306	0,689126	0,752461	0,893165	-1,0809	0,981913
AnkleRot	-7,91531	-0,16638	-3,21232	5,395725	8,53964	0,561151	0,945017	5,52633

Table B.0.2: Intrasection ICC of Session 1 (Peak Left, Peak Right, Range of Motion Left, Range of Motion Right)

Peak Left	CGM10KAD	CGM10Med	CGM11KAD	CGM11Med	CGM21	CGM22	CGM23	PiG
HipFlexExt	0,82758639	0,963074516	0,82594019	0,701425037	0,74425701	0,56598991	0,644091	0,892834
HipAbAd	0,85103515	0,885728894	0,85097153	0,859186837	0,2505828	0,11338677	0,340408	0,869145
HipRot	0,67214185	0,996921947	0,6840857	0,729927408	0,89610026	0,73431146	0,941582	0,930806
KneeFlexExt	0,95466991	0,986140147	0,9544828	0,939923701	0,94691369	0,94598474	0,897192	0,92498
KneeVarVal	0,96463317	0,999440329	0,96585954	0,957733216	0,9874727	0,84862756	0,985481	0,882738
KneeRot	0,85674315	0,3771544	-0,1204069	-0,11589173	0,17488701	0,78565603	0,195532	0,80113
AnkleDorPla	0,76926345	0,216143211	0,83920693	0,884669326	0,88945349	0,89552162	0,88776	0,847341
AnkleInvAd	0,98441613	0,995416046	0,96299243	0,930150068	0,93567429	0,85612181	0,64862	0,979402
AnkleRot	0,52880085	0,99024482	0,47489971	0,423770642	0,40532313	0,31518328	0,658697	0,077204

Peak Right	CGM10KAD	CGM10Med	CGM11KAD	CGM11Med	CGM21	CGM22	CGM23	PiG
HipFlexExt	0,69786895	0,938091927	0,69482145	0,67672317	0,73519433	0,59965508	0,451763	0,726677
HipAbAd	0,96268673	0,968466587	0,96268549	0,963197341	0,92584571	0,93855736	0,942081	0,965366
HipRot	0,90387602	0,996232192	0,90612171	-0,02233645	0,67674211	0,70976992	0,099063	0,978319
KneeFlexExt	0,69251002	0,963983154	0,68969594	0,716606976	0,77287754	0,77611411	0,59068	0,534082
KneeVarVal	0,98319687	0,997952605	0,98355238	0,794065006	0,97446524	0,90825893	0,980376	0,950612
KneeRot	0,94063612	0,175413871	0,97044761	0,913759442	0,95043495	0,86024684	0,865496	0,927265
AnkleDorPla	0,16098925	0,773741333	0,88716629	0,854663558	0,85912175	0,87545661	0,853792	0,908396
AnkleInvAd	0,30791678	0,993679029	0,86149664	0,902211831	0,9120934	0,75690658	0,953107	0,987521
AnkleRot	0,14174167	0,983271437	0,04548064	0,313498481	0,46250193	0,80812032	0,793761	0,698157

ROM Left	CGM10KAD	CGM10Med	CGM11KAD	CGM11Med	CGM21	CGM22	CGM23	PiG
HipFlexExt	0,66859681	0,638709018	0,66892236	0,629909478	0,64286881	0,64555428	0,592375	0,819303
HipAbAd	0,97273254	0,971858847	0,97273671	0,971566354	0,97178297	0,97693075	0,966746	0,951678
HipRot	0,09329504	-0,01962097	0,10188688	-0,07874977	-0,0218212	0,09719543	0,485929	0,030157
KneeFlexExt	0,92543518	0,918626599	0,92545132	0,926398329	0,90616438	0,90907873	0,043322	0,935481
KneeVarVal	0,0729395	0,98617856	0,09065018	0,239016347	0,72603403	0,29774231	0,471987	-0,1183
KneeRot	-0,06579815	0,737540648	-0,0630294	-0,0988601	0,19281327	0,01611988	-0,03429	-0,10315
AnkleDorPla	0,97918827	0,954542049	0,97904437	0,978741808	0,97905489	0,98019477	0,976175	0,97783
AnkleInvAd	0,97197941	0,898571243	0,97368218	0,949257118	0,95418107	0,92567539	0,776164	0,951411
AnkleRot	-0,09668924	-0,09372095	-0,0969418	-0,10079102	-0,0930835	0,2408765	-0,09804	0,180962

ROM Right	CGM10KAD	CGM10Med	CGM11KAD	CGM11Med	CGM21	CGM22	CGM23	PiG
HipFlexExt	0,00650414	-0,02102174	0,00693107	-0,02799201	0,01058272	-0,0371587	0,009682	0,241867
HipAbAd	0,90661012	0,889230695	0,90670794	0,900863175	0,9014875	0,90005492	0,839861	0,908275
HipRot	0,01416638	0,411628944	0,00383033	0,465467254	0,67981739	0,85249797	0,247924	0,83249
KneeFlexExt	0,81110616	0,585528183	0,81151341	0,758933979	0,63784478	0,6496532	0,78184	0,838693
KneeVarVal	0,89400088	0,976804532	0,89422592	0,859075659	0,94012504	0,93286193	0,594037	0,834886
KneeRot	-0,0193727	0,8067581	-0,0178373	0,000284522	0,62015874	0,09869506	0,044014	0,064066
AnkleDorPla	0,987068	0,980959847	0,98681681	0,986281388	0,98654752	0,98758575	0,991376	0,992592
AnkleInvAd	0,79324025	0,966121602	0,92399307	0,955323097	0,96049878	0,9237595	0,960318	0,993811
AnkleRot	0,14600191	0,314360966	0,11414893	0,152446831	0,10429465	0,14728847	0,120175	0,112461

Table B.0.3: Intrasection ICC of Session 2 (Peak Left, Peak Right, Range of Motion Left, Range of Motion Right)

Peak Left	CGM10KAD	CGM10Med	CGM11KAD	CGM11Med	CGM21	CGM22	CGM23	PiG
HipFlexExt	-0,11852	0,581628	-0,11915	0,000265	-0,09215	-0,13277	-0,08739	0,029149
HipAbAd	-0,00641	0,299968	-0,00578	-0,01573	0,755106	0,192801	0,048097	0,512814
HipRot	0,707386	0,995417	0,716094	0,033791	0,829488	-0,09508	0,854475	0,756443
KneeFlexExt	0,651967	0,951483	0,650583	0,535392	0,677037	0,693508	0,285912	0,229276
KneeVarVal	0,732489	0,994001	0,742137	0,010912	0,869733	-0,10818	0,990084	0,129132
KneeRot	0,845849	0,785425	0,911718	0,941557	0,930202	0,942263	0,94256	0,849858
AnkleDorPla	0,894929	0,864643	0,666139	0,607521	0,617884	0,643701	0,753033	0,73589
AnkleInvAd	0,075697	0,975345	0,13801	0,770116	0,783549	0,743451	0,812227	0,270984
AnkleRot	0,795793	0,94741	0,791043	0,741726	0,76833	0,475377	0,364927	0,49317

Peak Right	CGM10KAD	CGM10Med	CGM11KAD	CGM11Med	CGM21	CGM22	CGM23	PiG
HipFlexExt	0,447114	0,896747	0,441239	0,189499	0,37337	-0,18284	0,297578	0,017399
HipAbAd	0,950035	0,977084	0,950001	0,95261	0,865002	0,7868	0,073608	0,965705
HipRot	0,850752	0,997342	0,855968	0,505693	0,835388	0,268435	0,643258	0,97921
KneeFlexExt	0,156182	0,989966	0,144305	-0,07262	0,250888	0,298008	0,109544	0,714588
KneeVarVal	0,891835	0,997578	0,895503	0,653438	0,94707	0,355236	0,985186	0,942857
KneeRot	0,566035	0,961234	0,937285	0,818101	0,787575	0,305608	0,720925	0,885371
AnkleDorPla	-0,07802	0,709942	0,19438	-0,02606	-0,02834	-0,04022	0,339904	0,369924
AnkleInvAd	0,931493	0,976402	0,294149	0,790688	0,82971	0,914187	0,199514	0,970505
AnkleRot	0,46979	0,78165	0,433825	0,294148	0,385911	0,672684	-0,1285	0,96775

ROM Left	CGM10KAD	CGM10Med	CGM11KAD	CGM11Med	CGM21	CGM22	CGM23	PiG
HipFlexExt	0,814879	0,814082	0,814821	0,810535	0,822351	0,886743	0,848874	0,891718
HipAbAd	0,923861	0,914575	0,923794	0,926767	0,929828	0,900311	0,78356	0,932975
HipRot	0,463117	0,218629	0,467797	0,238828	0,011453	-0,05498	-0,09668	0,621467
KneeFlexExt	0,863598	0,926836	0,863887	0,859732	0,822941	0,828026	0,196269	0,861333
KneeVarVal	0,725653	0,993909	0,728806	0,024275	0,648845	0,759769	-0,05425	0,123876
KneeRot	0,155574	-0,1199	0,150948	0,35184	0,000576	0,661815	0,300609	0,165748
AnkleDorPla	0,951361	0,91029	0,95171	0,947114	0,947417	0,952504	0,931248	0,91931
AnkleInvAd	0,924547	0,841964	0,909427	0,951245	0,953855	0,936516	0,95465	0,883727
AnkleRot	0,20286	0,155745	0,202715	0,249791	0,264863	0,484794	0,555543	-0,05155

ROM Right	CGM10KAD	CGM10Med	CGM11KAD	CGM11Med	CGM21	CGM22	CGM23	PiG
HipFlexExt	0,813092	0,821325	0,812932	0,811238	0,825048	0,47433	-0,16194	0,823471
HipAbAd	0,948748	0,965214	0,948672	0,952096	0,953702	0,973801	0,948348	0,961411
HipRot	0,957791	0,962393	0,957479	0,96789	0,970801	0,963869	0,463601	0,971515
KneeFlexExt	0,065547	0,898254	0,068544	-0,0147	0,05511	0,022837	0,933416	0,601995
KneeVarVal	0,940937	0,996697	0,940459	0,925603	0,946767	0,882963	0,762586	0,979769
KneeRot	0,644798	0,952193	0,643782	0,682122	0,550896	0,607786	-0,10773	0,128697
AnkleDorPla	0,956617	0,933519	0,956724	0,95502	0,954863	0,951162	0,968758	0,980588
AnkleInvAd	0,570315	0,939203	-0,07675	0,627479	0,758472	0,905241	0,406802	0,992266
AnkleRot	-0,05729	0,126893	-0,02886	-0,10468	-0,09503	-0,11546	0,172557	-0,14915

Table B.0.4: Intrasection ICC of Session 3 (Peak Left, Peak Right, Range of Motion Left, Range of Motion Right)

Peak Left	CGM10KAD	CGM10Med	CGM11KAD	CGM11Med	CGM21	CGM22	CGM23	PiG
HipFlexExt	0,296532	0,32112	0,302518	0,260054	0,028781	-0,11839	-0,11701	0,715524
HipAbAd	0,892095	0,878397	0,892175	0,882948	0,254372	0,816662	0,718094	0,920742
HipRot	0,983006	0,990741	0,983144	0,58117	0,870107	0,945186	0,785166	0,984959
KneeFlexExt	0,704613	0,861147	0,70415	0,771588	0,829719	0,812344	0,78196	0,583614
KneeVarVal	0,979512	0,991176	0,979782	0,833986	0,977401	0,989669	0,976651	0,975663
KneeRot	0,854352	0,922902	0,773108	0,971016	0,95513	0,971571	0,98218	0,907906
AnkleDorPla	0,932407	0,936182	0,911975	0,88923	0,892277	0,911118	0,8896	0,934143
AnkleInvAd	0,83815	0,974553	0,306477	0,426273	0,511472	0,104885	0,692506	0,617619
AnkleRot	0,844376	0,985848	0,864245	0,888435	0,882875	0,481402	0,681288	0,910739

Peak Right	CGM10KAD	CGM10Med	CGM11KAD	CGM11Med	CGM21	CGM22	CGM23	PiG
HipFlexExt	0,493999	0,974051	0,481328	0,703196	0,783822	0,395685	-0,06054	0,214525
HipAbAd	0,983552	0,988104	0,98357	0,983185	0,968871	0,946332	0,895683	0,984321
HipRot	0,993053	0,998862	0,993209	0,898024	0,950718	0,911529	0,876951	0,996135
KneeFlexExt	0,866347	0,990202	0,865499	0,901032	0,925123	0,926548	0,846713	0,862268
KneeVarVal	0,988392	0,99955	0,988502	0,006235	0,872826	0,363509	0,929326	0,98144
KneeRot	0,641468	0,346529	0,981581	0,788956	0,612638	0,310102	-0,14816	0,021513
AnkleDorPla	-0,04934	0,908159	0,103283	-0,00784	-0,02658	-0,05072	0,269214	0,414576
AnkleInvAd	0,96051	0,988986	0,828526	0,724155	0,755655	0,877609	0,340837	0,893329
AnkleRot	-0,1791	0,993078	-0,1035	0,528737	0,596774	0,924143	0,059796	0,947103

ROM Left	CGM10KAD	CGM10Med	CGM11KAD	CGM11Med	CGM21	CGM22	CGM23	PiG
HipFlexExt	0,966538	0,965648	0,966536	0,965514	0,966966	0,978211	0,969942	0,967733
HipAbAd	0,969381	0,965097	0,969383	0,967279	0,968168	0,972153	0,937893	0,97873
HipRot	0,814264	0,850041	0,813558	0,838867	0,88445	0,935182	0,728425	0,749898
KneeFlexExt	0,937728	0,919431	0,937728	0,913672	0,880763	0,866086	-0,05691	0,947657
KneeVarVal	0,96026	0,986883	0,960806	0,969279	0,988679	0,991086	0,963559	0,939091
KneeRot	0,443665	0,179278	0,442837	0,298332	-0,00015	0,692803	0,040209	0,377575
AnkleDorPla	0,977835	0,935926	0,978215	0,9765	0,976562	0,978749	0,959907	0,972591
AnkleInvAd	0,909701	0,847093	0,914012	0,97146	0,973327	0,945283	0,975044	0,954671
AnkleRot	0,355002	0,33509	0,368856	0,161774	0,233881	0,837767	0,854472	0,484135

ROM Right	CGM10KAD	CGM10Med	CGM11KAD	CGM11Med	CGM21	CGM22	CGM23	PiG
HipFlexExt	0,924667	0,923442	0,924668	0,922709	0,92886	0,905525	0,821187	0,943729
HipAbAd	0,979409	0,978266	0,97942	0,979308	0,979501	0,978586	0,965421	0,979417
HipRot	0,973882	0,98386	0,973675	0,981438	0,988878	0,989239	-0,02706	0,9567
KneeFlexExt	0,822702	0,93073	0,824772	0,657905	0,440879	0,475036	0,843715	0,891577
KneeVarVal	0,928876	0,997626	0,92379	0,941216	0,961344	0,957735	-0,03708	0,906061
KneeRot	-0,03043	0,828241	-0,03685	-0,10539	-0,0456	0,063538	0,050841	0,051936
AnkleDorPla	0,974754	0,867591	0,974937	0,967239	0,967999	0,970011	0,976206	0,985668
AnkleInvAd	0,597616	0,92748	0,51448	0,666211	0,727531	0,853039	-0,14946	0,986227
AnkleRot	0,510891	0,058882	0,517003	0,287415	0,314502	0,81936	0,555497	0,155318

Appendix C

Standard Error Measurement

Table C.0.1: Intersession Standard Error Measurement (SEM)

Peak L	CGM10KAD	CGM10Med	CGM11KAD	CGM11Med	CGM21	CGM22	CGM23	PiG
HipFlexExt	1,66186	2,61117	1,65887	1,33850	1,24487	0,73713	0,99438	2,08735
HipAbAd	1,09393	0,95483	1,09381	1,09232	1,04736	0,93138	0,90573	0,99764
HipRot	3,23324	9,50239	3,22594	1,18038	1,46302	1,69961	0,93430	2,73970
KneeFlexExt	2,09442	4,01436	2,08929	1,68782	1,56309	1,59143	1,23412	1,87476
KneeVarVal	1,97157	5,63914	1,96450	0,99165	1,05589	2,00238	0,40018	2,42096
KneeRot	4,12524	4,08898	3,48870	4,63164	4,73835	4,67531	3,41691	4,41483
AnkleDorPla	0,71343	1,48445	0,80057	1,15968	1,16653	1,06372	1,02394	0,91252
AnkleInvAd	2,36393	1,78646	1,32395	0,58967	0,57230	0,78791	0,63813	1,42176
AnkleRot	1,46258	5,93540	1,59136	1,63906	1,60345	0,38739	0,63726	3,33351

Peak R	CGM10KAD	CGM10Med	CGM11KAD	CGM11Med	CGM21	CGM22	CGM23	PiG
HipFlexExt	0,46469	1,159903	0,468236	0,536422	0,508582	0,839706	1,108553	0,633494
HipAbAd	1,139431	1,164283	1,140685	1,084644	1,048697	1,124265	1,590085	1,055391
HipRot	5,02707	6,601574	5,07403	1,341555	1,143056	1,317538	1,449065	4,243402
KneeFlexExt	1,338669	4,573052	1,339244	1,846776	1,824353	1,847891	1,525741	1,035632
KneeVarVal	1,467274	5,951069	1,46374	0,439902	0,626168	1,547592	0,440029	1,505021
KneeRot	3,210602	4,870169	1,512859	1,009974	1,817199	1,139267	1,943909	3,121652
AnkleDorPla	0,479999	0,51932	1,457501	1,551843	1,556146	1,585473	1,008238	1,255853
AnkleInvAd	1,102747	1,586537	0,865445	0,179181	0,141131	0,45357	0,802968	0,611362
AnkleRot	1,484322	10,63354	1,589718	0,543781	0,457679	1,413422	1,576471	5,973292

ROM L	CGM10KAD	CGM10Med	CGM11KAD	CGM11Med	CGM21	CGM22	CGM23	PiG
HipFlexExt	1,783886	1,832577	1,781885	1,858714	1,834314	2,191269	1,925561	1,535051
HipAbAd	1,421736	1,343946	1,421615	1,380575	1,330017	1,359571	1,06492	1,41565
HipRot	2,595619	2,346598	2,602256	2,297542	2,220737	2,848347	1,867101	2,005389
KneeFlexExt	1,714676	0,846292	1,714685	1,562919	1,444895	1,560635	0,480628	1,802806
KneeVarVal	1,06181	4,682376	1,060296	1,899684	1,848851	4,316809	1,774966	0,907535
KneeRot	1,439061	2,757972	1,439791	1,444499	1,172353	2,546455	0,833313	1,234241
AnkleDorPla	1,766175	1,135398	1,679955	2,036706	2,047941	2,153111	1,965508	1,217491
AnkleInvAd	0,821733	0,220882	0,862006	0,801358	0,781445	0,800223	1,516547	0,166974
AnkleRot	1,603225	1,542513	1,626812	1,460406	1,456097	1,497465	1,856409	0,597828

ROM R	CGM10KAD	CGM10Med	CGM11KAD	CGM11Med	CGM21	CGM22	CGM23	PiG
HipFlexExt	1,969626	1,992354	1,967935	2,040161	1,980542	1,69788	1,485446	1,965112
HipAbAd	1,752004	1,52212	1,752728	1,725266	1,651407	1,390473	1,009981	1,673994
HipRot	4,761685	4,78424	4,759068	4,857576	5,587327	5,493908	0,50584	3,014787
KneeFlexExt	1,554635	2,013287	1,558493	1,276581	1,380818	1,409219	1,010976	1,290261
KneeVarVal	0,687803	5,658708	0,688468	0,960866	1,00064	1,269399	0,514625	1,072159
KneeRot	1,411794	1,434555	1,3904	1,430036	1,594383	2,754061	0,337924	0,497053
AnkleDorPla	2,362188	2,631797	2,295141	2,44441	2,444158	2,324771	1,763839	0,742331
AnkleInvAd	0,796021	0,079923	0,901755	0,632385	0,606313	0,243537	1,017726	1,322921
AnkleRot	1,661695	1,392042	1,621888	1,35502	1,279364	1,743587	0,482681	1,062893

Table C.0.2: Intrasection Standard Error Measurement (SEM): Session1

Peak L	CGM10KAD	CGM10Med	CGM11KAD	CGM11Med	CGM21	CGM22	CGM23	PiG
HipFlexExt	1,294083	1,276282	1,294291	1,283823	1,238452	1,185947	1,152939	1,031582
HipAbAd	0,796205	0,777939	0,796522	0,792029	0,755786	0,729437	0,766221	0,83608
HipRot	1,719125	1,648869	1,720252	1,640801	1,698415	1,379813	0,914116	1,147862
KneeFlexExt	1,104491	1,342758	1,10406	1,094909	1,093139	1,118809	1,009707	1,101547
KneeVarVal	0,594547	0,329051	0,594412	0,556784	0,644179	1,332953	0,394263	0,707759
KneeRot	1,263826	2,470954	1,262625	1,200818	1,231997	1,268656	0,767748	1,600194
AnkleDorPla	0,958694	0,937366	0,958642	0,949099	0,952733	0,937668	0,98567	1,064629
AnkleInvAd	0,468275	0,505818	0,474228	0,485145	0,486519	0,724074	0,39742	0,370486
AnkleRot	2,222371	2,18378	2,219119	2,216228	2,117178	2,466412	2,164738	2,445841

Peak R	CGM10KAD	CGM10Med	CGM11KAD	CGM11Med	CGM21	CGM22	CGM23	PiG
HipFlexExt	1,104884	1,087099	1,105039	1,096966	1,058821	1,069962	1,116619	0,916699
HipAbAd	1,080477	1,074656	1,080675	1,071207	1,021849	0,972833	0,932173	0,945881
HipRot	1,705081	1,583788	1,707343	1,609681	1,644506	1,823144	1,175634	1,050263
KneeFlexExt	1,227857	1,370757	1,227822	1,232831	1,197713	1,187217	1,10421	1,235952
KneeVarVal	0,582212	0,849438	0,581621	0,581531	0,622072	1,007203	0,378457	0,486891
KneeRot	1,328846	1,891429	1,3296	1,264202	1,213312	1,565541	1,284822	0,991236
AnkleDorPla	1,057385	1,027093	1,052391	1,039032	1,037288	0,983461	0,928339	1,060642
AnkleInvAd	0,260396	0,291786	0,267541	0,264422	0,269097	0,465571	0,204439	0,173616
AnkleRot	1,694187	1,64121	1,717006	1,685163	1,788714	1,951086	1,365024	2,140958

ROM L	CGM10KAD	CGM10Med	CGM11KAD	CGM11Med	CGM21	CGM22	CGM23	PiG
HipFlexExt	2,04925	2,058358	2,048962	2,061877	1,989148	1,896008	1,779987	1,858829
HipAbAd	0,982319	0,908562	0,98229	1,001976	0,969873	0,894213	0,735299	1,44527
HipRot	1,729956	2,208689	1,730619	1,707691	1,760421	1,567535	1,495552	1,509639
KneeFlexExt	1,93517	2,08203	1,936323	1,840517	1,912876	1,907017	1,825922	1,662125
KneeVarVal	0,716267	0,807278	0,714872	0,80738	0,9888	1,652786	0,572305	0,824966
KneeRot	2,167567	3,116798	2,162576	2,150076	1,621903	2,257884	1,330676	2,525743
AnkleDorPla	2,064962	1,836423	2,058146	2,03908	2,035593	2,132087	2,115442	1,737615
AnkleInvAd	0,675396	0,490315	0,66575	0,657327	0,653464	0,887112	0,601308	0,467996
AnkleRot	2,658487	2,635582	2,654107	2,635542	2,488715	3,228047	2,31301	2,976059

ROM R	CGM10KAD	CGM10Med	CGM11KAD	CGM11Med	CGM21	CGM22	CGM23	PiG
HipFlexExt	1,627551	1,629987	1,627441	1,627677	1,564058	1,627372	1,730985	1,337397
HipAbAd	1,070803	1,047686	1,07118	1,054487	1,006944	1,073462	1,088806	0,923789
HipRot	1,877047	1,890841	1,878753	1,800456	1,891722	2,205994	1,230652	1,409648
KneeFlexExt	1,528907	1,633711	1,530193	1,497905	1,51249	1,542125	1,575331	1,541563
KneeVarVal	0,807234	1,291533	0,806678	0,80152	0,806139	1,513732	0,482938	0,661292
KneeRot	2,060487	2,129712	2,061733	1,943027	2,319287	2,557348	1,130009	0,669664
AnkleDorPla	1,005537	1,008974	1,013254	0,986973	0,97736	0,96565	0,851547	1,011058
AnkleInvAd	0,430573	0,488063	0,350456	0,36199	0,360825	0,540008	0,27794	0,32667
AnkleRot	2,256926	2,055851	2,271495	2,229552	2,263974	2,64918	1,650894	2,460078

Table C.0.3: Intrasession Standard Error Measurement (SEM): Session2

Peak L	CGM10KAD	CGM10Med	CGM11KAD	CGM11Med	CGM21	CGM22	CGM23	PiG
HipFlexExt	1,502709	1,513179	1,503005	1,484517	1,417277	1,52423	1,614235	0,989773
HipAbAd	0,717627	0,767342	0,717636	0,714488	0,677306	0,718172	0,678559	0,532712
HipRot	1,152998	1,123714	1,153573	1,107623	1,022498	1,548217	0,858019	1,196302
KneeFlexExt	1,367069	1,571095	1,36669	1,393741	1,386077	1,398108	1,464533	1,334181
KneeVarVal	0,743802	1,416812	0,741585	1,054872	1,139464	1,660646	0,282856	0,504013
KneeRot	2,261987	2,136965	2,260146	2,284059	2,208104	2,661444	1,744191	1,941537
AnkleDorPla	1,024379	0,924263	1,026232	0,984634	0,974901	1,015515	0,893778	1,113174
AnkleInvAd	0,835551	0,738429	0,854141	0,951892	0,947602	1,091792	0,888041	0,563716
AnkleRot	2,583038	2,542331	2,590065	2,596399	2,390182	1,86069	2,244278	2,966398

Peak R	CGM10KAD	CGM10Med	CGM11KAD	CGM11Med	CGM21	CGM22	CGM23	PiG
HipFlexExt	1,550289	1,484585	1,550871	1,526703	1,47529	1,458944	1,566343	1,54358
HipAbAd	1,018859	0,936275	1,019373	0,997246	0,952797	0,84707	0,687347	0,817769
HipRot	1,325944	1,31853	1,327529	1,236107	1,274487	1,88481	0,976571	0,53968
KneeFlexExt	0,791896	0,998592	0,791741	0,800479	0,794801	0,820383	0,706586	0,831598
KneeVarVal	0,576982	0,626305	0,576566	0,616692	0,635493	0,983002	0,155355	0,409969
KneeRot	1,250588	1,363504	1,25224	1,235751	1,240697	2,012005	0,540203	1,134431
AnkleDorPla	1,689597	1,605737	1,685482	1,66383	1,653316	1,645496	1,521786	1,707742
AnkleInvAd	0,405487	0,594565	0,465256	0,412043	0,426854	0,58641	0,25114	0,465907
AnkleRot	3,132235	2,947024	3,117405	3,078459	2,976544	2,808519	2,507413	3,091567

ROM L	CGM10KAD	CGM10Med	CGM11KAD	CGM11Med	CGM21	CGM22	CGM23	PiG
HipFlexExt	1,566816	1,579742	1,566885	1,557544	1,490122	1,612972	1,589372	1,443453
HipAbAd	0,873624	0,890937	0,873713	0,86135	0,820579	0,976192	0,99617	0,786025
HipRot	1,632655	1,541984	1,632654	1,664952	1,661574	1,881679	1,516317	1,303604
KneeFlexExt	1,739756	1,890592	1,739658	1,756423	1,791854	1,849838	1,982487	1,821346
KneeVarVal	1,074443	1,40747	1,073706	1,182618	1,25044	1,901271	0,746473	1,032366
KneeRot	3,168385	2,809595	3,173534	3,183685	2,922098	3,366952	2,23407	2,008404
AnkleDorPla	2,318385	2,189593	2,301637	2,230028	2,219043	2,172112	2,69893	2,498261
AnkleInvAd	0,873376	0,793865	0,900845	1,03187	1,021518	1,248923	0,935697	0,555272
AnkleRot	2,609295	2,563658	2,61521	2,633859	2,434091	1,422795	2,383845	2,718824

ROM R	CGM10KAD	CGM10Med	CGM11KAD	CGM11Med	CGM21	CGM22	CGM23	PiG
HipFlexExt	1,557157	1,496992	1,557739	1,535489	1,483017	1,465931	1,478136	1,624525
HipAbAd	0,652468	0,624078	0,65288	0,637784	0,608094	0,578513	0,534324	0,575794
HipRot	1,804222	1,849595	1,804466	1,7827	1,898982	2,224951	0,942696	1,309488
KneeFlexExt	1,194321	1,307244	1,194137	1,204715	1,201508	1,24928	1,220319	1,215001
KneeVarVal	0,978415	0,879337	0,974515	0,951519	1,027879	1,470204	0,367834	0,584919
KneeRot	1,991841	1,467384	1,989973	1,934174	1,965874	4,029774	0,874358	1,46178
AnkleDorPla	1,607256	1,764032	1,611807	1,602927	1,601585	1,64496	1,799127	1,994999
AnkleInvAd	0,533183	0,52917	0,618932	0,577286	0,478378	0,591733	0,41507	0,478483
AnkleRot	3,054913	2,849153	3,043575	2,989433	2,940296	2,750616	2,246017	3,112475

Table C.0.4: Intrasession Standard Error Measurement (SEM): Session 3

Peak L	CGM10KAD	CGM10Med	CGM11KAD	CGM11Med	CGM21	CGM22	CGM23	PiG
HipFlexExt	1,017736	1,015276	1,017673	1,020541	0,983182	0,919429	1,011891	0,952676
HipAbAd	0,821369	0,818202	0,821343	0,825963	0,788655	0,681118	0,904501	0,744051
HipRot	0,925367	0,875419	0,926414	0,865559	0,963332	1,010295	1,131108	0,941765
KneeFlexExt	1,406609	1,64006	1,406063	1,401072	1,364745	1,32693	1,380261	1,420398
KneeVarVal	0,782048	1,005804	0,778199	0,489183	0,435697	0,374218	0,485833	0,745349
KneeRot	1,309962	1,082828	1,31118	1,596934	1,867877	2,04328	0,85546	0,834445
AnkleDorPla	1,113362	0,976923	1,117133	1,077655	1,072964	1,073334	1,037016	1,082578
AnkleInvAd	0,575158	0,514783	0,57566	0,593891	0,594255	0,72065	0,541376	0,434379
AnkleRot	2,082775	2,080099	2,080719	2,005894	1,88293	2,284821	1,770694	1,672139

Peak R	CGM10KAD	CGM10Med	CGM11KAD	CGM11Med	CGM21	CGM22	CGM23	PiG
HipFlexExt	1,180177	1,174304	1,179773	1,191448	1,143652	1,05465	0,917827	1,154373
HipAbAd	0,841062	0,851261	0,841092	0,831453	0,795953	0,823092	0,835324	0,805968
HipRot	0,87759	1,031128	0,878652	0,853031	0,840924	1,405705	0,384048	0,764558
KneeFlexExt	1,37172	1,771272	1,371208	1,420944	1,346862	1,351844	1,312263	1,384543
KneeVarVal	0,479275	0,662944	0,471956	0,822387	0,840989	1,318389	0,51795	0,571521
KneeRot	1,002838	1,38487	0,993497	0,837796	1,130236	1,778704	1,443436	0,690697
AnkleDorPla	0,866963	0,643909	0,86895	0,787575	0,779174	0,81257	0,941439	1,195435
AnkleInvAd	0,485848	0,917666	0,478906	0,586995	0,622702	0,829418	0,308737	0,720243
AnkleRot	2,789327	2,753402	2,79355	2,769795	2,707087	2,288614	2,273318	2,07608

ROM L	CGM10KAD	CGM10Med	CGM11KAD	CGM11Med	CGM21	CGM22	CGM23	PiG
HipFlexExt	1,198868	1,202742	1,198525	1,211873	1,171585	1,067636	1,158366	1,20049
HipAbAd	1,174912	1,214693	1,174157	1,214413	1,159037	0,870543	1,277845	1,028442
HipRot	1,301733	1,397954	1,300446	1,2861	1,230119	1,047531	1,080216	1,23301
KneeFlexExt	1,299188	1,532951	1,298649	1,302557	1,270792	1,205088	1,097847	1,299114
KneeVarVal	0,452698	0,70709	0,449622	0,580503	0,405028	0,954834	0,441365	0,423998
KneeRot	2,641554	1,939046	2,641178	2,843053	3,060568	3,602448	1,16291	1,421092
AnkleDorPla	1,602943	1,431881	1,605382	1,543313	1,525295	1,537514	1,790459	1,699676
AnkleInvAd	0,695357	0,59571	0,664234	0,625689	0,582031	0,747413	0,565068	0,525631
AnkleRot	1,905431	1,901306	1,917075	1,817316	1,592605	2,121328	1,731515	1,509811

ROM R	CGM10KAD	CGM10Med	CGM11KAD	CGM11Med	CGM21	CGM22	CGM23	PiG
HipFlexExt	1,58971	1,58085	1,589024	1,610763	1,551335	1,424275	1,208157	1,532037
HipAbAd	0,94	0,982492	0,939746	0,948378	0,90933	0,886294	0,848606	0,898807
HipRot	1,248775	0,900633	1,251217	1,12637	1,109462	1,42843	0,679375	1,266067
KneeFlexExt	1,584727	1,974105	1,584381	1,652022	1,587746	1,579583	1,564755	1,558104
KneeVarVal	0,771469	0,977175	0,761087	1,256971	1,262352	1,76519	0,809826	0,772793
KneeRot	1,537176	2,540895	1,535669	1,988267	1,691534	3,311806	1,573495	0,739522
AnkleDorPla	1,396216	1,214914	1,401968	1,273123	1,258932	1,170515	1,224152	1,552431
AnkleInvAd	0,390745	0,755999	0,380023	0,458903	0,49918	0,680691	0,387661	0,598532
AnkleRot	2,223793	2,157706	2,228174	2,208755	2,180913	1,795705	1,808566	1,481874

Appendix D

Minimal Detectable Change

Table D.0.1: Intersession Minimal Detectable Change

Peak L	CGM10KAD	CGM10Med	CGM11KAD	CGM11Med	CGM21	CGM22	CGM23	PiG
HipFlexExt	4,606441	7,237801	4,598145	3,710141	3,450604	2,043226	2,756272	5,785838
HipAbAd	3,032218	2,64664	3,031876	3,027769	2,903125	2,581648	2,510549	2,765315
HipRot	8,962075	26,33928	8,94185	3,271836	4,055291	4,711092	2,589761	7,594059
KneeFlexExt	5,805444	11,12723	5,791225	4,67841	4,332678	4,411231	3,420807	5,196563
KneeVarVal	5,464912	15,6309	5,445324	2,748713	2,926774	5,550315	1,109249	6,710562
KneeRot	11,43459	11,33408	9,670183	12,83826	13,13404	12,95929	9,471203	12,23729
AnkleDorPla	1,977514	4,114688	2,219079	3,214464	3,233449	2,948486	2,838218	2,529386
AnkleInvAd	6,552469	4,95181	3,669799	1,634489	1,586324	2,183973	1,768807	3,940912
AnkleRot	4,054077	16,4521	4,411015	4,543242	4,444535	1,07379	1,766398	9,240029

Peak R	CGM10KAD	CGM10Med	CGM11KAD	CGM11Med	CGM21	CGM22	CGM23	PiG
HipFlexExt	1,288054	3,215088	1,297885	1,486886	1,409717	2,327546	3,072752	1,755956
HipAbAd	3,15834	3,227227	3,161817	3,006479	2,906839	3,116304	4,40749	2,925394
HipRot	13,93433	18,29863	14,06449	3,718601	3,168388	3,652028	4,016602	11,76211
KneeFlexExt	3,7106	12,67585	3,712196	5,119001	5,056849	5,122093	4,229138	2,870625
KneeVarVal	4,067075	16,49552	4,057281	1,219345	1,735648	4,289707	1,219698	4,171704
KneeRot	8,899336	13,49942	4,193432	2,799506	5,037018	3,157887	5,388241	8,652779
AnkleDorPla	1,330489	1,439481	4,039988	4,301489	4,313417	4,394706	2,794694	3,481046
AnkleInvAd	3,05666	4,397657	2,398891	0,496664	0,391196	1,257232	2,225713	1,694609
AnkleRot	4,114331	29,47467	4,406474	1,507285	1,268621	3,917805	4,369753	16,55712

ROM L	CGM10KAD	CGM10Med	CGM11KAD	CGM11Med	CGM21	CGM22	CGM23	PiG
HipFlexExt	4,944679	5,079645	4,939133	5,152092	5,084458	6,073888	5,337383	4,254945
HipAbAd	3,940852	3,725229	3,940514	3,826759	3,686618	3,768538	2,951809	3,923982
HipRot	7,194688	6,504438	7,213085	6,36846	6,155568	7,895215	5,17534	5,558655
KneeFlexExt	4,75284	2,3458	4,752865	4,332191	4,005045	4,325859	1,332233	4,997124
KneeVarVal	2,943188	12,97888	2,938991	5,265654	5,124754	11,96558	4,919954	2,515559
KneeRot	3,988874	7,644709	3,990897	4,003948	3,249596	7,058412	2,309827	3,421142
AnkleDorPla	4,895589	3,147164	4,656597	5,64546	5,676604	5,96812	5,448111	3,374713
AnkleInvAd	2,277727	0,612253	2,389359	2,221252	2,166054	2,218105	4,203655	0,462828
AnkleRot	4,443914	4,275629	4,509293	4,048038	4,036094	4,15076	5,145702	1,657096

ROM R	CGM10KAD	CGM10Med	CGM11KAD	CGM11Med	CGM21	CGM22	CGM23	PiG
HipFlexExt	5,459525	5,522522	5,454838	5,655039	5,489781	4,706284	4,117447	5,447014
HipAbAd	4,856308	4,219102	4,858315	4,782192	4,577468	3,854194	2,799524	4,640074
HipRot	13,19872	13,26124	13,19146	13,46452	15,48728	15,22833	1,402116	8,356562
KneeFlexExt	4,309229	5,580548	4,319922	3,538501	3,827431	3,906157	2,802283	3,576422
KneeVarVal	1,906493	15,68514	1,908336	2,663384	2,773633	3,518595	1,426466	2,971873
KneeRot	3,913293	3,976384	3,853991	3,963857	4,419405	7,633867	0,936677	1,37776
AnkleDorPla	6,547652	7,294969	6,361807	6,775558	6,774859	6,443935	4,889113	2,057638
AnkleInvAd	2,206457	0,221535	2,499537	1,752881	1,680613	0,675049	2,820992	3,666951
AnkleRot	4,605984	3,858543	4,495644	3,755925	3,546217	4,832975	1,337924	2,946188

Table D.0.2: Intrasession Minimal Detectable Change: Session 1

Peak L	CGM10KAD	CGM10Med	CGM11KAD	CGM11Med	CGM21	CGM22	CGM23	PiG
HipFlexExt	3,587016	3,537672	3,587592	3,558575	3,432813	3,287279	3,195785	2,859398
HipAbAd	2,206967	2,156336	2,207846	2,195393	2,094933	2,021896	2,123855	2,317496
HipRot	4,765171	4,570432	4,768295	4,548068	4,707767	3,824647	2,533801	3,181712
KneeFlexExt	3,061492	3,721935	3,060298	3,034933	3,030027	3,10118	2,798765	3,053333
KneeVarVal	1,648	0,912083	1,647626	1,543326	1,785574	3,694756	1,092841	1,961807
KneeRot	3,503148	6,849136	3,499818	3,328498	3,414921	3,516535	2,128089	4,435512
AnkleDorPla	2,657364	2,598246	2,65722	2,630768	2,64084	2,599084	2,732139	2,951001
AnkleInvAd	1,297992	1,402056	1,314494	1,344754	1,348563	2,00703	1,101593	1,026935
AnkleRot	6,160099	6,053129	6,151084	6,14307	5,868518	6,836546	6,000348	6,779525

Peak R	CGM10KAD	CGM10Med	CGM11KAD	CGM11Med	CGM21	CGM22	CGM23	PiG
HipFlexExt	3,062583	3,013284	3,063012	3,040636	2,934902	2,965783	3,09511	2,540961
HipAbAd	2,994929	2,978793	2,99548	2,969233	2,832421	2,696557	2,583852	2,621847
HipRot	4,726242	4,390036	4,732514	4,461807	4,558339	5,053496	3,258692	2,91118
KneeFlexExt	3,403446	3,799544	3,40335	3,417233	3,31989	3,290798	3,060715	3,425884
KneeVarVal	1,613809	2,354522	1,612172	1,611922	1,724296	2,791826	1,04903	1,349594
KneeRot	3,683372	5,242773	3,685463	3,504189	3,363129	4,339457	3,561346	2,747566
AnkleDorPla	2,930921	2,846957	2,917079	2,880048	2,875214	2,726014	2,573225	2,939948
AnkleInvAd	0,72178	0,80879	0,741585	0,73294	0,745898	1,290498	0,566676	0,481239
AnkleRot	4,696046	4,549201	4,759299	4,671032	4,958063	5,408136	3,783653	5,934434

ROM L	CGM10KAD	CGM10Med	CGM11KAD	CGM11Med	CGM21	CGM22	CGM23	PiG
HipFlexExt	5,68023	5,705478	5,679434	5,715231	5,513638	5,255466	4,933873	5,152412
HipAbAd	2,722848	2,518407	2,722768	2,777334	2,68835	2,478632	2,038144	4,006085
HipRot	4,795194	6,122173	4,797032	4,733478	4,879639	4,344986	4,145458	4,184505
KneeFlexExt	5,364019	5,771091	5,367214	5,101652	5,302222	5,285981	5,061196	4,607174
KneeVarVal	1,98539	2,237661	1,981524	2,237943	2,740815	4,58129	1,58635	2,286689
KneeRot	6,00819	8,639323	5,994355	5,959707	4,495686	6,258534	3,688445	7,001002
AnkleDorPla	5,723783	5,090305	5,70489	5,652041	5,642376	5,909843	5,863706	4,816424
AnkleInvAd	1,872103	1,359084	1,845364	1,822018	1,81131	2,458949	1,666742	1,29722
AnkleRot	7,368951	7,305462	7,35681	7,305351	6,898366	8,947689	6,411336	8,249215

ROM R	CGM10KAD	CGM10Med	CGM11KAD	CGM11Med	CGM21	CGM22	CGM23	PiG
HipFlexExt	4,51134	4,518093	4,511035	4,511689	4,335346	4,510846	4,798045	3,707074
HipAbAd	2,968113	2,904038	2,969159	2,92289	2,791105	2,975484	3,018017	2,560612
HipRot	5,202908	5,241145	5,207639	4,990609	5,243587	6,114703	3,411194	3,907344
KneeFlexExt	4,237913	4,528415	4,241479	4,151981	4,192408	4,274552	4,366595	4,272995
KneeVarVal	2,237538	3,579947	2,235998	2,2217	2,234502	4,195852	1,338637	1,833007
KneeRot	5,711378	5,90326	5,714834	5,385797	6,428735	7,088607	3,132225	1,856214
AnkleDorPla	2,787207	2,796734	2,808596	2,735751	2,709103	2,676645	2,360369	2,802509
AnkleInvAd	1,193486	1,352843	0,971414	1,003386	1,000156	1,496826	0,770411	0,905482
AnkleRot	6,25588	5,698528	6,296263	6,180004	6,275417	7,343153	4,576046	6,818988

Table D.0.3: Intrasession Minimal Detectable Change: Session 2

Peak L	CGM10KAD	CGM10Med	CGM11KAD	CGM11Med	CGM21	CGM22	CGM23	PiG
HipFlexExt	4,165297	4,194318	4,166118	4,114871	3,928491	4,22495	4,474432	<u>2,74351</u>
HipAbAd	1,98916	2,126963	1,989186	1,98046	1,877396	1,990672	1,88087	<u>1,476603</u>
HipRot	3,195947	3,114776	3,19754	3,070174	2,83422	4,291438	2,378307	<u>3,315981</u>
KneeFlexExt	3,789321	4,354852	3,788272	3,863253	3,842008	3,875358	4,059479	<u>3,698162</u>
KneeVarVal	2,061713	3,927202	2,055568	2,923955	3,158432	4,603076	0,784036	<u>1,397052</u>
KneeRot	6,269907	5,923364	6,264804	6,331089	6,120552	7,377146	<u>4,834651</u>	<u>5,381667</u>
AnkleDorPla	2,839433	2,561928	2,844571	2,729267	2,702287	2,814865	<u>2,477425</u>	<u>3,085562</u>
AnkleInvAd	2,316028	2,046821	2,367558	2,63851	2,626619	3,026294	2,461524	<u>1,56254</u>
AnkleRot	7,159816	7,046982	7,179293	7,196851	6,625247	<u>5,15757</u>	6,220822	<u>8,222435</u>

Peak R	CGM10KAD	CGM10Med	CGM11KAD	CGM11Med	CGM21	CGM22	CGM23	PiG
HipFlexExt	4,297182	4,115059	4,298795	4,231804	4,089296	<u>4,043988</u>	4,34168	<u>4,278585</u>
HipAbAd	2,824133	2,595221	2,825559	2,764225	2,641019	2,347958	1,905228	<u>2,26674</u>
HipRot	3,67533	3,654779	3,679723	3,426313	3,532698	5,224426	2,706915	<u>1,495917</u>
KneeFlexExt	2,195022	2,767957	2,194594	2,218815	<u>2,203077</u>	2,273985	<u>1,958556</u>	<u>2,305072</u>
KneeVarVal	1,599312	1,736029	1,598158	1,709382	<u>1,761497</u>	2,724742	<u>0,430622</u>	<u>1,136376</u>
KneeRot	3,466453	3,779442	3,471032	3,425326	3,439037	5,576994	<u>1,497368</u>	<u>3,144481</u>
AnkleDorPla	4,683325	4,450875	4,671917	4,611902	4,582758	4,561083	<u>4,218175</u>	<u>4,733619</u>
AnkleInvAd	1,123952	1,648049	1,289624	1,142125	1,18318	1,625445	<u>0,696123</u>	<u>1,29143</u>
AnkleRot	8,682112	8,168735	8,641006	8,533054	8,250559	7,784818	<u>6,950193</u>	<u>8,569386</u>

ROM L	CGM10KAD	CGM10Med	CGM11KAD	CGM11Med	CGM21	CGM22	CGM23	PiG
HipFlexExt	4,342994	4,378821	4,343183	4,317291	4,130408	4,470931	4,405514	<u>4,001048</u>
HipAbAd	2,421562	2,46955	2,421808	2,387539	2,274528	2,705868	2,761243	<u>2,178749</u>
HipRot	4,525489	4,274162	4,525487	4,615013	4,605649	5,215747	4,203017	<u>3,613407</u>
KneeFlexExt	4,822358	5,240454	4,822085	4,868556	4,966765	5,12749	5,495173	<u>5,048515</u>
KneeVarVal	2,978205	3,901308	<u>2,976161</u>	3,278049	3,466043	5,270055	<u>2,069117</u>	<u>2,861571</u>
KneeRot	8,782315	7,7878	8,796586	8,824726	8,099643	9,332715	6,192527	<u>5,567012</u>
AnkleDorPla	6,426236	6,069242	6,379813	6,181323	6,150874	<u>6,020788</u>	7,481052	<u>6,924827</u>
AnkleInvAd	2,420874	2,200482	2,497015	2,860197	2,831502	<u>3,461837</u>	2,59362	<u>1,539136</u>
AnkleRot	7,232595	7,106098	7,248991	7,300685	6,746957	<u>3,943788</u>	6,607681	<u>7,536196</u>

ROM R	CGM10KAD	CGM10Med	CGM11KAD	CGM11Med	CGM21	CGM22	CGM23	PiG
HipFlexExt	4,316218	4,14945	4,317833	4,256157	4,110715	<u>4,063354</u>	4,097184	<u>4,502954</u>
HipAbAd	1,80855	1,729856	1,80969	1,767848	1,685551	1,603557	1,48107	<u>1,59602</u>
HipRot	5,00105	5,126815	5,001724	4,941393	5,263709	6,167249	<u>2,613021</u>	<u>3,629715</u>
KneeFlexExt	3,310488	3,623497	<u>3,309979</u>	3,339298	3,33041	3,462829	3,38255	<u>3,36781</u>
KneeVarVal	2,712028	2,437399	<u>2,701219</u>	2,637476	2,849134	4,075198	<u>1,019583</u>	<u>1,621313</u>
KneeRot	5,5211	4,067381	5,515922	5,361256	5,449124	11,16996	<u>2,423597</u>	<u>4,051847</u>
AnkleDorPla	4,455086	4,889648	4,4677	4,443088	<u>4,439367</u>	4,559597	4,986925	<u>5,529855</u>
AnkleInvAd	1,477907	1,466784	1,715593	1,600155	1,325995	1,640199	<u>1,150516</u>	<u>1,326288</u>
AnkleRot	8,467787	7,897451	8,436361	8,286285	8,150086	7,624318	<u>6,225641</u>	<u>8,62734</u>

Table D.0.4: Intrasession Minimal Detectable Change: Session 3

Peak L	CGM10KAD	CGM10Med	CGM11KAD	CGM11Med	CGM21	CGM22	CGM23	PiG
HipFlexExt	2,821019	2,8142	2,820846	2,828796	<u>2,725241</u>	2,548528	2,80482	2,640684
HipAbAd	2,276717	2,26794	2,276647	2,289451	<u>2,186039</u>	1,887963	2,507148	2,062405
HipRot	2,564986	2,426538	2,567889	2,399207	<u>2,67022</u>	2,800394	3,135271	2,610439
KneeFlexExt	3,898922	4,546014	3,897409	3,883574	<u>3,782879</u>	3,678063	3,825887	3,937143
KneeVarVal	2,167725	2,787947	2,157059	1,355947	<u>1,207691</u>	1,037279	1,346662	2,066001
KneeRot	3,631028	3,001446	3,634406	4,426476	5,177491	5,663682	2,371215	<u>2,312964</u>
AnkleDorPla	3,086081	<u>2,707894</u>	3,096536	2,987107	2,974104	2,975131	2,874461	3,000752
AnkleInvAd	1,594257	1,426907	1,595649	1,646182	1,64719	1,997541	1,500617	1,204036
AnkleRot	5,773157	5,765741	5,76746	5,560053	5,219216	6,333202	4,908113	<u>4,634934</u>

Peak R	CGM10KAD	CGM10Med	CGM11KAD	CGM11Med	CGM21	CGM22	CGM23	PiG
HipFlexExt	3,271284	3,255005	3,270163	3,302526	3,170042	2,923342	<u>2,544085</u>	3,199758
HipAbAd	2,331306	2,359574	2,331388	2,30467	<u>2,20627</u>	2,281494	2,3154	2,234031
HipRot	2,432555	2,85814	2,4355	2,364481	2,330921	3,896415	<u>1,064526</u>	2,119247
KneeFlexExt	3,802214	4,909715	3,800794	3,938657	3,733311	3,74712	<u>3,637407</u>	3,837758
KneeVarVal	1,328484	1,837588	<u>1,308196</u>	2,279542	2,331104	3,654389	1,435684	1,584175
KneeRot	2,779725	3,838663	2,753832	2,322253	3,132856	4,930317	4,001	<u>1,914515</u>
AnkleDorPla	2,403099	<u>1,784825</u>	2,408606	2,183047	2,159759	2,25233	2,609535	3,313575
AnkleInvAd	1,346701	2,543641	1,327459	1,627068	1,726043	2,29903	<u>0,855776</u>	1,996411
AnkleRot	7,73162	7,632041	7,743325	7,677481	7,503662	6,343713	6,301315	<u>5,754599</u>

ROM L	CGM10KAD	CGM10Med	CGM11KAD	CGM11Med	CGM21	CGM22	CGM23	PiG
HipFlexExt	3,323093	3,333831	3,322142	3,35914	3,247468	<u>2,959336</u>	3,210828	3,32759
HipAbAd	3,256691	3,366958	3,254598	3,36618	3,212687	<u>2,413023</u>	3,542005	2,850696
HipRot	3,60822	3,874931	3,604651	3,564887	3,409715	<u>2,903607</u>	2,994205	3,417729
KneeFlexExt	3,601165	4,249124	3,599672	3,610504	3,522454	3,340334	<u>3,043077</u>	3,600961
KneeVarVal	1,254815	1,959955	1,246287	1,609072	1,122681	2,646666	<u>1,223402</u>	1,175261
KneeRot	7,322015	5,374762	7,320973	7,88054	8,483462	9,985477	<u>3,223423</u>	3,939065
AnkleDorPla	4,443131	<u>3,96897</u>	4,449891	4,277844	4,227903	4,261772	4,962899	4,711263
AnkleInvAd	1,92743	1,651223	1,841162	1,734323	1,613308	2,071723	1,566289	<u>1,456974</u>
AnkleRot	5,281585	5,270152	5,31386	5,037342	4,414477	5,880022	4,799515	<u>4,184982</u>

ROM R	CGM10KAD	CGM10Med	CGM11KAD	CGM11Med	CGM21	CGM22	CGM23	PiG
HipFlexExt	4,406451	4,381892	4,40455	4,464806	4,300081	3,947888	<u>3,348841</u>	4,246591
HipAbAd	2,605547	2,723329	2,604842	2,62877	2,520535	2,456681	2,352217	2,491366
HipRot	3,461428	2,496428	3,468197	3,122137	3,07527	3,959407	<u>1,883131</u>	3,509358
KneeFlexExt	4,392639	5,47194	4,39168	4,579172	4,401008	4,37838	4,337279	<u>4,318844</u>
KneeVarVal	2,138403	2,70859	<u>2,109626</u>	3,484145	3,499062	4,892857	2,244724	<u>2,142072</u>
KneeRot	4,260834	7,043001	4,256657	5,511196	4,688693	9,179858	4,361505	<u>2,049851</u>
AnkleDorPla	3,870113	3,36757	3,886058	3,528917	3,489582	<u>3,244502</u>	3,393176	4,30312
AnkleInvAd	1,083089	2,095522	1,053369	1,272014	1,383655	1,886779	<u>1,074543</u>	1,659045
AnkleRot	6,164041	5,980856	6,176182	6,122356	6,045184	4,977439	5,013089	<u>4,107544</u>

Does the lower limb kinematic CGM2.i model form a suitable alternative to the PiG model in a clinical setting?

Louise Missault

Student number: 01409686

Supervisors: Prof. Malcolm Forward, Prof. Frank Plasschaert

Master's dissertation submitted in order to obtain the academic degree of
Master of Science in Biomedical Engineering

Academic year 2018-2019